

© Copyright 2018

Ting Qiu

Planning and Operation of Energy Storage Systems in Power Systems

Ting Qiu

A dissertation

submitted in partial fulfillment of the
requirements for the degree of

Doctor of Philosophy

University of Washington

2018

Reading Committee:

Daniel Kirschen, Chair
Miguel A. Ortega-Vazquez
Baosen Zhang

Program Authorized to Offer Degree:

Electrical Engineering

ProQuest Number: 10750367

All rights reserved

INFORMATION TO ALL USERS

The quality of this reproduction is dependent upon the quality of the copy submitted.

In the unlikely event that the author did not send a complete manuscript and there are missing pages, these will be noted. Also, if material had to be removed, a note will indicate the deletion.



ProQuest 10750367

Published by ProQuest LLC (2018). Copyright of the Dissertation is held by the Author.

All rights reserved.

This work is protected against unauthorized copying under Title 17, United States Code
Microform Edition © ProQuest LLC.

ProQuest LLC.
789 East Eisenhower Parkway
P.O. Box 1346
Ann Arbor, MI 48106 – 1346

University of Washington

Abstract

Planning and Operation of Energy Storage Systems in Power Systems

Ting Qiu

Chair of the Supervisory Committee:
Professor Daniel S. Kirschen
Electrical Engineering

The increase in renewable power generation has greatly changed the current energy market dynamics. The cheaper, cleaner but intermittent characteristics of renewable power generation such as wind has accelerated the retirement of large coal plants and investments in flexible resources such as fast response generators, energy storage and transmission facilities. However, this transition requires tremendous effort on how to improve the market design to better handle the uncertainty on renewable generation, and to facilitate the deployment of more flexible resources such as energy storage.

In this dissertation, we focus on the planning and operation of energy storage systems. To begin with, we discuss in detail different optimization methods that have been proposed to handle this growing uncertainty. Yearly simulations were performed to compare the solution accuracy and the

computing efficiency. Then two stochastic multi-stage co-planning models are proposed to coordinate investments in battery energy storage and transmission expansion, and in battery energy storage and fast generation. These co-planning models have a 25-year horizon and consider not only the uncertainty on both wind capacity and load increase, but also the degradation of the batteries. A sensitivity analysis is performed to study the competition and cooperation relationship between these resources, their investment patterns under different geography, and the correlation between the profiles of wind generation and load. At the end of this dissertation, a stochastic energy and ancillary service co-optimization model is proposed to evaluate the contribution of storage to both energy arbitrage and ancillary services. The actual requirements for regulation reserve and spinning reserve are quantified by combining intra-hour system operation with day-ahead stochastic optimization.

TABLE OF CONTENTS

List of Figures	iv
List of Tables	vii
Chapter 1. Introduction	12
1.1 Operation of the electric power system under uncertainty	12
1.2 Energy storage in power systems.....	13
1.3 The Effect of Energy Storages Costs	18
1.4 Objective and Structure of the Dissertation	19
Chapter 2. An Overview of Mathematical Methods to Deal with Uncertainty	21
2.1 Introduction.....	21
2.2 Base Unit Commitment Modeling.....	21
2.3 Stochastic Optimization Unit Commitment Model	25
2.4 Interval optimization.....	28
2.5 robust optimization or scheduling.....	30
2.6 Other day-ahead optimization methods and trends.....	35
2.7 Test system and Results	36
2.8 Summary	42
Chapter 3. Stochastic Multi-Stage Co-Planning of Transmission Expansion and Energy Storage	44
3.1 Introduction.....	44

3.2	Modeling.....	46
3.3	Formulation of the Planning Problem.....	50
3.4	Test system.....	58
3.5	Test Results and sensitivity analysis.....	60
3.6	Conclusions.....	69
Chapter 4. Stochastic Multi-Stage Co-Planning of Generation and Battery Energy Storage.....		71
4.1	Introduction.....	71
4.2	Modeling Assumptions	74
4.3	Formulation of the Planning Problem.....	77
4.4	Test System.....	82
4.5	Test Results and Analysis	85
4.6	Conclusions.....	96
Chapter 5. Stochastic Energy and Ancillary Service Co-Optimization with BESS		97
5.1	Introduction.....	97
5.2	Model Assumptions	101
5.3	Formulation of the Problem	102
5.4	Test System.....	108
5.5	Test Results and Analysis	111
5.6	Conclusions.....	124
Chapter 6. Conclusions and Future Work.....		125
6.1	Conclusions.....	125
6.2	Suggested Future Work.....	126

Bibliography	129
Appendix A.....	145

LIST OF FIGURES

Figure 1.1. Effect of Renewable Generation on Load Shape [5].....	12
Figure 2.1. Centralized and Decomposition Methods	27
Figure 2.2. Generation level transit process.....	29
Figure 2.3. Robust optimization and OA Solving Process	34
Figure 2.4. Scatter Plot of Day-ahead Unit Commitment Solution Time.....	38
Figure 2.5. CDF Plot of Day-ahead Unit Commitment Solution Time	39
Figure 2.6. Scatter Plot of Real-time Cost	40
Figure 2.7. CDF Plot of Day-Ahead Start-up Cost.....	41
Figure 2.8. CDF Plot of Real-time Cost	41
Figure 3.1. BESS Investment Unit [29].....	47
Figure 3.2. Load and Wind generation capacity scenarios	49
Figure 3.3. Test System Topology	59
Figure 3.4. Total available BESS energy and power capacity as a function of time.....	62
Figure 3.5. Total BESS energy capacity installed at each bus.....	62
Figure 3.6. Total BESS power capacity installed at each bus.	63
Figure 3.7. Energy capacity installed each year at each bus of the planning horizon using the co-planning method.....	63
Figure 3.8. Energy capacity installed each year at each bus of the planning horizon using the BESS only planning method.....	64
Figure 3.9. Total BESS energy capacity installed each year at each bus using stochastic optimization	65

Figure 3.10. Total BESS energy capacity installed each year at each bus using deterministic optimization	65
Figure 3.11. Total Available Energy Capacity	66
Figure 3.12. Total available BESS energy capacity for different initial transmission capacities.	69
Figure 4.1. Examples of representative days	76
Figure 4.2. Test System Topology	83
Figure 4.3. Total Available BESS Power Capacity over time	95
Figure 4.4. Total Available BESS Energy Capacity over time.....	96
Figure 5.1. California’s average hourly ancillary service prices for 2002. [109].....	98
Figure 5.2. Test System Topology	110
Figure 5.3. Total Hourly Generation Output	112
Figure 5.4. Total Hourly Regulation Reserve Provided by Generators	113
Figure 5.5. Total Hourly Spinning Reserve Provided by Generators	113
Figure 5.6. CDF of the Different Costs in Day-ahead and Real Time Market	115
Figure 5.7. CDF of Relative Cost Savings in Day-ahead Energy and Ancillary Service Procurement Costs	116
Figure 5.8. CDF of Relative Savings in Real-time, Day-ahead, and Total Cost	117
Figure 5.9. Histograms of Average Hourly Regulation Up Reserve	118
Figure 5.10. Histograms of Average Hourly Spinning Up Reserve	119
Figure 5.11. Histograms of Average Hourly Regulation Down Reserve	119
Figure 5.12. Histograms of Average Hourly Spinning Down Reserve	120
Figure 5.13. Relative increase in the day-ahead costs caused by the BESS O&M cost.....	121
Figure 5.14. CDF of the cost of real-time corrective actions.....	122

Figure 5.15. Real-time Wind Curtailment in Monte-Carlo Simulation 123

LIST OF TABLES

Table 1.1. Costs of Storage Options	19
Table 3.1. Unit Category.....	60
Table 3.2. Investments in Transmission Line Capacity.....	60
Table 3.3. BESS Investment Location.....	61
Table 3.4. BESS Investments.....	66
Table 3.5. Line Capacity Upgrades.....	67
Table 3.6. Line Capacity Upgrades.....	68
Table 3.7. BESS Investment Location.....	68
Table 4.1. Features Used for Identifying Representative Days	76
Table 4.2. Unit Categories	84
Table 4.3. Co-planning of Generation Capacity for 9 Combinations of Wind penetrations and Wind/load Correlations.....	85
Table 4.4. Co-planning of Storage for 9 Combinations of Wind Penetrations and Wind/load Correlations.....	86
Table 4.5. Total Generation Capacity (MW) with the Co-Planning Model	88
Table 4.6. Total BESS Energy Capacity (MWh) in Co-Planning Model.....	89
Table 4.7. Total BESS Power Capacity at Each Location (MW).....	90
Table 4.8. Generation Only Planning	92
Table 4.9. Differences between Co-planning and Generation Only Planning.....	92
Table 4.10. Total Installed Capacity (MW) with Generation Only Planning.....	93
Table 4.11. Generation Investment in TEST1 and TEST2.....	96

Table 5.1. Comparison of Day-ahead and Expected Real-Time Costs..... 111

ACKNOWLEDGEMENTS

First and foremost, I would like to express my utmost appreciation to my advisor Prof. Daniel S. Kirschen for his consistent guidance and support through all the periods when I was in Seattle, Boise and Austin. This dissertation would not have been possible without his inspiration and careful editing. My gratitude also goes to my reading committee members, Prof. Miguel A. Ortega-Vazquez and Prof. Baosen Zhang for their insightful feedback and suggestions along my research. I would also like to thank Prof. Liu Shan for serving the GSR committee and providing many constructive suggestions.

I must acknowledge the friends and collaborators from Renewable Energy Analysis Lab (REALab): Prof. Yury Dvorkin, Dr. Ahlmahz Negash, Yisheng Wang, Prof. Hrvoje Pandzic, Marco Au, Ryan Elliot, Zeyu Wang, Dr. Mush_q Sarker, Yushi Tan, Jesus Elmer Contreras, Bolun Xu, Dr. Ricardo Fernandez-Blanco, Daniel Olsen, Ahmad Milyani, Abeer Almaimouni, Yao Long, Agustina Gonzalez, Kelly Kozdras, Rebecca Breiding, Dr. Pierre Henneaux, Dr. Tu Nguyen, Dr. Remy Rigo-Mariani, Pan Li, Yuanyuan Shi, Dr. Hao Wang, Yize Chen, Chenghui Tang, Dr. Weiling Zhang, Dr. Yangwu Shen, Dr. Yang Wang, Yao Chang, Jingkun Liu, YiWang, Prof. YunfengWen, Dr. Tobias Haring, Leonardo H. Macedo. Thank you all for the many beautiful memory along the different stages of PhD study, and I feel honored to work with such a talented group.

I would like to thank the EE department staff for their kindly help during the past years. I thank Brenda Larson for setting up the PhD general and final exams, payroll officer Eric Eto's effort during each of my status change.

Last but not the least, I would like to thank my husband Xiaohu Xue for all the encouragement and support, my son Darren Xue for being such a lovely angel that I spare some time on research even during the busiest time., my parents for their unconditional love and care. My special thanks to Grandma Louise Holert for the hospitality during the years when I was in Seattle. I could not finish this dissertation without them. This dissertation is dedicated to all of you.

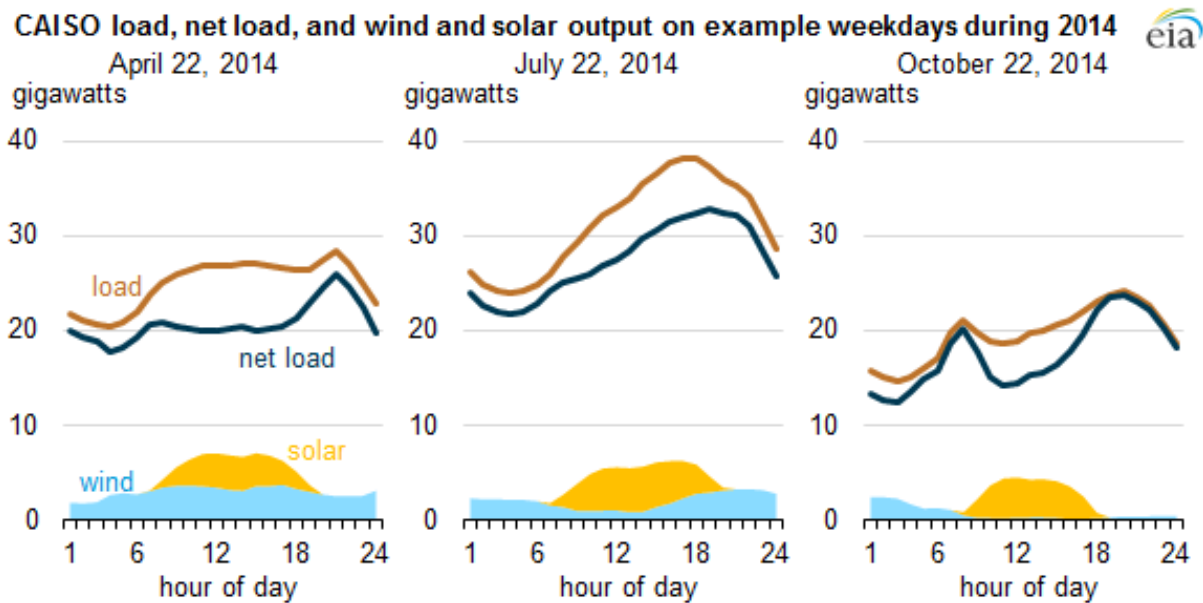
DEDICATION

This thesis is dedicated to my family.

Chapter 1. INTRODUCTION

1.1 OPERATION OF THE ELECTRIC POWER SYSTEM UNDER UNCERTAINTY

Unlike traditional generation, renewable resources, such as wind and solar do not incur any fuel cost to generate electricity. They are therefore among the first to be used by the power system operator. However, due to their highly variable nature, a large proportion of renewable generation, will further increase the uncertainty affecting system operation and reliability. As shown in Figure 1.1, as more wind and solar generation is added to the system, the California Independent System Operator (CAISO), is facing increasingly different types of net load patterns. More flexibility is therefore needed to deal with the increasing uncertainty.



Source: California Independent System Operator (CAISO), Daily Renewables Watch

Figure 1.1. Effect of Renewable Generation on Load Shape [5]

In the short-term operational time frame, increased flexibility can be achieved by a better management of existing dispatchable capacity through advanced optimization techniques (such as stochastic optimization, interval optimization, robust optimization and etc.), by improving renewable generation forecast accuracy, by enhancing market design (such as introducing intra-hour scheduling and adding flexible ramping constraints), or simply by increasing the reserve requirements [1-4]. Over a longer planning timeframe, one should consider deploying flexible resources such as energy storage systems and expanding the generation and transmission capacity to increase the dispatchable capacity of the current system

1.2 ENERGY STORAGE IN POWER SYSTEMS

Compared with conventional technologies, electricity storage offers price arbitrage opportunities and fast-response services which could be widely deployed throughout an electric power system—functioning as generation, transmission, distribution, or end-use assets. Energy storage systems, when placed at key locations with an appropriate technology, can alleviate the impact of renewable generation variation, enhance system reliability, defer transmission expansion, or postpone the need for new generation capacity.

- RENEWABLE GENERATION SUPPLY RELIABILITY

Energy storage systems, when installed in combination with wind farms or PV plants, could greatly facilitate their generation scheduling and improve the reliability of their energy supply by mitigating fluctuations in their output. Ghosh and Kamalasan [6] design an optimal control strategy based on energy functions for flywheel energy storage. Their aim is to improve the low voltage ride-through characteristics of an integrated doubly fed induction wind generator (DFIG)

and keep the grid power isolated from wind power output and voltage fluctuations. A rank-based battery energy storage system dispatch control algorithm is developed in Abdullah et al. [7] to achieve assured wind farm power output levels and dispatch for wind farm profit maximization. Islam et al. [8] use a supervisory control unit combined with short-term wind speed prediction for management of the stored energy in a small capacity flywheel energy storage system to mitigate the output fluctuations of an aggregated wind farm. A dual layer BESS control strategy consisting of a fluctuation mitigation control layer and a power allocation control layer is proposed in Jiang et al. [9] to control the wind farm power output within fluctuation mitigation requirements. Wang et al. [10] designed a hybrid energy storage system composed of a vanadium redox battery and a supercapacitor bank to smooth the fluctuating output power of a PV plant. In Song et al. [11], a new energy storage model based on a Markov chain is used to enhance photovoltaic generation power supply availability considering the energy storage capacity degradation.

- ECONOMIC MARKET OPERATION

On the electric market side, energy storage systems can participate in both energy and ancillary services markets to facilitate higher renewable integration. Li et al. [12] use a two-step framework to evaluate the benefits of battery energy storage in power system operation with the aim of decreasing the curtailment of wind generation, reduce load and reserve shortfalls as well as the commitment of thermal units, and lower the total system costs. A multi-period Nash-Cournot equilibrium model for the joint energy and ancillary services markets is proposed to evaluate the contribution of the ESSs in supporting renewable generation by Zou et al. [13]. O'Dwyer and Flynn [14] propose a sub-hourly UCED analysis to evaluate the role of energy storage in reducing the cycling cost of conventional plants in systems with high wind penetrations.

Jabr et al. [15], used robust optimization to set the base-point of conventional generation and storage for the forecasted net load, and participation factors that dictate how conventional generation and storage should be adjusted to maintain feasible operation whenever the renewables realization deviates from the forecast. In Ghofrani et al. [16], a combination of genetic algorithm (GA)-based optimization and probabilistic optimal power flow is used to evaluation energy storage for reliability and operability enhancement of wind integration considering uncertainty on wind generation, load and equipment availability.

- RELIEVE TRANSMISSION CONGESTION

As energy storage systems respond much faster than conventional generators, they are effective at relieving transmission congestion by controlling the charging and discharging sequence and rate. Vargas et al. [17] exploit the fast ramping capabilities of energy storage to deal with transmission congestion in the case of insufficient ramping from conventional power plants. In Wen et al. [18, 19], as well as Del Rosso and Eckroad [20], battery storage system respond before conventional generators to relieve line overloading following a contingency. Khani et al. [21] propose a real-time optimal dispatch algorithm that aims to optimally prepare a compressed-air energy storage system to maximize its contribution to congestion relief.

- FREQUENCY REGULATION

The fast response characteristic of energy storage systems also makes them an ideal resource for frequency regulation following a generation contingency or a sudden change in renewable generation. A unit commitment formulation constrained by frequency dynamics is proposed by Wen et al. [22], where both the synchronous units' primary reserve requirements and the storage

units' corrective actions are modeled for post-contingency inertial response and primary frequency control to guarantee dynamic frequency security following a contingency. Zhang et al. [23] propose a fuzzy-logic based frequency controller for wind farms augmented with a battery energy storage system to improve the primary frequency response of low-inertia hybrid power systems. Pulendran and Tate [24] proposed a model predictive approach to control an energy storage system for preventing load shedding due to transient declines in frequency. Datta and Senjyu [25], describe a fuzzy-logic based frequency control method for distributed PV inverters, energy storage systems (ESSs) and EVs. This method provides frequency control and reduces tie-line power fluctuations caused by a large penetration of PV or sudden load variations. Yang and Walid [26] proposed a secure scheduling and dispatch approach to investigate the relationship between outages and the energy storage capacity during the frequency regulation process considering both distributed renewable energy sources failure and renewable generation supply uncertainties. In Banham-Hall et al. [27], a Vanadium Redox Flow Battery is attached to a wind farm to time shift energy and provide frequency response.

- DISTRIBUTION

In distribution systems, energy storage could be used to deal with voltage fluctuations, to enhance the stability of the network and to smooth renewable generation.

In Wang et al. [28], a coordinated voltage control scheme using energy storage system is proposed for distribution networks to solve the voltage problems caused by large, clustered distributions of low carbon technologies (wind generation, photovoltaic generation, electric vehicles, heat pumps and etc.). In Mokhtari et al. [29], energy storage units are used for both voltage support and load management by controlling the reactive and active power respectively.

Sugihara et al. [30] addressed the voltage fluctuation problem in a distribution network with high penetration of PV, and proposed to subsidize customer-side energy storage systems to help with voltage regulation. In Alam et al. [31], a distributed energy storage system is controlled to mitigate the neutral current and neutral potential problems in four-wire multi-grounded low voltage systems under unbalanced allocation of rooftop solar PV.

The utilization of energy storage system is proposed to solve the phase balancing problem in power system through Lyapunov optimization in Sun et al. [32]. In Jayasekara et al. [33], battery energy storage systems are used for peak shaving, voltage regulation, and loss reduction in distribution systems considering battery cycling cost. A supervisory controller is proposed in Liu et al. [34] to facilitate the high-level penetration of renewable energy distributed generations. Nagarajan and Ayyanar [35] provide a generalized framework for strategic deployment of lithium-ion-based energy storage to reduce the substation transformer losses, and the life cycle cost of the battery storage system, as well as to mitigate PV variability. In Tant et al. [36], battery energy storage systems are installed in residential distribution feeders to reduce voltage deviations and facilitate the integration of PV. The trade-offs between voltage regulation, reductions in peak apparent power, and the annual energy utilization cost is also discussed. Somayajula and Crow [37], integrate an ultra-capacitor in a power conditioner system to improve the power quality in the distribution grid by compensating voltage sags and swells, and smoothing renewable intermittency.

- END USERS

On-site energy storage systems provide opportunities for the electricity end users to reduce their electricity bill (i.e., for energy use and for demand charges) [38]. In Wang et al. [39], a

reinforcement learning technique is used for consumers to coordinate PV energy generation and energy storage with the goal of shaving the peaks of their power demand profile, thereby minimizing their electricity bill. In Paterakis et al. [40] and Erdinc et al. [41], Mixed-Integer Linear Programming (MILP) is used to minimize the total energy procurement cost for a smart household with assets such as electric vehicles, controllable appliances, energy storage and distributed generation. The energy cost minimization performance of different energy storage devices in building energy systems is compared in Xu et al. [42] through scenario based stochastic optimization, considering uncertainties in demand profiles and solar irradiance.

1.3 THE EFFECT OF ENERGY STORAGE COSTS

The future application of storage technologies depends on the one hand on how rapidly the technologies advance and the costs drop. On the other hand, it will be essential to develop novel energy storage planning techniques that are robust to the inevitable long-term forecasting errors, and advanced operational schemes that make better use of the services that storage can provide.

Table 1.1 shows the different types of energy storage, their costs and their possible applications in power systems. Storage technologies such as thermal storage and pumped hydro are mature and fully commercial. But others listed in this table, such as battery and flywheel energy storage, are still evolving in terms of technology and operational roles [5]. Since the cost can be high when it comes to building new flexible assets such as storage, particularly with emerging technologies, the risk of stranded investments can be significant.

Table 1.1. Costs of Storage Options [43]

Storage Options	Cost(\$/kw)	Typical Applications
Li-ion	\$1000-\$2000	Frequency regulation; ancillary services; black start; renewable shifting, smoothing and firming; arbitrage; peak load shift; reactive power
Compressed Air	\$1600-\$2200	Ancillary services; black start; renewable shifting and firming; area regulation; spinning reserve; reactive power
Pumped Hydro Storage	\$1200-\$2100	Same as CAES
NaS Battery	\$3500-\$6000	Arbitrage; renewable shifting and firming; frequency regulation and other ancillary services; peak load shift; black start; reactive power
Flywheel	\$2100-\$2600	Frequency regulation; renewable energy smoothing; reactive power

Source: Energy Storage Cost and Performance Report 2015 by FC Business Intelligence

1.4 OBJECTIVE AND STRUCTURE OF THE DISSERTATION

The goal of this dissertation is to investigate how energy storage systems, combined with advanced optimization techniques could improve the system operational efficiency and reliability. In particular, we focus on improving energy storage planning and operation models and methods.

The remainder of this dissertation is organized as follows. Chapter 2 gives an overview of the many optimization techniques applied to the day-ahead unit commitment problem to deal with wind uncertainty. Some of these optimizations are explained in more detail as they are the mathematical foundations of energy storage system planning and operations techniques developed in the later chapters; Chapter 3 proposes a stochastic multi-stage co-planning model for energy storage and transmission lines. This model can be used to determine the long-term optimal site and size of energy storage, the transmission that should be enhanced; Chapter 4 proposes a multi-stage approach for co-planning energy storage and fast response generators. This chapter also discusses the co-operative and competitive relationships between BESS and fast generators, as well as the patterns of location and size for BESS and fast generators for nine different scenarios of wind power output/load ratios and hourly wind-load correlations; Chapter 5 describes the optimization of energy storage in power system for energy arbitrage and ancillary service support from the perspective of the system operator; Chapter 6 concludes, summarizes the contributions made and discusses future work.

Chapter 2. AN OVERVIEW OF MATHEMATICAL METHODS TO DEAL WITH UNCERTAINTY

2.1 INTRODUCTION

Wind power has become a significant part of the total power generation in many power systems. The accompanying uncertainty has also brought huge challenges to the system operator. In this chapter, we will first discuss several different ways of modeling wind uncertainty that have been discussed in the literature. Then, we will introduce different methods for solving these different models. A small example will be used to exemplify each method. Finally, we will test these methods using the IEEE RTS and compare the performance of these different methods.

2.2 BASE UNIT COMMITMENT MODELING

- NOTATIONS

Sets

t : $(1 \cdots T)$ - Index to the time interval in the unit commitment

i : $(1 \cdots I)$ - Index to the generators

b : $(1 \cdots NB)$ - Index to the piece-wise linear cost segments

l : $(1 \cdots L)$ - Index to the transmission lines

s : $(1 \cdots S)$ - Index to the nodes

w : $(1 \cdots W)$ - Index to the wind farms

Variables

$x_{i,t}$: Binary variable, generator i on-off state at period t

$p_{i,t}$: Generator i power output at period t

$p_{i,b,t}$: Generator i power output of segment b at period t

$w p_{w,t}$: Wind power produced by wind farm W at period t

$w s_{w,t}$: Wind power curtailed from wind farm W at period t

$SU_{i,t}$: Generator i start-up cost at period t

Parameters

NL_i : No-load cost of generator i

$w f_{w,t}$: Wind forecast

\bar{F}_l : Transmission line rating

$\Gamma_{l,i}^U, \Gamma_{l,s}^D, \Gamma_{l,w}^W$: Contribution factor of generator, load and wind to power flow on line l

$D_{s,t}$: Demand at bus s at period t

Δ_i : Ramping ability of generator i

$\bar{p}_{i,b}$: Maximum generation of each segment of a cost curve

$\underline{p}_i, \bar{p}_i$: Minimum and maximum generation of each generator

$u^1 \dots u^{10}$: Dual variables for the corresponding constraints

- OBJECTIVE FUNCTION

The objective of the base unit commitment problem is to minimize the total generation cost and wind curtailment penalty cost.

$$\min J = \sum_{i=1,t=1,b=1}^{I,T,NB} k_{i,b} \cdot p_{i,b,t} + \sum_{i=1,t=1}^{I,T} (C_{i,t}^{Noload} + SU_{i,t}) + M \cdot \sum_{w=1,t=1}^{W,T} wS_{w,t} \quad (2.1)$$

$$u_{i,t}^7 : C_{i,t}^{Noload} \geq NL_i \cdot x_{i,t} \quad (2.2)$$

- SYSTEM CONSTRAINTS

System constraints include the system balance constraint (2.3) and the DC line flow constraint (2.4) and (2.5).

$$u_t^6 : \sum_{i=1}^I p_{i,t} + \sum_{w=1}^W wp_{w,t} = \sum_{k=1}^K D_{k,t} \quad (2.3)$$

$$u_{l,t}^9 : \sum_{i=1}^I \Gamma_{l,i}^U \cdot p_{i,t} + \sum_{w=1}^W \Gamma_{l,w}^W \cdot wS_{w,t} \geq -\bar{F}_l + \sum_{k=1}^K \Gamma_{l,k}^D \cdot D_{k,t} \quad (2.4)$$

$$u_{l,t}^{10} : -\sum_{i=1}^I \Gamma_{l,i}^U \cdot p_{i,t} - \sum_{w=1}^W \Gamma_{l,w}^W \cdot wp_{w,t} \geq -\bar{F}_l - \sum_{k=1}^K \Gamma_{l,k}^D \cdot D_{k,t} \quad (2.5)$$

- MINIMUM UP-DOWN TIME AND START-UP COST

There are several different ways to model the minimum up-down time constraints and start-up cost, and here we eliminate the details and only gives its abbreviation. Detailed information can be found in Pandzic et al. [44]

$$H(x) = 0 \quad (2.6)$$

- GENERATION CONSTRAINT

The generation constraint includes the generation capacity constraints (2.7) and (2.8), the generation equation constraint (2.9) and the ramping rate constraints (2.10) to (2.13).

$$u_{i,t}^1 : \sum_{b=1}^{NB} p_{i,b,t} \geq x_{i,t} \cdot \underline{P}_i \quad (2.7)$$

$$u_{i,t}^2 : -p_{i,b,t} \geq -x_{i,t} \cdot \bar{P}_{i,b} \quad (2.8)$$

$$u_{i,t}^3 : \sum_{b=1}^{NB} p_{i,b,t} - p_{i,t} = 0 \quad (2.9)$$

$$u_{i,t}^4 : p_{i,t} - p_{i,t-1} \geq -\underline{\Delta}_i \quad t \geq 2 \quad (2.10)$$

$$u_{i,t=1}^4 : p_{i,t=1} \geq -\underline{\Delta}_i + p_{i,0} \quad (2.11)$$

$$u_{i,t}^5 : p_{i,t-1} - p_{i,t} \geq -\bar{\Delta}_i \quad t \geq 2 \quad (2.12)$$

$$u_{i,t=1}^5 : -p_{i,1} \geq -\bar{\Delta}_i + p_{i,0} \quad (2.13)$$

- WIND CONSTRAINT

$$u_{w,t}^8 : wp_{w,t} + ws_{w,t} = wf_{w,t} \quad (2.14)$$

The above constraints frame the basic unit commitment problem. When integrating other resources such as wind generation into the system, additional constraints may be added, and the objective function could also be modified for different optimization goals. We will only mention the modified part of this basic model when discussing the different optimization models used to solve the day-ahead unit commitment problem with wind uncertainty in the following part. To simplify the notation, we name the remaining constraints ED constraints

$$G(P) = 0 \quad (2.15)$$

2.3 STOCHASTIC OPTIMIZATION UNIT COMMITMENT MODEL

There are several ways to model wind uncertainty. The most common and straight forward way is to represent wind uncertainty by different scenarios. The more scenarios are used, the more wind dynamics can be caught for a certain time period. Wind uncertainty models of this type are generally used in stochastic optimization unit commitment model.

- NOTATIONS

n : 1... N Wind scenario set

π_n : Probability of wind power scenario n

$wf_{w,t,n}$: Wind farm power output forecast at period t of scenario n

$ws_{w,t,n}$: Wind farm power curtailment at period t of scenario n

$p_{i,b,t,n}$: Generator i power output of segment b at period t of scenario n

- FORMULATIONS AND SOLVING METHODS

The objective of stochastic unit commitment is to minimize the sum of the expected total generation and wind curtailment penalty costs.

$$\min J = \sum_{n=1}^N \pi_n \cdot \left(\sum_{i=1, t=1, b=1}^{I, T, NB} k_{i,b} \cdot p_{i,b,t,n} + M \cdot \sum_{w=1, t=1}^{W, T} ws_{w,t,n} \right) + \sum_{i=1, t=1}^{I, T} (SU_{i,t} + C_{i,t}^{Noload}) \quad (2.16)$$

For all scenarios $n = 1 \dots N$, the system and generation constraints as shown in the base case.

Stochastic optimization unit commitment tries to find common generator on-off states for all possible wind realization. Compared with the base unit commitment model, the stochastic optimization unit commitment model shares the same one set of unit commitment constraints

$H(x) = 0$, and there is a whole set of economic constraints $G(P) = 0$ for each of the N possible wind scenarios.

Currently, the UC problem with scenario-based wind model is solved using the following methods:

1. *Centralized solution method*

The centralized method solves the N scenarios together. As the number of wind scenarios increase, the number of ED constraints increases correspondingly, which also increase the computation burden for large power systems. The centralized method can therefore be used only for small systems or cases with shorter scheduling periods or with a small number of wind scenarios.

2. *Decomposed solution method*

As mentioned above, the N scenarios share the same set of UC constraints, however, each scenario has its independent ED constraints, the problem can be decomposed into two stage problem. The first stage solves a pure unit commitment problem to determine the on-off status of the generators, while the second stage solves N economic dispatch problems. Since the N economic dispatch problems are independent of each other, parallel computation is possible. This is quite beneficial when applying stochastic optimization to larger power systems. The commonly used decomposition method is Benders' Decomposition (BD). However other decomposition methods can also used, for example see Papavasiliou and Oren [45, 46].

The following figures illustrates the centralized and decomposition methods.

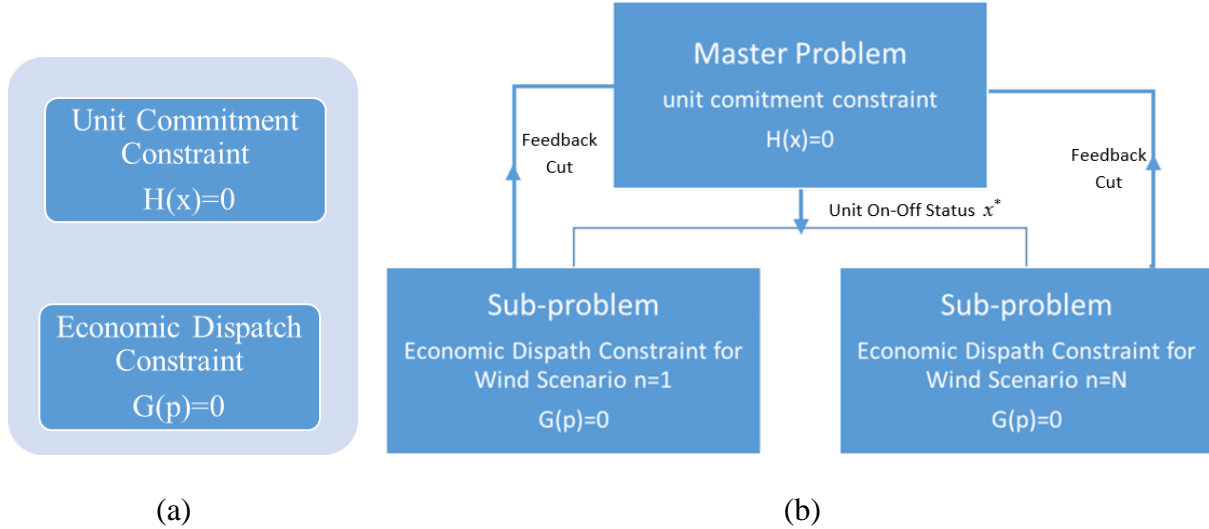


Figure 2.1. Centralized and Decomposition Methods

- VARIANTS OF STOCHASTIC OPTIMIZATION MODEL

Variants of stochastic optimization unit commitment model have been proposed by Chen et al. [47] and Wang et al. [48]. In these papers, the authors model the connections among all scenarios such as the transit limit among different scenarios. These constraints require the generation level of a generator under the expected wind forecast scenario should be able to transit to the generation level in other scenarios within 10-15 minutes.

$$|p_{i,t} - p_{i,t,n}| \leq \frac{10}{60} \Delta_i, \text{ if } x_{i,t} > 0 \quad (2.17)$$

A stochastic optimization unit commitment attempts to minimize the expected total cost as calculated on the day ahead. It has gained popularity because of the easy modeling and the possibility of parallel computing. However, some difficulties persist with stochastic optimization unit commitment:

1. Scenario generation

In order to capture the wind dynamics, enough scenarios should be generated and added to

the model. These wind scenarios should be sufficiently representative to reduce the risk of violations of operational constraints in real-time.

2. *Scenario reduction*

Even though a larger number of wind scenarios is better for describing wind uncertainty, it could put on too much burden on the computing resources. Reducing the number of scenarios is thus necessary, especially when stochastic optimization is applied to large power systems or long-term system operation and planning.

2.4 INTERVAL OPTIMIZATION

Another way of modeling wind uncertainty is using an uncertainty bound or interval that describes the possible lower and upper bounds of wind generation at each time period. Interval optimization is another way of solving the unit commitment problem with uncertainty modeling. Interval optimization can be considered as a variant of stochastic optimization, in which only three scenarios are considered: the upper and lower bound wind forecasts, and the expected wind forecast. The objective of interval optimization is to minimize the cost of the expected wind forecast scenario, while the system should have enough ramping capability to transition between the lower and upper bound of wind realization.

Interval optimization considers all possible transitions among different scenarios. This transition process is shown in Figure 2.2 as published by Wang et al. [49]. D_t is the net load.

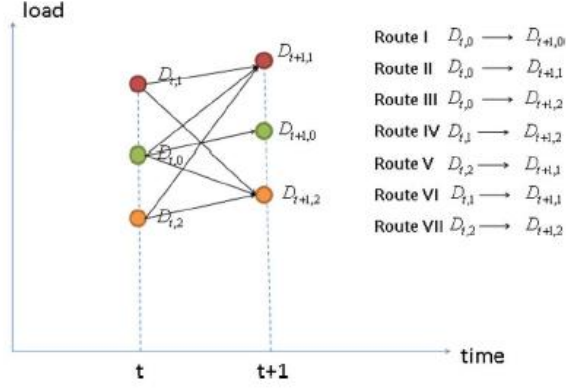


Figure 2.2. Generation level transit process

Based on the scenario-based model, the following transition constraints between these three scenarios are added to the model [49]:

$$\left| p_{i,t,n_2} - p_{i,t-1,n_1} \right| \leq \Delta_i \quad (2.18)$$

$$\left| p_{i,t,n_1} - p_{i,t-1,n_2} \right| \leq \Delta_i \quad (2.19)$$

$$\left| p_{i,t,n_2} - p_{i,t-1} \right| \leq \Delta_i \quad (2.20)$$

$$\left| p_{i,t,n_2} - p_{i,t-1} \right| \leq \Delta_i \quad (2.21)$$

To guarantee that the system constraints are satisfied for all wind realizations, the line flow constraints (2.4) and (2.5) are replaced by the following:

$$-\bar{F}_l + \max_{k=1}^K \sum_{l,s} \Gamma_{l,s}^D D_{s,t} \leq \sum_{i=1}^I \Gamma_{l,i}^U p_{i,t,n} \leq \bar{F}_l + \min_{k=1}^K \sum_{l,s} \Gamma_{l,s}^D D_{s,t} \quad (2.22)$$

The interval optimization unit commitment model guarantees the feasibility of all wind realization within the given bounds. It reduces the risks of not having enough ramping capacity or transmission capacity when the wind generation drops or increases suddenly. The selection of the upper and lower bounds plays a significant role and must be chosen carefully to avoid making the model too conservative. Yu et al. [50] set the uncertain wind generation bound using a Markov

chain to improve the robustness of the original interval optimization unit commitment model.

2.5 ROBUST OPTIMIZATION OR SCHEDULING

The robust optimization unit commitment model aims to protect the system against the worst wind realization over a given uncertainty set. Generally, robust optimization model involve two steps: the first searches for the worst realization scenario, and the second is the base unit commitment under this worst-case scenario. Formally, the robust optimization unit commitment model is defined as follows:

$$\min Zu = \max_{wg_{w,t}} \min_{P_{i,b,t}, ws_{w,t}, x_{i,t}} \left(\sum_{i=1, t=1}^{I, T} k_{i,b} P_{i,b,t} + C_{i,t}^{Noload} + M \sum_{w=1, t=1}^{W, T} ws_{w,t} + \sum_{i=1, t=1}^{I, T} SU_{i,t} \right) \quad (2.23)$$

St. (2.6), (2.15)

$$\sum_{w=1}^W \frac{|wg_{w,t} - wf_{w,t}|}{\Delta w_{w,t}} \leq \Gamma_t \quad (2.24)$$

$$wf_{wt} - \Delta w_{w,t} \leq wg_{w,t} \leq wf_{wt} + \Delta w_{w,t} \quad (2.25)$$

Equation (2.23) is the objective function with a max-min part. Problems of this type are hard to solve. Equations (2.6), (2.15) are the same constraints as appeared in the base unit commitment model. The worst wind realization $wf_{w,t}$ is a decision variable in the outer maximum optimization problem under the uncertainty area defined by (2.24) and (2.25).

As the worst wind realization $wf_{w,t}$ only appears in the economic dispatch constraints which contain no binary variables, a common method for solving the robust optimization model is to use a decomposition technique such as Benders' Decomposition. The decomposed model is formulated as the following:

- FIRST STAGE: BENDERS' MASTER PROBLEM

$$\min_{x_{i,t}} Zl = \sum_{i=1,t=1}^{I,T} SU_{i,t} + \beta \quad (2.26)$$

St. (2.6)

The first stage minimizes the start-up cost with only the unit commitment constraints, namely the minimum up and down time constraints. A Benders' cut generated by the second stage problem is added to the master problem to update the value of β .

- SECOND STAGE: BENDERS' SUB-PROBLEM:

$$\min Zu = \max_{wg_{w,t}, p_{i,b,t}, ws_{w,t}} \min \left(\sum_{i=1,t=1}^{I,T} k_{i,b} \cdot p_{i,b,t} + C_{i,t}^{Noload} + M \sum_{w=1,t=1}^{W,T} ws_{w,t} \right) \quad (2.27)$$

St. (2.15), (2.24), (2.25)

The second stage solves an economic dispatch problem under the worst wind realization scenario, which first needs to be identified within the given uncertainty set. The max-min second stage sub-problem can be transformed into the following using primal-dual theory.

$$\begin{aligned} \max_{wg_{w,t}, u} Zu = & \sum_{i=1,t=1}^{I,T} \left(u_{i,t}^1 \cdot \hat{x}_{i,t} \cdot \underline{P}_i - u_{i,t}^2 \cdot \hat{x}_{i,t} \cdot \bar{P}_i - u_{i,t}^4 \cdot \underline{\Delta}_i - u_{i,t}^5 \cdot \bar{\Delta}_i \right) + \sum_{i=1}^I \left(u_{i,t_0}^4 \cdot p_{i,0} - u_{i,t_0}^5 \cdot p_{i,0} \right) \\ & + \sum_{t=1}^T u_t^6 \cdot D_t + \sum_{i=1,t=1}^{I,T} u_{i,t}^7 \cdot NL_i \cdot \hat{x}_{i,t} - \sum_{w=1}^W u_{w,t}^8 \cdot wg_{w,t} \\ & + \sum_{l=1,t=1}^{L,T} u_{l,t}^9 \cdot \left(-\bar{F}_l + \sum_{s=1}^S \Gamma_{l,s}^D \cdot D_{s,t} \right) + \sum_{l=1,t=1}^{L,T} u_{l,t}^{10} \cdot \left(-\bar{F}_l - \sum_{s=1}^S \Gamma_{l,s}^D \cdot D_{s,t} \right) \end{aligned} \quad (2.28)$$

$$p_{i,b,t} : u_{i,t}^1 - u_{i,b,t}^2 + u_{i,t}^3 \leq k_{i,b} \quad (2.29)$$

$$p_{i,t} : -u_{i,t}^3 + u_{i,t}^4 - u_{i,t}^5 + u_{i,t}^6 - u_{i,t+1}^4 + u_{i,t+1}^5 + \Gamma_{l,i}^U \cdot \left(u_{i,t}^8 - u_{i,t}^9 \right) \leq 0, \quad t < T \quad (2.30)$$

$$p_{i,T} : -u_{i,T}^3 + u_{i,T}^4 - u_{i,T}^5 + u_T^6 + \Gamma_{l,i}^U \cdot (u_{i,T}^8 - u_{i,T}^9) \leq 0 \quad (2.31)$$

$$C_{i,t}^{Noload} : u_{i,t}^7 \leq 1 \quad (2.32)$$

$$wp_{w,t} : u_t^6 + u_{w,t}^8 + \sum_{l=1}^L \Gamma_{l,w}^W \cdot u_{l,t}^9 - \sum_{l=1}^L \Gamma_{l,w}^W \cdot u_{l,t}^{10} \leq 0 \quad (2.33)$$

$$ws_{w,t} : u_{w,t}^8 \leq M \quad (2.34)$$

$$\sum_{w=1}^W \frac{|wg_{w,t} - wf_{w,t}|}{\Delta w_{w,t}} \leq \Gamma_t \quad (2.35)$$

$$wf_{w,t} - \Delta w_{w,t} \leq wg_{w,t} \leq wf_{w,t} + \Delta w_{w,t} \quad (2.36)$$

Due to the bilinear term $u_{w,t}^8 \cdot wg_{w,t}$ in the objective function (2.28), the above problem is NP-hard and an efficient ways to solve this problem is still under research. In Zhao and Zeng [51], Xiong and Jirutitijaroen [52] and An and Zeng [53], a column-and-constraint generation method has been used to solve the sub-problem. Jiang et al. [54] use a Monte-Carlo sampling method to find the worst wind scenario. Bertsimas et al. [55] use an outer approach method in the sub-problem to linearize the bilinear part. In our comparison, the outer approach method is adopted to find the worst wind scenario.

- OUTER APPROACH MASTER PROBLEM

$$\begin{aligned} \max_{wg_{w,t}, u} Zu = & \sum_{i=1, t=1}^{I, T} \left(u_{i,t}^1 \cdot \hat{x}_{i,t} \cdot \underline{P}_i - u_{i,t}^2 \cdot \hat{x}_{i,t} \cdot \bar{P}_i - u_{i,t}^4 \cdot \underline{\Delta}_i - u_{i,t}^5 \cdot \bar{\Delta}_i \right) + \sum_{i=1}^I \left(u_{i,t_0}^4 \cdot p_{i,0} - u_{i,t_0}^5 \cdot p_{i,0} \right) \\ & + \sum_{t=1}^T u_t^6 \cdot D_t + \sum_{i=1, t=1}^{I, T} u_{i,t}^7 \cdot NL_i \cdot \hat{x}_{i,t} \\ & + \sum_{l=1, t=1}^{L, T} u_{l,t}^9 \cdot \left(-\bar{F}_l + \sum_{s=1}^S \Gamma_{l,s}^D \cdot D_{s,t} \right) + \sum_{l=1, t=1}^{L, T} u_{l,t}^{10} \cdot \left(-\bar{F}_l - \sum_{s=1}^S \Gamma_{l,s}^D \cdot D_{s,t} \right) \\ & + \beta \end{aligned} \quad (2.38)$$

Subject to: (2.24)-(2.25), (2.29)-(2.34)

$$\beta \leq - \sum_{t=1, w=1}^{T,W} \left(\hat{u}_t^8 \cdot \hat{w} g_{w,t}^w + \hat{u}_t^8 \cdot (w g_{w,t}^w - \hat{w} g_{w,t}^w) + (u_t^8 - \hat{u}_t^8) \cdot \hat{w} g_{w,t}^w \right) \quad (2.39)$$

In the outer approach (OA, thereafter) master problem, the bilinear part of objective function is linearized.

- OUTER APPROACH SUB-PROBLEM

$$\begin{aligned} \max_{w, g_{w,t}, u} Zu = & \sum_{i=1, t=1}^{I,T} \left(u_{i,t}^1 \cdot \hat{x}_{i,t} \cdot \bar{P}_i - u_{i,t}^2 \cdot \hat{x}_{i,t} \cdot \bar{P}_i - u_{i,t}^4 \cdot \Delta_i - u_{i,t}^5 \cdot \bar{\Delta}_i \right) + \sum_{i=1}^I \left(u_{i,t_0}^4 \cdot p_{i,0} - u_{i,t_0}^5 \cdot p_{i,0} \right) \\ & + \sum_{t=1}^T u_t^6 \cdot D_t + \sum_{i=1, t=1}^{I,T} u_{i,t}^7 \cdot NL_i \cdot \hat{x}_{i,t} - \sum_{w=1}^W u_{w,t}^8 \cdot \hat{w} g_{w,t} \\ & + \sum_{l=1, t=1}^{L,T} u_{l,t}^9 \cdot \left(-\bar{F}_l + \sum_{s=1}^S \Gamma_{l,s}^D \cdot D_{s,t} \right) + \sum_{l=1, t=1}^{L,T} u_{l,t}^{10} \cdot \left(-\bar{F}_l - \sum_{s=1}^S \Gamma_{l,s}^D \cdot D_{s,t} \right) \end{aligned} \quad (2.37)$$

Subject to (2.29)-(2.34)

The OA sub-problem solves an economic dispatch problem in its dual form given a wind realization scenario. During the OA iteration, the sub-problem solves an economic dispatch problem for a given wind realization, and the master problem updates the wind scenario within the defined uncertainty set for a better objective value. The whole process is repeated until the results of the outer approach sub-problem and of the master problem are equal. Figure 2.3 shows the iteration process as illustrated in Bertsimas et al. [55]:

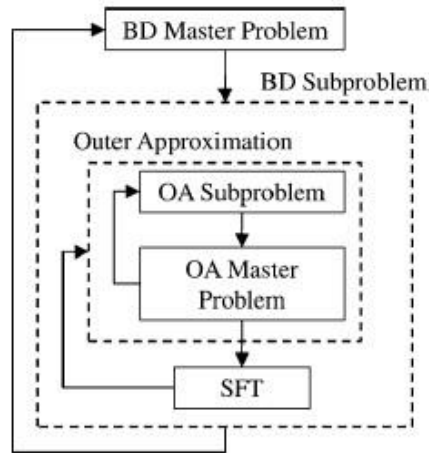


Figure 2.3. Robust optimization and OA Solving Process

The robust optimization unit commitment model minimizes the total system cost under the worst-case wind scenarios, and guarantees the feasibility of all wind realization scenarios within the defined uncertainty set. However, this model has drawbacks:

1. *Computation Time*

Due to the special structure of the robust optimization unit commitment model, it can only be solved using a decomposition method. It may take a number of iterations for the problem to converge in some cases. Several heuristics have been suggested to improve the solution efficiency, such as adding some economic dispatch constraints to the Benders' master problem as mentioned by Bertsimas et al. [55], or by making a good estimation of the possible worst wind scenario as suggested by Zhao and Guan [56].

2. *Worst-case Wind Scenario*

As mentioned above the bi-linear term in the Benders' sub-problem makes it hard to guarantee a global optimal solution when searching for the worst-case wind scenario, especially when there are many wind farms in the system. The search for the worst-case wind

scenarios has become an independent research topic in the literature [51-55].

3. *Uncertainty Budget*

Unlike the interval optimization unit commitment model which can be really conservative in some cases, the conservativeness of the robust optimization model can be adjusted by changing the uncertainty budget. However, there is no strict rule on how to set this uncertainty budget, and historical information may be needed to get the right setting.

2.6 OTHER DAY-AHEAD OPTIMIZATION METHODS AND TRENDS

Beside the three optimization techniques discussed above, other day-ahead unit commitment optimization methods dealing with uncertainty are discussed in the literature. These include rolling optimization (Tuohy et al. [57], Madaeni and Sioshansi [58] and Qiu et al. [59]), robust min-max regret optimization (Jiang et al. [60]), and the combined optimization methods (Zhao and Guan [56] and [61-63]).

- ROLLING OPTIMIZATION

Rolling optimization is one way of dealing with wind power output uncertainty by using a more accurate wind forecast. This can be realized by reducing the forecast time period. Madaeni and Sioshansi [58] propose a way of rolling scheduling (optimization) that makes full use of wind data updates. In the rolling optimization, the day-ahead unit commitment problem is solved first using the original wind forecast information. In the economic dispatch period, economic dispatch problem is solved every 15 minutes using the updated wind forecast.

- MIN-MAX REGRET OPTIMIZATION

In practice, it is unlikely to have a zero-error wind forecast on the day ahead. There will therefore always be an adjustment cost associated with errors in the wind forecast. To protect the system against the worst possible adjustments in real-time, Jiang et al. [60] propose a robust min-max regret optimization unit commitment. Min-max regret optimization has the same structure as robust optimization except for the objective function. The former aims at protecting the system against the worst wind realization in real-time, while the latter protects the system against the worst real-time wind change from that forecast on the day ahead.

- COMBINATIONS OF DIFFERENT OPTIMIZATION METHODS

As discussed above, each optimization model has its own advantages and disadvantages, and their performance is highly dependent on the case and the setting of the optimization parameters. More and more research has focused on the combinations of different optimization methods. The combination of stochastic and chance constrained optimization is discussed by Wu et al. [61] [62]. Zhao and Guan [60] propose a combination of stochastic optimization and robust optimization in day-ahead unit commitment. By adjusting the weight of the two different objective functions, they control the conservativeness of the model. A combination of stochastic and interval optimization described by Dvorkin et al. [63] reduces the computing time. The conservativeness of the solution can be optimized by choosing a good switching time between the two methods.

2.7 TEST SYSTEM AND RESULTS

Tests were carried out on a modified version of the IEEE-RTS 24 bus system. Full system data can be downloaded from [64]. The wind power profile used are from NREL's Eastern

interconnection wind integration study [65]. Four wind farms with capacities of 112MW, 138.4MW, 243.8MW and 223.2MW are located at bus 2, bus 18, bus 21 and bus 23 of the original system.

The Eastern interconnection study year 2006 observed data are used for testing, and the history (2004-2005) forecast and observed data and 2006 forecast data are used to generate 11 scenarios for stochastic optimization and bounds for interval and robust optimization.

Other important testing parameters include:

- For the robust optimization, the uncertainty budget is set to be $1.5\sqrt{W} = 3$.
- The gap of the Benders master problem is 0.5% and the convergence gap is $1e-4$. The outer-approach inner convergence gap is $1e-5$.
- For the robust optimization, the economic dispatch constraints of the average wind forecast are added into the master problem to predict the worst-case scenario and accelerate the convergence.
- The optimization gap for both the interval and stochastic day-ahead optimization is set to 0.5%.
- The wind curtailment penalty is \$20/MWh and load curtailment penalty is \$5000/MWh.
- The system transmission capacity is reduced to 80% of its original value.

1. Day-ahead unit commitment solution time

The size and structure of the day-ahead optimization are the main factors that affect the solution time of the model. Robust optimization has the smallest problem size, while the stochastic optimization has the largest size because it considers more scenarios. However, the robust optimization can only be solved using a decomposition method, and the search for the worst-case scenario is not easy. Many heuristics have been proposed in the literature to help accelerate the

speed of the search and the overall convergence rate. This makes the solution time quite unstable. Figure 2.1 is a scatter plot of the solution time of the day-ahead unit commitment. It illustrates this observation about the effect of these heuristics.

The left part of Figure 2.4 (a) shows the whole data set. In the plot on the right side of Figure 2.4(b) the extreme points of the robust optimization have been eliminated. We can see from the 2.4(a) that there are days when it may take an extremely long time to find the worst-case wind scenario. However, for most of the days, the solution time is shorter than for the interval and stochastic optimizations.

As stochastic optimization formulation has the largest problem size, we observe longer solution time compared with both interval and robust optimization in Figure 2.4(b).

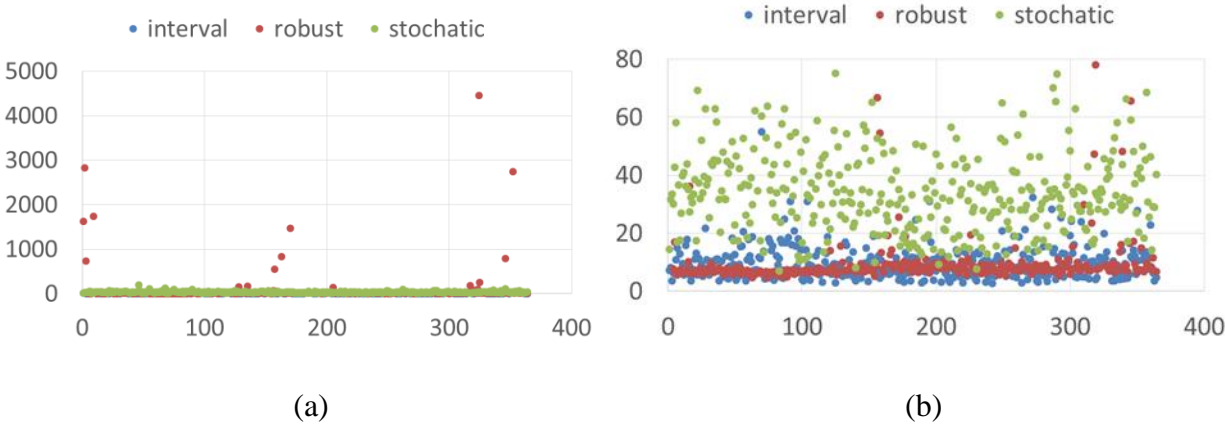


Figure 2.4. Scatter Plot of Day-ahead Unit Commitment Solution Time

The CDF plot in figure 2.5 provides a more straightforward comparison of these three optimization methods in terms of solution time. For a better comparison, the extreme points in robust optimization method have been removed from the figure. We can see from Figure 2.5 that the solution time is no more than 20 seconds for over 95% of the days. If stochastic optimization

is applied, the solution time is no more 20 seconds than only 10% of the days. Figure 2.5 also shows that the solution time of the robust optimization is not always shorter than the solution time of the interval optimization problem due to the heuristics used to search for the worst-case wind scenario.

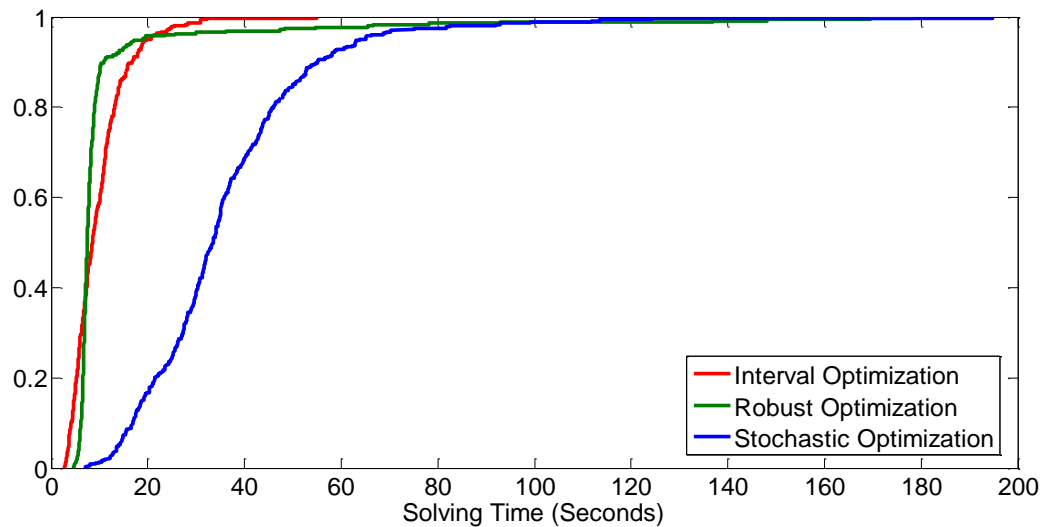


Figure 2.5. CDF Plot of Day-ahead Unit Commitment Solution Time

2. Total Cost in Real-time

The real-time total cost includes both the start-up and dispatch costs. Since the generator on-off status is optimized on the day-ahead and cannot be changed in real-time, the start-up cost is determined by the day-ahead unit commitment. The day-ahead scheduled generator output can be adjusted in real-time, so the dispatch cost is determined by the real-time wind and load realizations. As the three optimization methods are aimed at different objectives, their distributions of real-time total cost are different as shown in Figures 2.6, 2.7 and 2.8.

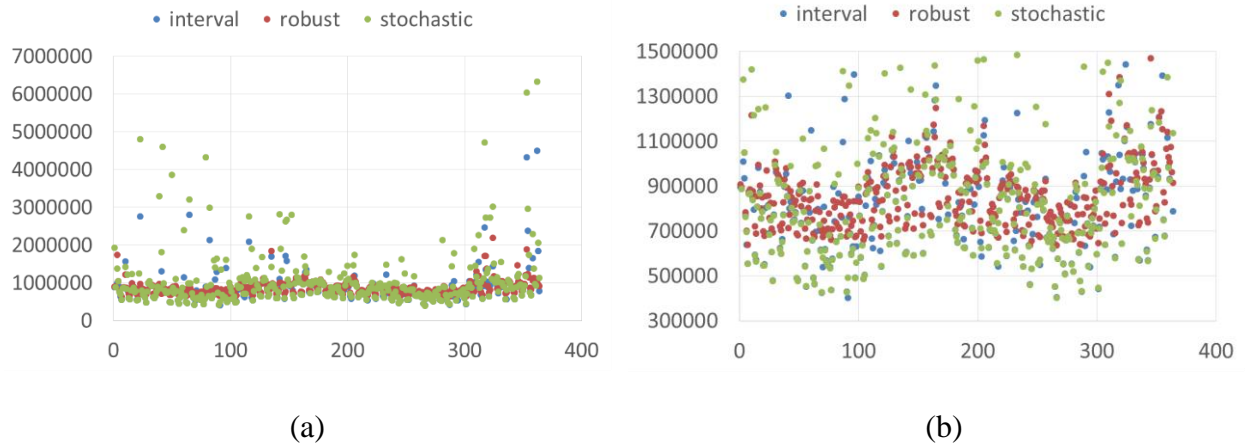


Figure 2.6. Scatter Plot of Real-time Cost

Figure 2.6 is a scatter plot of the real-time total cost. Figure 2.6 (a) shows the whole data set. In Figure 2.6(b) the extreme points of the stochastic optimization have been removed. We can see from Figure 2.6 (a) that there are more days when the total real-time cost is high when using stochastic optimization, which means that there is more wind or load curtailment on these days. These extreme situations happen less frequently when using interval optimization. And there are rarely extreme situations when using robust optimization.

Figure 2.6 (b) shows that despite the more extreme days resulting from the stochastic optimization, the total real-time cost is much less using stochastic optimization than with the other two optimization methods on days when the wind realization is close to the day-ahead forecasted wind scenario compared.

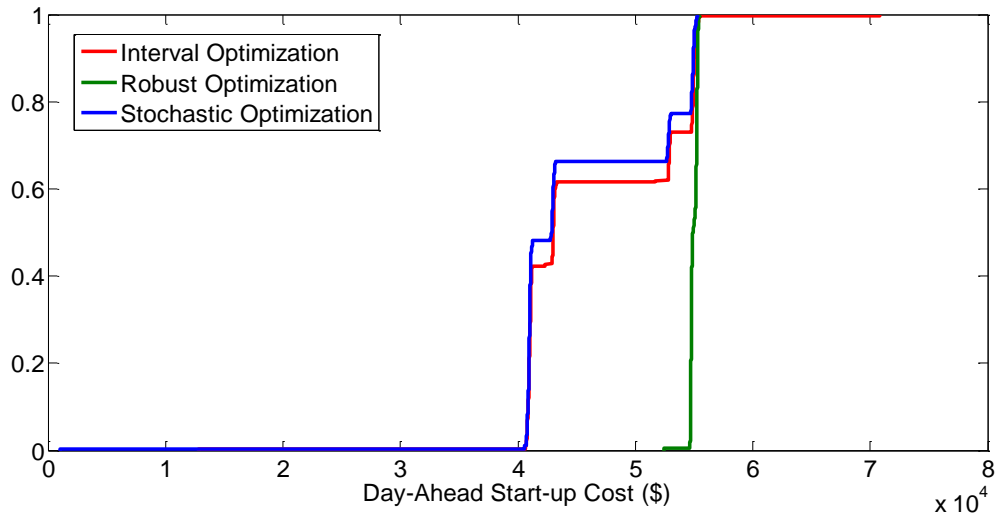


Figure 2.7. CDF Plot of Day-Ahead Start-up Cost

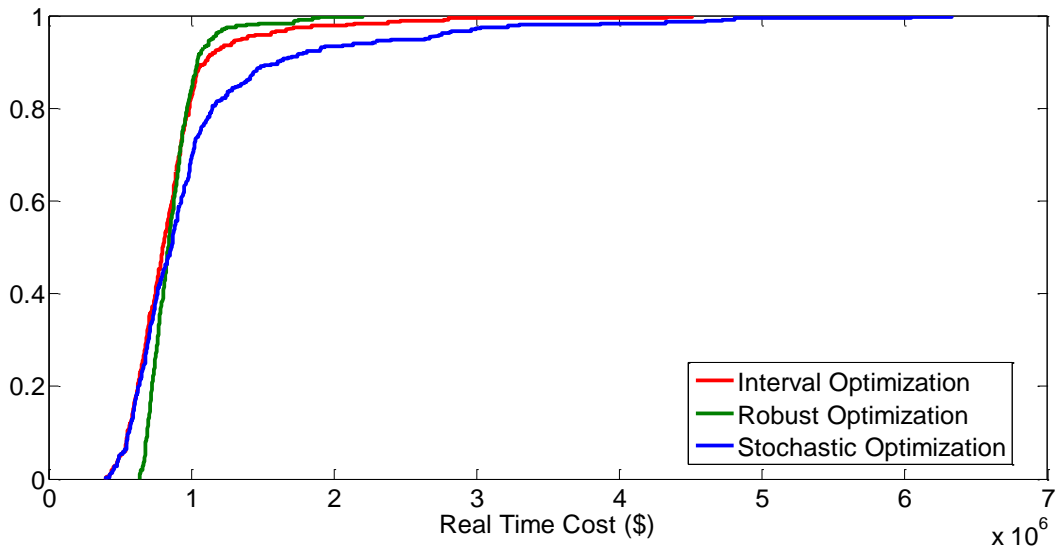


Figure 2.8. CDF Plot of Real-time Cost

The CDF plots in Figures 2.7 and 2.8 provide a more straightforward comparison of the three different optimization methods in terms of day-ahead start-up and total real-time costs. Even though the day-ahead start-up cost is likely to be highest using robust optimization (as shown by Figure 2.7), we can see from Figure 2.8 that the total real-time cost is no more than \$1,000,000 for

about 95% of the days when using robust optimization. That percentile is slightly less when using interval optimization and drops to about 70% when using stochastic optimization.

As robust optimization is aimed at minimizing the cost under the worst-case wind scenario, the tail of its CDF plot is much shorter as shown in Figure 2.8, which in turn makes the costs under preferable wind scenarios bigger than with the other two methods. Interval optimization and stochastic optimization aim to minimize the cost under average forecast and the expected cost under all forecast instead. Therefore, their CDF has a longer tail, which means that high real-time cost are likely to happen occasionally using these two methods. However, interval and stochastic optimization have better performance on days when the day-ahead forecast does not deviate significantly from the real-time wind realization.

2.8 SUMMARY

In this chapter, we investigated the various optimization techniques used to solve the day-ahead unit commitment under wind generation uncertainty. Special attention was given to stochastic, interval and robust optimization. The IEEE RTS and the NREL Eastern wind data were used to test and compare their performance. In summary, each of the three main optimization method has its own advantages and disadvantages in terms of both computing time and real-time performance.

- Robust optimization has a relatively smaller problem size, and the solution efficiency can be quite high if there is fast way to find the worst-case wind scenario. Since the size of the interval optimization problem is fixed, its solution time depends only on the different cases. Even though the problem size is largest for the stochastic optimization method, the solution efficiency can be improved significantly using advanced forecast and scenarios reduction techniques.

- The real-time performance of the three optimization models is highly dependent on the wind forecast and the parameter settings. In cases of high uncertainty, robust optimization could greatly reduce the probability of incurring an extremely high real-time cost if an adequate uncertainty budget is chosen. When the day-ahead forecast is accurate, stochastic optimization, or tighter wind generation bounds and a smaller uncertainty budget in interval and robust optimization may be a better option.

Chapter 3. STOCHASTIC MULTI-STAGE CO-PLANNING OF TRANSMISSION EXPANSION AND ENERGY STORAGE

3.1 INTRODUCTION

Generation and transmission system planning have been extensively studied in the literature. Hemmati et al. [66] provide a comprehensive review of the topic while Munoz et al. [67] as well as Martinez Cesena et al. [68] discuss recent progress. With the development of battery technologies, the combined operation and planning of storage devices with other power system resources is drawing increasing attention. Zach and Auer [69] point out that energy storage and transmission investments increase system flexibility but that cost/benefit analyses are needed to determine which measures are preferable.

Various studies [70-76] focus on the planning of energy storage systems alone in power systems. Oh [70] uses a DCOPF model and a limited number of time periods per year to make the problem of siting and sizing storage units tractable. A full unit commitment model is used in Pandzic et al. [71] to determine both the optimal sizes and sites for energy storage using wind and load profile over a whole year, and some heuristics are introduced to limit the problem size. Other authors [72-74] focus on the size of energy storage without considering the effects of the transmission network. The statistical properties of renewable generation are used in Liu et al. [72], and the power spectrum density of deviations of renewable generation from forecasts is applied in Li et al. [73]. Bayram et al. [74] developed a stochastic analytical framework to determine the proper size of energy storage and conducted a benefit/cost analysis to evaluate storage investments.

Co-planning of energy storage and transmission systems is addressed in [75-78]. Hu et al. [75] solve a MILP problem iteratively to determine the ESS investment size and locations by replacing

part of the transmission investment while satisfying the same system requirement. Zhang et al. [76] propose a MILP model to determine the size and location of a single energy storage unit to minimize both the operation and investment costs taking line losses into account. Hedayati et al. [77] and Konstantelos et al. [78] propose multi-stage co-planning models to determine the location of a given size energy storage that minimizes the one-time investment cost and the long-term operation cost. A DCOPF based deterministic planning model is used in Hedayati et al. [77], while a SCOPF based stochastic planning framework is used by Konstantelos et al. [78], who take into account N-1 security criteria as well as the uncertainty on the long-term wind capacity.

As the size of the planning model tends to be large, the computing burden can be tremendous when the planning horizon is long or the model accuracy is high. Researchers either choose a shorter planning horizon or simplify the UC(ED) operation model to make the problem tractable. To overcome the above mentioned limitations, this chapter describes a more accurate technique for co-planning the multi-stage expansion of transmission capacity and the deployment of battery energy storage systems (BESS). Its contributions can be summarized as follows:

- a. It models the degradation in energy storage capacity due to shelf life and charge/discharge cycles, which have been ignored in all the other BESS planning models.
- b. It accounts for the delays associated with the planning and construction of transmission lines.
- c. It incorporates a unit commitment with reserve requirements to represent accurately the operation of the system.
- d. It optimizes both the size and the location of investments in energy storage at each year of the horizon.
- e. It implements a stochastic optimization to take into account the effect of uncertainty on load as well as renewable generation.

The remainder of this chapter is organized as follows: Section 3.2 describes the modeling assumptions while Section 3.3 provides the detailed mathematical formulation of the optimization problem. Section 3.4 describes the test system. Section 3.5 presents the results of the optimization and of the sensitivity analysis. Section 3.6 concludes.

3.2 MODELING

Multi-stage planning problems can easily get very large. Careful choices about modeling assumptions must therefore be made to achieve a balance between the accuracy of the results and the computing time.

- BATTERY ENERGY STORAGE SYSTEMS

The calendar life of a battery as well as the charge and discharge cycles it has undergone affect its energy capacity. A number of papers (e.g. [79-81]) offer detailed and accurate models of battery degradation. However, because these models are non-linear and involve multiple variables and non-linearities, the computational burden that they would impose on a planning study is not acceptable. In our study, we assume instead a flat degradation rate of 94%, which means that 6% of the energy capacity is lost each year, 3% of which is due to calendar aging and 3% to utilization.

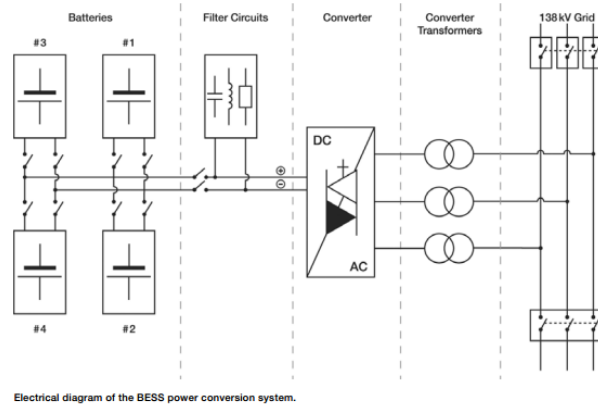


Figure 3.1. BESS Investment Unit [29]

Energy storage planning techniques described in the literature (e.g. [77-78]) typically determine the optimal location for storage unit of a given size and for a one-time investment. This is a rather restrictive assumption as storage lends itself to incremental investments over time at the same location. Instead, as shown in Figure 3.1, we assume that BESS units can be added over time at each location, providing a variable power/energy capacity ratio. Each BESS unit is retired independently when it reaches the end of its useful life.

- SYSTEM OPERATION

Enhancing the fidelity of the modeling of system operation increases the numbers of variables and constraints. In a planning model, these numbers increase further as the number of years considered as part of the planning horizon is extended. Different strategies have been used to streamline the operation model. Most planning models ignore or simplify the Unit Commitment (UC) decisions and constraints or use very broad time periods. Konstantelos and Strbac [78] removed all time coupling constraints (such as the ramp rate limits on the generators), and considered a 15-year planning horizon with a 5-year epoch. Hedayati et al. [77] ignore the

uncertainty on future wind generation and load and consider an 8-year horizon with a 4-year epoch. These assumptions have serious drawbacks. First, it is impossible to know all the committed units in advance under the current market structure and it is quite unlikely that all the peaking units will be online at all times. The contribution of storage in dealing with the uncertainty in renewable generation and in reducing the number of start-ups of peaking units would therefore be undervalued. Second, because the available capacity of an energy storage system is likely to fade substantially over a 5- or 8-year timeframe, using such a long planning epoch could lead to inaccurate planning decisions.

Our study adopts a 25-year planning horizon with a 1-year epoch. To reduce the number of binary variables used to reflect the generators' status, all generators are divided into two types: those that are assumed to be always committed and those that are free, i.e. which can start up or shut down at any time. In other words, slow and fast generators. Two methods can be used to divide the generators into these two types. We can run a 24-hour unit commitment for 25 years and assign the generators that are committed more often than a given threshold to the slow category while the others are considered free. Alternatively, generators with a one-hour minimum up/down time can be assumed to be fast generators, while the remaining ones are assigned to the slow category. Testing showed that the two techniques produce very similar results.

- **LOAD AND WIND GENERATION CAPACITY SCENARIOS**

To reduce the risk of stranded assets, investments in transmission or storage capacity should be robust with respects to errors in the long-term evolution of the load and the renewable generation capacity. The proposed optimal co-planning approach therefore considers 3 scenarios that combine the load and wind generation uncertainty. Figure 3.2 illustrates these scenarios.

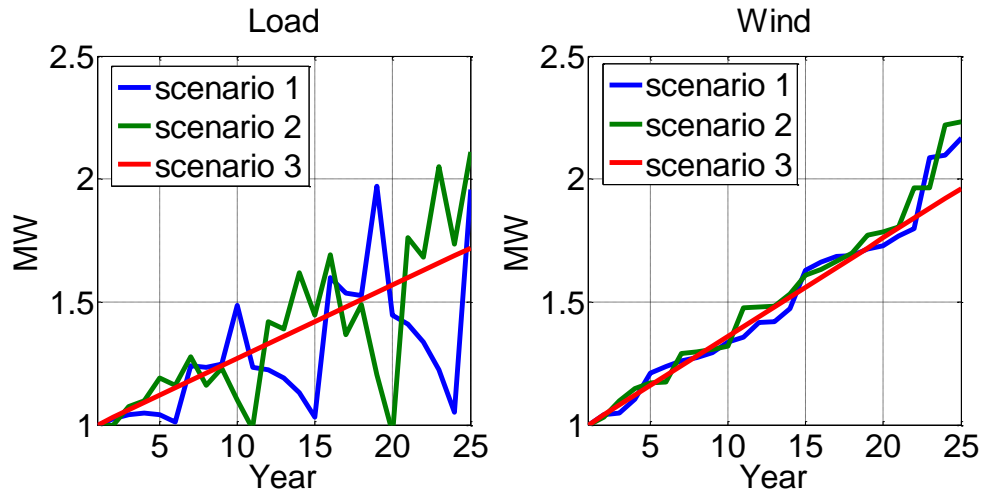


Figure 3.2. Load and Wind generation capacity scenarios

- RESERVE REQUIREMENT

Most planning models do not consider the need to provide operating reserve. As the proportion of stochastic renewable generation increases, this simplification becomes untenable. The proposed model considers the reserve constraint in the unit commitment and uses the 3+5 rule to specify the amount of operating reserve, which means that the reserve required is equal to 3% of the forecast load prediction plus 5% of the forecast wind generation [2, 83]. The amount of reserve provided by BESS follows the model described by Hu et al. [84]. This model is explained in detail later in this chapter.

- LOCATIONS FOR BESS AND ADDITIONAL TRANSMISSION CAPACITY

Limiting the number of locations where BESS could be installed and the number of transmission lines that could be upgraded significantly reduces the computational burden. To determine a good set of likely candidates, a planning problem with a 1-year horizon was run to determine the best

locations for each of the 25 years in the actual horizon. Locations where this short-term planning problem frequently installed BESS were selected as candidates for the long-term planning problem. Lines where the power flow frequently exceeded 55% of their rating were considered for a capacity upgrade.

- REPRESENTATIVE DAYS

In long-term planning, considering a whole year of operation is unnecessary and makes the problem intractable. When integrating renewables, the shape of net load could be quite different from that of the original one due to the increasing renewable capacity. Thus, 5 days are selected to represent typical wind generation and load profiles for each year based on how the daily wind is changing with daily load. The correlation coefficient of daily load and wind is calculated, and net load profiles are clustered into 5 groups using the K-means method. The profile which is closest to the centroid of each group is selected as a representative day of that group. Since these 5 days are usually not consecutive, the initial ramp constraints are relaxed.

3.3 FORMULATION OF THE PLANNING PROBLEM

- NOTATIONS

Sets and Indices:

y : $(1 \cdots Y)$ - Index to the study year

Parameters:

τ : Number of days represented by each typical day in a year

r : Discount rate

ST : Life time of a BESS

LT : Life time of a transmission line

$k_{i,b}$: Marginal cost of a segment of generator cost curve

C^e : Cost per MWh of a BESS

C^p : Cost per MW of a BESS

C^l : Cost per MW of capacity of a transmission line

k^e : Annualized cost per MWh of a BESS

k^p : Annualized cost per MW of a BESS

k^l : Annualized cost per MW of a transmission line

δt : Spinning reserve response time

$\eta_s^{dis}, \eta_s^{ch}$: Storage device discharge and charge efficiency

E_s^{\min} : Minimum energy capacity of a BESS

$wf_{w,t}^y$: Wind forecast

$D_{s,t}^y$: Load forecast

$M_{i,s}^G$: Mapping of generators to nodes

$M_{w,s}^W$: Mapping of wind farms to nodes

$M_{l,s}^L$: Line connection

B_{ms} : B Matrix for DC power flow calculation

r_s : Energy capacity degradation factor of energy storage

k_{cal} : Calendar ageing rate

k_{cycle} : Cycling ageing rate

Binary variables:

$x_{i,t}^y$: Generator status, 1- online, 0 - offline

$I_{l,y}$: Line decision, 1- start construction, 0 - no construction

$Z_{l,y}$: New line status, 1- in service, 0 - not in service

Variables

C_y : Discounted annual operation cost

$C_{t,i}^{operation}$: Hourly unit operation cost

S_INV_y : Discounted annual storage investment cost

L_INV_y : Discounted annual line investment cost

$P_{i,b,t}^y$: Generation on each segment of the cost curve

$P_{i,t}^y$: Total generation of each generator

$ch_{s,t}^y$: Charging power of a BESS

$dis_{s,t}^y$: Discharging power of a BESS

$SoC_{s,t}^y$: State of charge of a BESS

$\theta_{s,t}^y$: Bus voltage angle

$f_{l,t}^y$: Power flow on an existing line

$Nf_{l,t}^y$: Power flow on a new line

$rg_{i,t}^y$: Reserve provided by a generator

$re_{s,t}^y$: Reserve provided by a BESS

$E_{s,y}$: Investment in energy capacity for a year

$Pe_{s,y}$: Investment in power capacity for a year

$APe_{s,y}$: Available power capacity by the end of a year

$AE_{s,y}$: Available energy capacity by the end of a year

- OBJECTIVE FUNCTION

For clarity of exposition, the equations below define the deterministic long-term planning problem. The stochastic optimization planning model can be easily obtained by adding one more dimension into the operation variable and related constraints, and detailed formulations follow the same structure as that shown in Chapter 2. Equation (3.1) shows that the long-term planning problem aims to minimize the sum of the operating cost over the horizon:

$$\min_{p_{i,t}, x_{i,t}, Pe_{s,y}, E_{s,y}, I_{l,y}} \sum_{y=1}^Y C_y + S_IN Y_y + L_IN Y_y \quad (3.1)$$

Equation (3.2) gives the discounted operating cost over the planning horizon. The penalty term discourages wind curtailments (at 20\$/MWh) and load curtailments (at 5000 \$/MWh).

$$C_y = \frac{\tau \cdot \left(\sum_{t=1}^T \sum_{i=1}^I C_{t,i}^{operation} + penalty \right)}{(1+r)^{y-1}} \quad (3.2)$$

$$C_{t,i}^{operation} = \sum_{b=1}^{NB} p_{i,b,t}^y \cdot k_{i,b} + NL_i + SU_i \cdot x_{i,t}^y \quad (3.2a)$$

Equation (3.3) gives the discounted BESS investment cost for each year. Equations (3.3a) and (3.3b) give the annualized BESS energy and power capacity cost while (3.3c) gives the annual

discount factor needed to ensure that all costs are to be paid off within the BESS life time.

$$S_INV_y = \sum_{n=1}^y \alpha_{y-n+1} \cdot \sum_{s=1}^S (k^e \cdot E_{s,n}^{\max} + k^p \cdot P_{s,n}^{\max})$$

(3.3)

$$k^e = C^E \cdot \frac{r(1+r)^{ST}}{(1+r)^{ST} - 1} \quad (\$/MWh \cdot Year) \quad (3.3a)$$

$$k^p = C^p \cdot \frac{r(1+r)^{ST}}{(1+r)^{ST} - 1} \quad (3.3b)$$

$$\alpha_n = \begin{cases} \frac{1}{(1+r)^{n-1}} & n \leq ST \\ 0 & n \geq ST + 1 \end{cases} \quad (3.3c)$$

Equation (3.4) gives the discounted transmission line investment cost for each year. An annual payment is assumed to be made each year after the investment decision is made. Equation (3.4a) gives the annualized line capacity cost while Equation (3.4b) gives the annual discount factor needed to ensure that the cost of the line is paid off over the line's life time.

$$L_INV_y = \sum_{n=1}^y \beta_{y-n+1} \cdot \sum_{l=1}^L k^l \cdot I_{l,n} \quad (3.4)$$

$$k^l = C^L \cdot \frac{r(1+r)^{LT}}{(1+r)^{LT} - 1} \quad (\$/Year) \quad (3.4a)$$

$$\beta_n = \begin{cases} \frac{1}{(1+r)^{n-1}} & n \leq LT \\ 0 & n \geq LT + 1 \end{cases} \quad (3.4b)$$

- GENERATOR CONSTRAINTS

Equations (3.5) to (3.8) describe the constraints on minimum and maximum generation capacity and maximum ramping.

$$p_{i,t}^y = \sum_{b=1}^{NB} p_{i,b,t}^y \cdot x_{i,t}^y \quad (3.5)$$

$$p_{i,t}^y \geq \underline{p}_i \cdot x_{i,t}^y \quad (3.6)$$

$$p_{i,b,t}^y \leq \bar{p}_{i,b} \cdot x_{i,t}^y \quad (3.7)$$

$$|p_{i,t}^y - p_{i,t-1}^y| \leq \Delta_i \quad (3.8)$$

- RESERVE CONSTRAINTS

Equations (3.9) and (3.10) determine the amount of reserve that each generator can provide:

$$p_{i,t}^y + rg_{i,t}^y \leq \bar{p}_i \cdot x_{i,t}^y \quad (3.9)$$

$$rg_{i,t}^y \leq \Delta_i \cdot \delta t \cdot x_{i,t}^y \quad (3.10)$$

- ENERGY STORAGE CONSTRAINTS

Equation (3.11) keeps track of the state of charge of each BESS while Equations (3.12) to (3.14) enforce their energy and power capacity limits. Equations (3.15) and (3.16) determine the amount of reserve that each BESS can provide:

$$SoC_{s,t}^y = SoC_{s,t-1}^y + ch_{s,t}^y - dis_{s,t}^y \quad (3.11)$$

$$E_{s,y}^{\min} \leq SoC_{s,t}^y \leq AE_{s,y} \quad (3.12)$$

$$ch_{s,t}^y \leq APe_{s,y} \quad (3.13)$$

$$dis_{s,t}^y \leq APe_{s,y} \quad (3.14)$$

$$0 \leq re_{s,t}^y + dis_{s,t}^y - ch_{s,t}^y \leq Pe_s^{\max} \quad (3.15)$$

$$E_s^{\min} \leq SoC_{s,t}^y - \frac{(re_{s,t}^y - ch_{s,t}^y)}{\eta_s^{ch}} \cdot \delta t \quad (3.16)$$

- POWER BALANCE CONSTRAINTS

Equation (3.17) enforces the system power balance at each node. Equation (3.18) limits the wind generation to the available wind power, which is assumed to be equal to the forecast:

$$\begin{aligned} & \sum_{i=1}^I p_{i,t}^y \cdot M_{i,s}^G - \sum_{w=1}^W wp_{w,t}^y \cdot M_{w,s}^W - \sum_{l=1}^L (f_{l,t}^y + Nf_{l,t}^y) \cdot M_{l,s}^L \\ & = D_{s,t}^y + \sum_{t=1}^{24} \left(\frac{ch_{s,t}^y}{\eta_s^{ch}} + dis_{s,t}^y \cdot \eta_s^{dis} \right) \end{aligned} \quad (3.17)$$

$$wp_{w,t}^y + ws_{w,t}^y = wf_{w,t}^y \quad (3.18)$$

- RESERVE REQUIREMENT

Equation (3.19) defines the 3+5 reserve requirement [2, 83], i.e. the total reserve should be no less than 3% of the forecasted load plus 5% of the forecasted wind power.

$$\sum_{i=1}^I rg_{i,t}^y + \sum_{s=1}^S re_{s,t}^y \geq 0.03 \cdot \sum_{s=1}^S D_{s,t}^y + 0.05 \cdot \sum_{w=1}^W wf_{w,t}^y \quad (3.19)$$

- LINE FLOWS AND TRANSMISSION CAPACITY

Equation (3.20) calculates the lines flows using a DC power flow. Equations (3.21) and (3.22) implement the line flow constraints.

$$f_{l,t}^y = B_{ms} (\theta_{m,t}^y - \theta_{s,t}^y) \quad (3.20)$$

$$-\bar{F}_{l,t} \leq f_{l,t}^y \leq \bar{F}_{l,t} \quad (3.21)$$

$$-\pi \leq \theta_{s,t}^y \leq \pi \quad (3.22)$$

- STORAGE PLANNING

Equation (3.23) gives the available BESS energy capacity for each year considering degradation. Equations (3.23a) and (3.23b) calculate the capacity factor at each year by combining the calendar aging and the aging caused by cycling. The energy capacity of a BESS is assumed to be zero once it reaches the end of its life.

$$AE_{s,y} = \sum_{t_0=1}^y a_{y-t_0+1} \cdot E_{s,t_0} \quad (3.23)$$

$$a_n = \begin{cases} 1 \cdot CF^{n-1} & n \leq ST \\ 0 & n \geq ST + 1 \end{cases} \quad (3.23a)$$

$$CF = 1 - k_{cal} - k_{cycle} \quad (3.23b)$$

Equation (3.24) gives the available power capacity of a BESS for each year. No degradation is assumed. Equation (3.24a) removes this power capacity once the BESS has reached the end of its life.

$$APE_{s,y} = \sum_{t_0=1}^y b_{y-t_0+1} \cdot Pe_{s,t_0} \quad (3.24)$$

$$b_n = \begin{cases} 1 & n \leq ST \\ 0 & n \geq ST + 1 \end{cases} \quad (3.24a)$$

Equations (3.25) and (3.26) are optional constraints that specify that a certain amount of available BESS in a certain year.

$$\sum_{s=1}^S AE_{s,Y} = AE^* \quad (3.25)$$

$$\sum_{s=1}^S APE_{s,Y} = APE^* \quad (3.26)$$

Equation (3.27) keeps the power/energy capacity ratio of each BESS within a technologically reasonable range:

$$0.25 \leq \frac{Pe_{s,y}}{E_{s,y}} \leq 8 \quad (3.27)$$

- LINE PLANNING AND OPERATION MODEL

Equation (3.28) enforces a construction delay of one year between the investment decision and the availability of an expanded transmission line. Equation (3.29) makes sure that once a transmission line is available, it remains available.

$$Z_{l,y} = \sum_{r=1}^{y-1} I_{l,r} \quad (3.28)$$

$$Z_{l,y} \geq Z_{l,y-1} \quad (3.29)$$

Equations (3.30) to (3.32) determine the flows on new transmission lines. The large number M prevents power from flowing in lines that have not yet been built [77].

$$Nf_{l,t}^y \geq B_{nm} (\theta_{m,t}^y - \theta_{n,t}^y) - (1 - Z_{l,y}) \cdot M \quad (3.30)$$

$$Nf_{l,t}^y \leq B_{nm} (\theta_{m,t}^y - \theta_{n,t}^y) + (1 - Z_{l,y}) \cdot M \quad (3.31)$$

$$-\bar{F}_{l,t} \cdot Z_{l,y} \leq Nf_{l,t}^y \leq \bar{F}_{l,t} \cdot Z_{l,y}$$

(3.32)

3.4 TEST SYSTEM

Tests were carried out on a modified version of the IEEE-RTS 24 bus system. Full system data can be downloaded from [64]. The wind power profile used are the same data from [64]. Only the three wind farms located at bus 20, 21 and 23 of subsystem I are selected with initial capacities 600MW, 300MW and 300MW. Wind energy generation accounts for 21.7% of the annual load at year 1. A line was added between buses 7 and 8 to make the system N-1 secure.

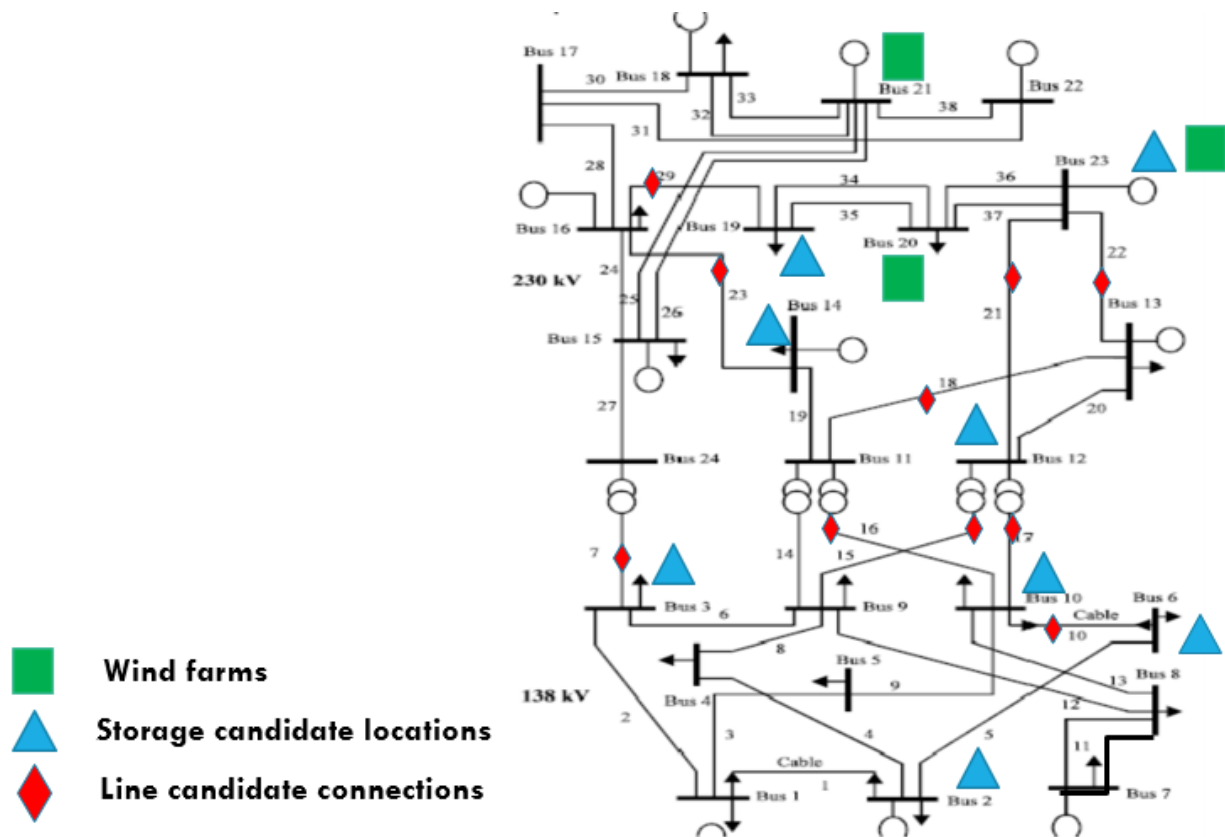


Figure 3.3. Test System Topology

Other important testing parameters include:

- Transmission capacity was reduced to 90% of its original value to increase congestion
- The cost of a BESS is assumed to be 500\$/kW plus 25\$/kWh, and its lifetime is 10 years
- The cost of building a line is assumed to be 927,000 \$, and lifetime 60 years [85]
- The discount rate was set at 5%.
- In the base case, the wind generation capacity increases by 4% per year and the load by 3%.
- Buses that are candidates for the installation of a BESS and lines that are candidates for transmission upgrades were selected using the technique described in Section 3.2E. Details are shown in Figure 3.3.

Table 3.1. Unit Category

Type	No	Min-Down (hr)	Min-Up (hr)	Committed Rate (%)	Category
1	15-19	1	2	0-30	Fast
2	1-2, 5-6	1	2	0-30	Fast
3	24-29	1	2	0-30	Fast
4	3-4, 7-8	2	3	100	Slow
5	9-11	2	4	100	Slow
6	20-21, 30-31	16	24	100	Slow
7	12-14	3	4	100	Slow
8	32	5	8	100	Slow
9	22-23	24	168	100	Slow

3.5 TEST RESULTS AND SENSITIVITY ANALYSIS

- CO-PLANNING VS. INDEPENDENT PLANNING

Using the base case settings, simulations for the three different planning models are carried out to compare the decisions under different planning methods: transmission expansion and ESS together co-planning, transmission expansion only and BESS only.

Table 3.2 shows that co-planning investments in transmission line and BESS capacity significantly reduces the number of lines that must be built.

Table 3.2. Investments in Transmission Line Capacity

	Upgraded lines	Line Capacity(MW)	Construction Start
Co-Planning	Line 21 (buses 12-23)	450	Year 09
Lines Only	Line 29 (buses 16-19)	450	Year 10
	Line 15 (buses 09-12)	360	Year 18
	Line 07 (buses 03-24)	360	Year 19
	Line 18 (buses 11-13)	450	Year 22

Similarly, Table 3.3 shows that co-planning the deployment of storage with upgrades in transmission line capacity results in the installation of BESS at fewer locations. However, Figure 3.4 shows that the total energy and storage capacities are installed at essentially the same rate, albeit at different locations. As illustrated by Figures 3.5 and 3.6, BESS capacity investments shift from buses at or near wind generation (e.g. buses 14 and 23) to buses close to the load centers (bus 03) to reduce the more expensive load curtailment.

Table 3.3. BESS Investment Location

	BESS Locations
Co-Planning	Bus 3, 6, 10, 12, 19
BESS Only	Bus 3, 6, 10, 12, 14, 19, 23

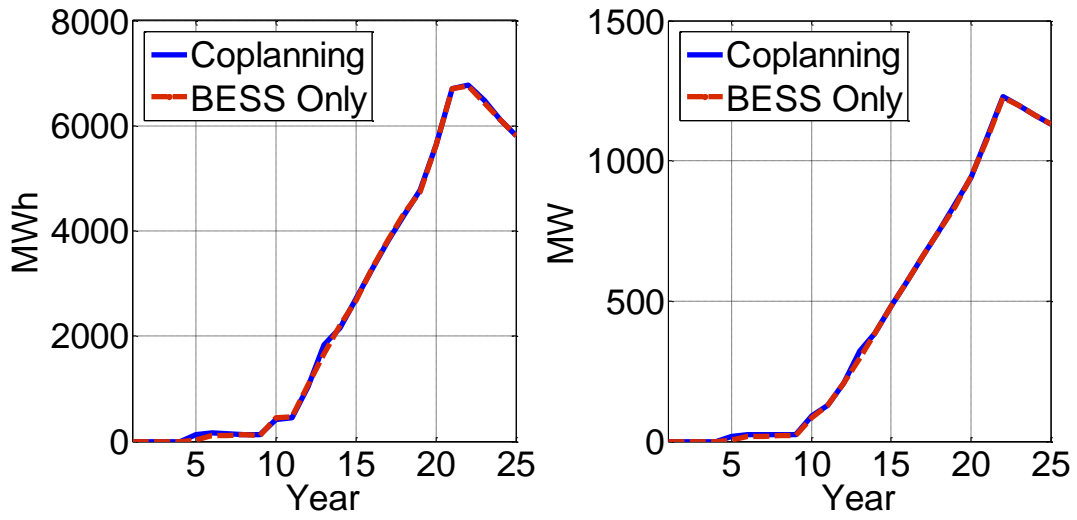


Figure 3.4. Total available BESS energy and power capacity as a function of time

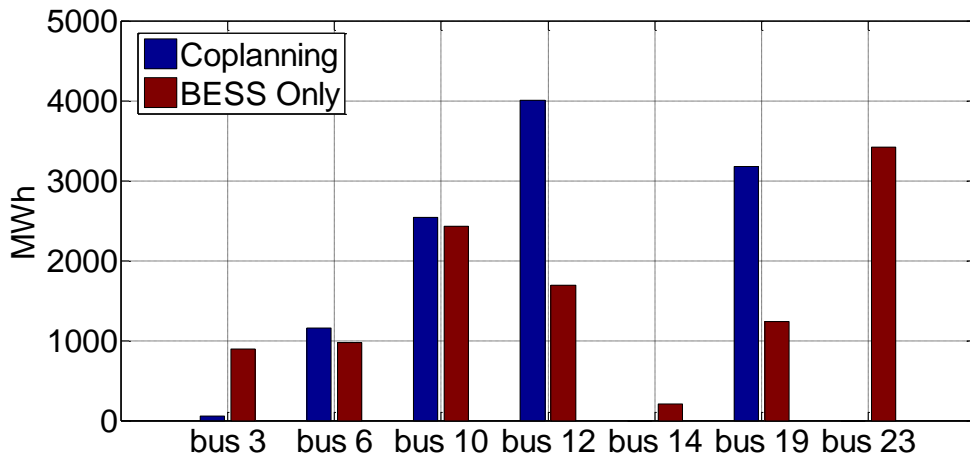


Figure 3.5. Total BESS energy capacity installed at each bus

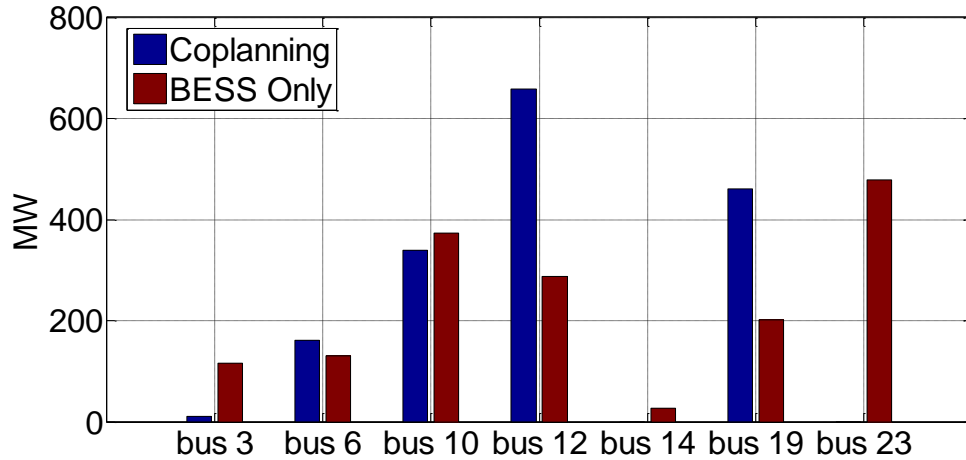


Figure 3.6. Total BESS power capacity installed at each bus.

Figures 3.7 and 3.8 further illustrate the differences in the timing and the location of the investments recommended by the two planning approaches.

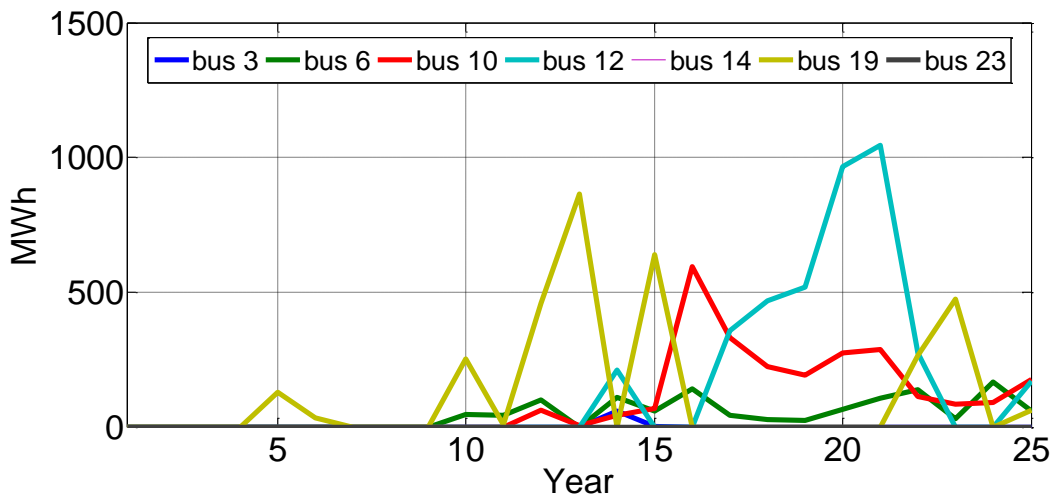


Figure 3.7. Energy capacity installed each year at each bus of the planning horizon using the co-planning method

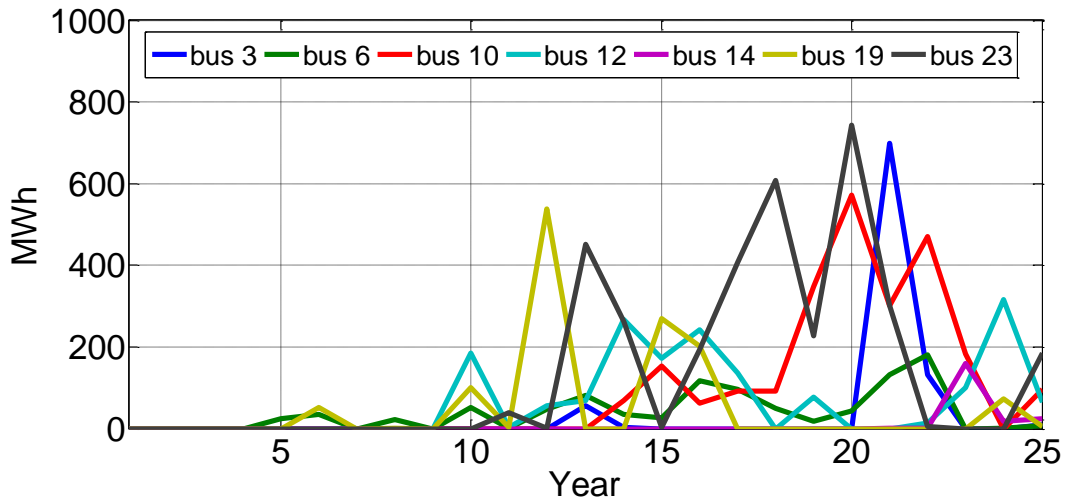


Figure 3.8. Energy capacity installed each year at each bus of the planning horizon using the BESS only planning method

- STOCHASTIC OPTIMIZATION

Because long-term forecasts of load growth and renewable energy development are inaccurate, considering multiple scenarios and performing the planning using a stochastic optimization provides a more robust investment plan. Figure 3.9 shows how much BESS energy capacity should be installed each year at each bus based on a stochastic optimization and the three wind generation and load growth scenarios described in Section 3.2D. Figure 3.10 shows the results obtained with a deterministic optimization using only the base scenario.

Comparing the results of Figure 3.9 and Figure 3.10 leads to the observation that deterministic planning distributes investments in BESS more widely over the years, while stochastic planning recommends larger investments in fewer years. The starting years, capacity at each bus, and total available energy and power capacities are also quite different.

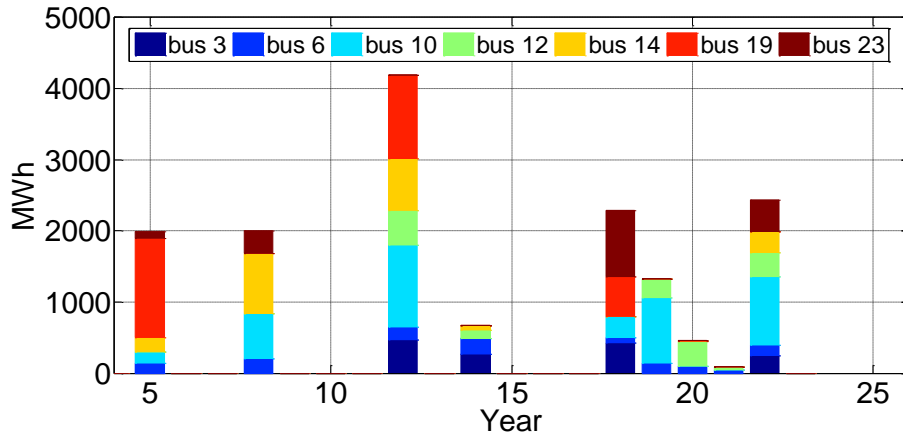


Figure 3.9. Total BESS energy capacity installed each year at each bus using stochastic optimization

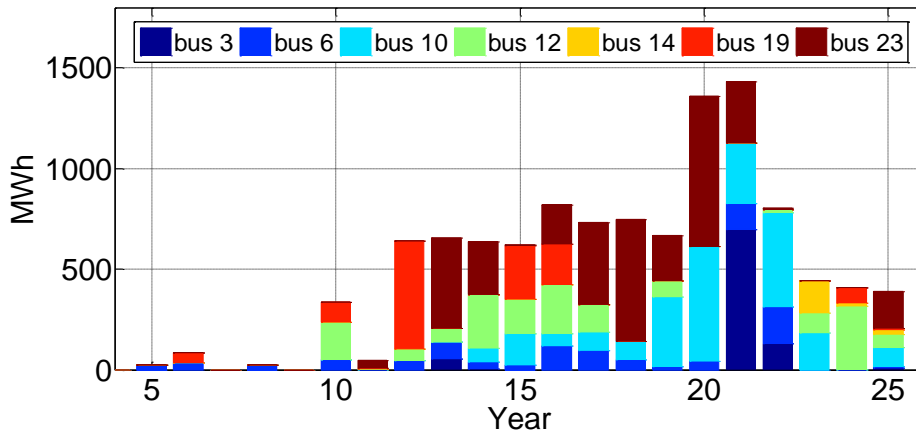


Figure 3.10. Total BESS energy capacity installed each year at each bus using deterministic optimization

- EFFECT OF BESS LIFETIME

The effect of changing the lifetime of each BESS from 10 to 15 years was studied using the co-planning approach. The annualized BESS energy and power capacity costs were changed accordingly, but all other parameters remained the same.

Table 3.4. BESS Investments

BESS lifetime	BESS Locations
10 years	Bus 3, 6, 10, 12, 19
15 years	Bus 6, 10, 12, 14, 19, 23

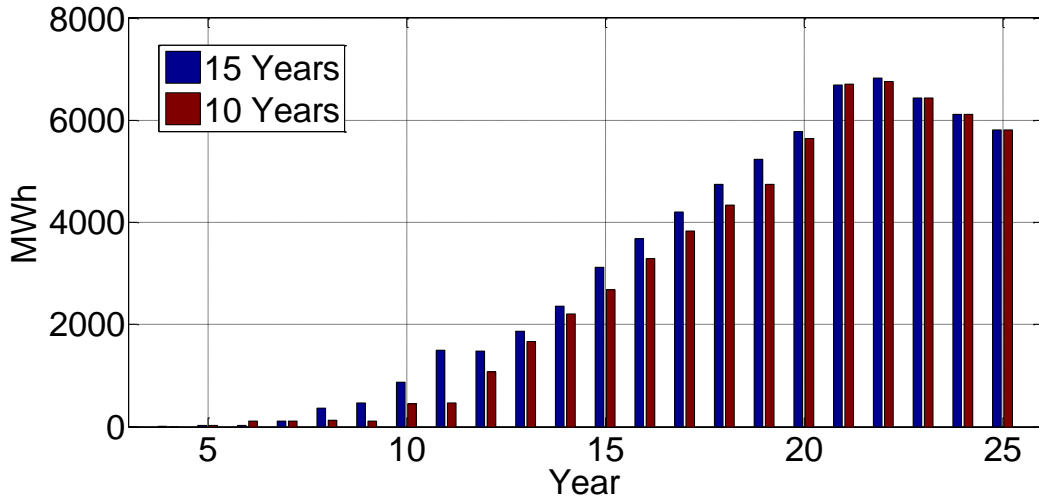


Figure 3.11. Total Available Energy Capacity

Table 3.4 shows that more BESS are installed when they have a longer lifetime and Figure 3.11 that their installation starts sooner.

Table 3.5 shows that more lines are built when the BESS operate for more years. This is reasonable, since a longer life time means the cost of using BESS has reduced, the saved cost can be used to upgrade more line capacities.

Table 3.5. Line Capacity Upgrades

BESS lifetime	Upgraded Lines	Line Capacity(MW)	Construction Year
10 years	Line 21 (bus 12-23)	450	Year 09
15 years	Line 23 (bus 14-16)	450	Year 09
	Line 22 (bus13-23)	450	Year 22
	Line 10 (bus 06-10)	157.5	Year 24

- EFFECT OF TRANSMISSION CAPACITY

To compare the effect of transmission capacity on co-planning, the initial transmission capacity was set at 100%, 90% and 80% of the original RTS transmission capacity. As one might expect and as Table 3.6 shows, fewer lines need to be upgraded if the initial transmission capacity is larger. On the other hand, as Table 3.7 shows, the locations where BESS are installed change. When less transmission capacity is available, the location of BESS shifts from corridors used to transport wind generation towards load centers (bus 03) to avoid load curtailments and to wind generation centers (bus 23) to reduce wind curtailments. Figure 3.12 shows that the transmission capacity has an almost negligible effect on the total installed BESS energy capacity in the system.

Table 3.6. Line Capacity Upgrades

Initial capacity	Upgraded Lines	Line Capacity(MW)	Construction Year
100%	None	NA	None
90%	line 21 (bus 12-23)	450	Year 09
80%	Line 22 (bus13-23)	400	Year 07
	Line 29 (bus16-29)	400	Year 11
	Line 10 (bus 6-10)	140	Year 21

Table 3.7. BESS Investment Location

	BESS Locations
100% Capacity	Bus 06, 10, 12, 14, 19, 23
90% Capacity	Bus 03, 06, 10, 12, 19
80% Capacity	Bus 03, 06, 10, 12, 14, 19, 23

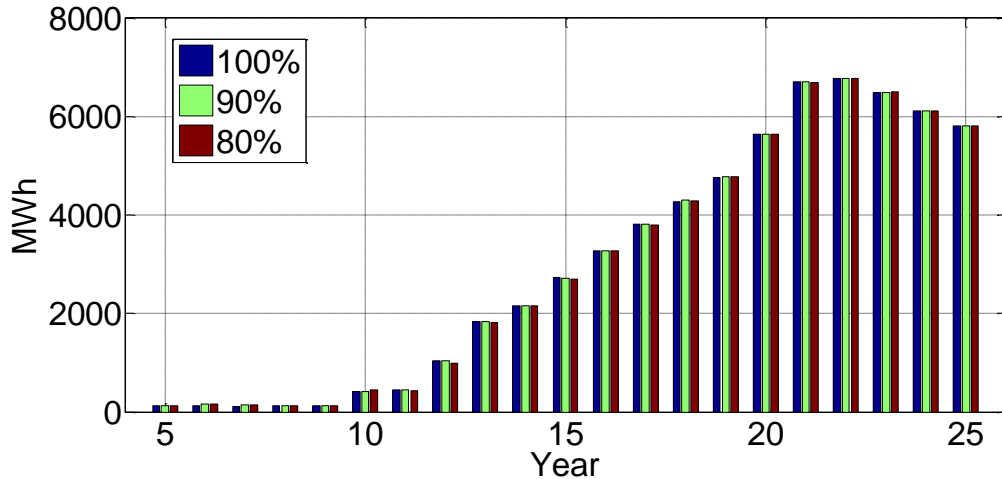


Figure 3.12. Total available BESS energy capacity for different initial transmission capacities

3.6 CONCLUSIONS

In this chapter, we have proposed a stochastic multi-stage method for co-planning transmission and BESS. Compared with the state of art, the proposed method uses more detailed and accurate models over a longer planning horizon. In particular, it takes into account the degradation and limited lifetime of BESS, it considers the reserve constraints and optimizes both the location and capacity of BESS. The size of the problem, and hence the computing burden, remain manageable because generators are grouped by types, and the locations where BESS be installed and the lines that can be upgraded are pre-selected. A sensitivity analysis has been performed to highlight the effect of different planning approaches, of the uncertainty on future load and wind developments, of the BESS lifetime and of the initial transmission capacity.

The reserve rate is defined as follows:

$$\frac{\text{Conventional Generation Capacity} + \text{Wind Generation}}{\text{Load Forecast}}$$

Over the course of 25 years planning horizon, this reserve rate will decrease. A negative reserve

rate may appear in times when the wind is low and the load is high such as in day 3 and 4. Despite the negative reserve rate, the system remain balanced because of the installed BESS. BESS charges during the early hours when the reserve rate is high and discharges during the hours when the reserve rate is low, so part of the capacity has been shifted. In hours when the reserve rate is negative, the BESS virtual generation capacity shifted from the high reserve rate hours is used to keep the system in balance. In the future, there may be significant value in co-planning generation, transmission and BESS to evaluate the benefit of BESS in providing both virtual transmission and generation capacity.

Chapter 4. STOCHASTIC MULTI-STAGE CO-PLANNING OF GENERATION AND BATTERY ENERGY STORAGE

4.1 INTRODUCTION

Because of their intermittency and stochasticity, wind and solar generation cannot be treated in the same way as conventional plants in generation planning. To ensure that enough generation is available when these renewable resources are not available, conventional fossil-fired units may still be required. Furthermore, as the proportion of renewable generation increases, flexible generating units or battery energy storage systems (BESS) [86-87] may be needed to keep the system in balance. Traditional generation expansion planning techniques must therefore be modified to consider the need for flexibility as well as the benefits of distributed energy storage.

Generation expansion planning has attracted a significant amount of interest in recent years [88-95]. Hua et al. [88] proposed a generation expansion planning model that incorporates operational flexibility through a convex relaxation of the unit commitment problem. Hinojosa and Gonzalez-Longatt [89] described a generation expansion model considering N-m contingencies, with the goal of enhancing system reliability under both normal operation and after the occurrence of a major disturbance. Kirschen et al. [90] proposed a stochastic method to optimize the flexibility of a portfolio of generating plants. De Jonghe et al. [91] discussed the effect of short term demand response on the optimization of the generation mix. All these methods are based on a snapshot of the system conditions for a given year. Multi-stage long-term planning methods are discussed in [93-95]. Saboori and Hemmati [93] developed a multi-stage generation expansion planning model to minimize the planning costs and the CO₂ emissions using a particle swarm optimization algorithm. Zhan et al. [94] introduced a stochastic programming model that maximizes total

profits, considering the effect of investment decisions on electricity prices. Dominguez et al. [95] proposed a multi-stage generation investment model that takes into consideration the demand growth and the generating units cost uncertainty. They used a linear decision rule (LDR) approach to reduce the computing burden.

Various studies [96-100] focus on the planning of energy storage systems. Oh [96] used a DC OPF model and a limited number of time periods per year to keep the problem of siting and sizing storage units tractable. Dvijotham et al. [97], developed a heuristic procedure for energy storage placement and sizing based on historical data. Wogrin and Gayme [98] discussed a co-optimizing model for siting and sizing of a storage technology portfolio consisting of four technologies in a transmission-constrained network. A stochastic optimization-based model is used by Xiong and Singh [99] to optimize both the location and size of an energy storage system considering the uncertainty on wind power generation. These authors use a capital/operating cost frontier to show how a budget constraint affects the ESS planning decisions. Pandzic et al. [71] used a full unit commitment model to determine both the optimal sizes and sites for energy storage based on wind and load profiles over a whole year. They introduced some heuristics to limit the problem size. Liu et al. [72] modeled wind fluctuation using power spectrum density and optimized only the size of the ESS to increase the level of wind power penetration while meeting the limits on grid frequency deviations. Xu et al [100] developed a bi-level formulation to optimize both the location and size of energy storage systems used for energy arbitrage and regulation services. Additional rate-of-return constraints are enforced to guarantee the profitability of investments in energy storage.

A few papers have dealt with the co-planning of energy storage and generation [101-107]. Yasuda et al. [101] proposed a model based on dynamic programming and a gradient search to co-optimize the mix of generation and storage, but did not consider transmission constraints or

renewable generation. Pudjianto et al. [102] developed an approach to simultaneously optimize investments in generation, network and storage capacity. However, the transmission and generator operating constraints are simplified to keep the computations tractable. Yang and Nehorai [103] used a consensus-based method to co-optimize investments in storage, renewable generation, and diesel generator capacities for a micro-grid. Carrión et al. [104] developed a coordinated generation and storage expansion formulation considering the primary frequency response constraints. Kargarian et al. [105] used a detailed hourly and intra-hourly operation model in a stochastic co-planning problem to optimize both the flexible generation and ESS capacity. Liu et al. [106] used a progressive hedging algorithm to solve a multi-stage stochastic planning model. To reduce the computation time, these authors considered only 4 investment periods over a 10-year horizon.

This chapter describes a multi-stage co-planning model for generation capacity and battery energy storage systems (BESS). Its contributions can be summarized as follows:

- a. It models the degradation of the energy storage capacity and time delays in the construction of generating plants.
- b. The multi-stage planning model optimizes both the size and the location of investments in energy storage and traditional generators at each year over the whole planning horizon.
- c. It provides a detailed analysis of common investment patterns and differences for 9 combinations of penetrations of renewable generation and hourly wind/load correlations.
- d. It discusses the effect of the choice of representative days on the planning results and provides a way to obtain near-optimal planning results for large systems.
- e. It analyzes competition and complementarity between storage and flexible generation.

Section 4.2 provides the detailed mathematical formulation of the optimization problem. Section

4.3 discusses the modeling assumptions. Section 4.4 describes the test system. Section 4.5 presents and discusses numerical results. Section 4.6 concludes this chapter.

4.2 MODELING ASSUMPTIONS

This chapter adopts a 25-year planning horizon with a 1-year resolution. Because multi-stage planning problems can easily get very large, careful modeling simplifications must be made to achieve a balance between the accuracy of the results and the computing time. The following paragraphs describe briefly these assumptions. More details can be found in [107].

- TYPES OF GENERATORS

A simplified generation expansion problem was first solved to determine the types of generators that should be considered as candidates for investments. At each location, additional generators of the type that are already connected there can be built, creating an aggregated generation capacity with larger ramping and operating limits but with the same up/down times and a single operating status. Nine different types of traditional generators are represented in the test system. The investment costs for these generators can be found in [90]. Units of types 1 and 4 with maximum capacities of 20MW and 76MW respectively turned out to be selected most frequently during this simplified generation expansion problem. Because units of type 4 are somewhat larger, they were selected for all further investments in flexible generation.

To further simplify the model and the amount of computation required, both existing and new generators were divided into two types: those that are assumed to be always committed and those that are free, i.e. that can start up or shut down at any time. In other words, slow and flexible generators. Generators with a minimum up/down time of less than 2 hours are assumed to be flexible generators, while the remaining ones are in the slow category. Units of Type 4 unit chosen

in the previous step are treated as flexible generators.

- REPRESENTATIVE DAYS

When planning a system with a large amount of renewable generation, simply providing enough generation to meet the expected peak load is not sufficient. One must also ensure that the system has enough flexibility from generation or storage to follow the net load profile. High wind generation from remote locations can also cause stress in the transmission network and thus require the availability of resources located closer to the load. One must also have enough generation to deal with days of minimal wind generation. Particular attention must therefore be paid to the shapes of the load and renewable generation profiles, which can be positively or negatively correlated. The difference between the load and renewable generation profiles define the shape of the net load, which drives decisions about investments in conventional generation. Being independent of the load value and wind capacity (which changes over the years), the correlation coefficient between these quantities is a good discriminating feature in the K-means clustering algorithm used to identify representative days. Using this algorithm, we divided a whole year into 3 clusters. Each cluster was then further divided into 3 subgroups based on the total wind output of that day. Our results are thus based on nine representative days based on the total wind generation level and how the daily wind is changing with the daily load. The day that is closest to the centroid of each subgroup is selected as representative of that subgroup. Table 4.1 summarizes these features.

Table 4.1. Features Used for Identifying Representative Days

HW	High ratio of wind generation to load
AW	Average ratio of wind generation to load
LW	Low ratio of wind generation to load
HC	High correlation between wind and load profiles
AC	Average correlation between wind and load profiles
LC	Low correlation between wind and load profiles

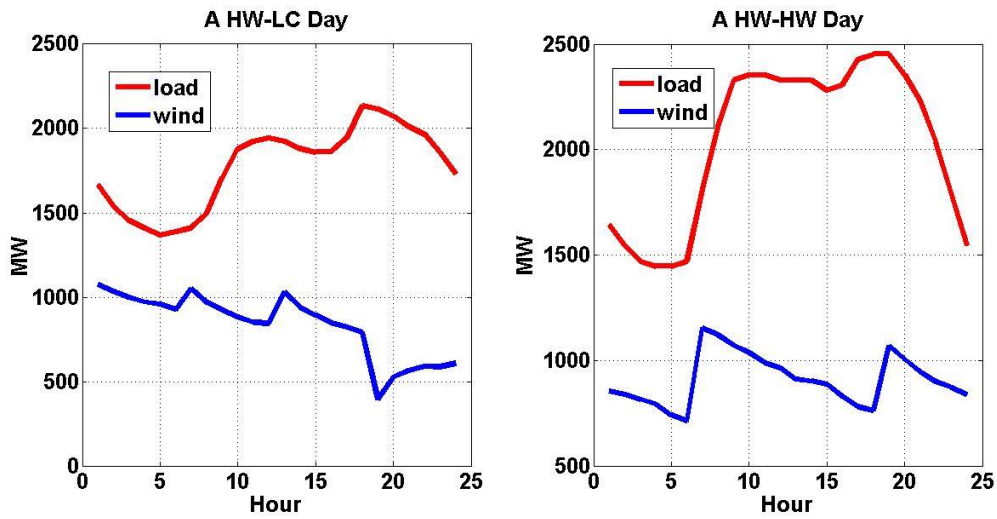


Figure 4.1. Examples of representative days

Figure 4.1 shows the load and wind generation profiles for two representative days. The one on the left represents the HW-HC cluster, while the one on the right represents the HW-LC cluster.

4.3 FORMULATION OF THE PLANNING PROBLEM

- NOTATIONS

Parameters:

GT Life time of a generator

Binary variables

$nx_{s,t}^y$ New invested generator investment status, 1- online, 0 – offline

$nz_{s,t}^y$ Construction status of new generators

Integer variables

$I_{s,y}$ Number of generators installed at bus in a single year

$Z_{s,y}$ Accumulated number of new generators in service

Variables

c_y Discounted annual operating cost

$C_{t,i}^{operation}$ Hourly unit operation cost

$NC_{t,s}^{operation}$ Hourly unit operation cost of new generators

$C_{t,s}^{nl}$ No-load cost of new generators

$C_{t,s}^{suc}$ Startup cost of new generators

G_INV_y Discounted annual generation investment cost

$np_{s,b,t}^y$ New generation on each segment of the cost curve

$np_{s,t}^y$ Total generation of installed new generators

$nrg_{s,t}^y$ Reserve provided by new built generators

- OBJECTIVE FUNCTION

For clarity of exposition, the equations below define the deterministic long-term planning problem. The stochastic version of this problem can be easily obtained by adding one more dimension to the operation variables and related constraints. The long-term planning problem aims to minimize the sum of the operating, generation investment and energy storage investment costs over the horizon:

$$\min \sum_{y=1}^y C_y + S_INV_y + G_INV_y \quad (4.1)$$

The total annual operating cost discounted over the planning horizon includes the operating cost of both existing and newly built generators, and a penalty term that discourages wind and load curtailments (at 20 \$/MWh and 5000 \$/MWh respectively):

$$C_y = \frac{\tau \cdot \left(\sum_{i=1, t=1}^{I, T} C_{t,i}^{operation} + \sum_{s=1, t=1}^{S, T} NC_{t,s}^{operation} + penalty \right)}{(1+r)^{y-1}} \quad (4.2)$$

Equation (4.2a) gives the operating cost of existing generators. Equations (4.2b) to (4.2f) give this cost for newly built generators, where (4.2c) and (4.2d) describes the no-load cost and (4.2e) to (4.2f) the startup cost.

$$C_{t,i}^{operation} = \sum_{b=1}^{NB} p_{i,b,t}^y \cdot k_{i,b} + NL_i + SU_i \cdot z_{i,t}^y \quad (4.2a)$$

$$NC_{t,s}^{operation} = \sum_{b=1}^{NB} p_{s,b,t}^y \cdot k_b + C_{s,t}^{nl} + C_{s,t}^{suc} \quad (4.2b)$$

$$C_{s,t}^{nl} \geq NL \cdot Z_{s,y} - (1 - nx_{s,t}^y) \cdot M \quad (4.2c)$$

$$C_{s,t}^{nl} \geq NL \cdot nx_{s,t}^y \quad (4.2d)$$

$$C_{s,t}^{suc} \geq SUC \cdot Z_{s,y} - (1 - nz_{s,t}^y) \cdot M \quad (4.2e)$$

$$C_{s,t}^{suc} \geq SUC \cdot nz_{s,t}^y \quad (4.2f)$$

Equation (4.3) gives the discounted annual BESS investment cost. Equations (4.3a) and (4.3b) specify the annualized BESS energy and power capacity costs while (4.3c) gives the annual discount factor needed to ensure that all costs are paid off within the battery lifetime.

$$S_INV_y = \sum_{n=1}^y \alpha_{y-n+1} \cdot \sum_{s=1}^S (k^e \cdot E_{s,n}^{\max} + k^p \cdot P_{s,n}^{\max}) \quad (4.3)$$

$$k^e = C^E \cdot \frac{r(1+r)^{ST}}{(1+r)^{ST} - 1} \quad (\$/MWh \cdot Year) \quad (4.3a)$$

$$k^p = C^p \cdot \frac{r(1+r)^{ST}}{(1+r)^{ST} - 1} \quad (\$/MW \cdot Year) \quad (4.3b)$$

$$\alpha_n = \begin{cases} \frac{1}{(1+r)^{n-1}} & n \leq ST \\ 0 & n \geq ST + 1 \end{cases} \quad (4.3c)$$

Equation (4.4) gives the discounted annual generation investment cost. An annual payment is assumed to be made each year after the investment decision. Equation (4.4a) gives the annualized generation investment cost while Equation (4.4b) gives the annual discount factor needed to ensure that the cost of the generator is paid off over the generator's life time.

$$G_INV_y = \sum_{n=1}^y \beta_{y-n+1} \cdot \sum_{s=1}^S k^g \cdot I_{s,n} \cdot \tilde{P} \quad (4.4)$$

$$k^g = C^g \cdot \frac{r(1+r)^{LT}}{(1+r)^{LT} - 1} \quad (\$/Year) \quad (4.4a)$$

$$\beta_n = \begin{cases} \frac{1}{(1+r)^{n-1}} & n \leq GT \\ 0 & n \geq GT + 1 \end{cases} \quad (4.4b)$$

- OPERATING CONSTRAINTS

Equations (4.5) to (4.8) enforce the constraints on minimum and maximum generation capacity and maximum ramping. Equations (4.9) and (4.10) specify the amount of reserve that each generator can provide:

$$P_{i,t}^y = \sum_{b=1}^{NB} P_{i,b,t}^y \cdot X_{i,t}^y \quad (4.5)$$

$$P_{i,t}^y \geq \underline{p}_i \cdot X_{i,t}^y \quad (4.6)$$

$$P_{i,b,t}^y \leq \bar{P}_{i,b} \cdot X_{i,t}^y \quad (4.7)$$

$$|P_{i,t}^y - P_{i,t-1}^y| \leq \Delta_i \quad (4.8)$$

$$P_{i,t}^y + rg_{i,t}^y \leq \bar{P}_i \cdot X_{i,t}^y \quad (4.9)$$

$$rg_{i,t}^y \leq \Delta_i \cdot \delta t \cdot X_{i,t}^y \quad (4.10)$$

Equation (4.11) keeps track of the state of charge of each BESS. Equations (4.12) to (4.14) enforce their energy and power capacity limits. Equations (4.15) and (4.16) determine the amount of reserve that each BESS can provide:

$$SoC_{s,t}^y = SoC_{s,t-1}^y + ch_{s,t}^y - dis_{s,t}^y \quad (4.11)$$

$$E_{s,y}^{\min} \leq SoC_{s,t}^y \leq AE_{s,y} \quad (4.12)$$

$$ch_{s,t}^y \leq APe_{s,y} \quad (4.13)$$

$$dis_{s,t}^y \leq APe_{s,y} \quad (4.14)$$

$$0 \leq re_{s,t}^y + dis_{s,t}^y - ch_{s,t}^y \leq APe_s^y \quad (4.15)$$

$$E_s^{\min} \leq SoC_{s,t}^y - \frac{(re_{s,t}^y - ch_{s,t}^y)}{\eta_s^{ch}} \cdot \delta t \quad (4.16)$$

Equation (4.17) enforces the power balance at each node:

$$\begin{aligned} & \sum_{i=1}^I P_{i,t}^y \cdot M_{i,s}^G + np_{s,t}^y - \sum_{w=1}^W wp_{w,t}^y \cdot M_{w,s}^W - \sum_{l=1}^L f_{l,t}^y \cdot M_{l,s}^L \\ & = D_{s,t}^y + \sum_{t=1}^T \left(\frac{ch_{s,t}^y}{\eta_s^{ch}} + dis_{s,t}^y \cdot \eta_s^{dis} \right) \end{aligned} \quad (4.17)$$

Equation (4.18) limits the wind generation to the available wind power, which is assumed to be equal to the forecast:

$$wp_{w,t}^y + ws_{w,t}^y = wf_{w,t}^y \quad (4.18)$$

Equation (4.19) defines the 3+5 reserve requirement [83-84], i.e. it specifies that the total reserve should be no less than 3% of the forecasted load plus 5% of the forecasted wind power.

$$\sum_{i=1}^I rg_{i,t}^y + \sum_{s=1}^S nrg_{s,t}^y + \sum_{s=1}^S re_{s,t}^y \geq 0.03 \cdot \sum_{s=1}^S D_{s,t}^y + 0.05 \cdot \sum_{w=1}^W wf_{w,t}^y \quad (4.19)$$

Equation (4.20) calculates the line flows using a dc model, while Equations (4.21) and (4.22) enforce the constraints on these flows.

$$f_{l,t}^y = B_{ms} \cdot (\theta_{m,t}^y - \theta_{s,t}^y) \quad (4.20)$$

$$-\bar{F}_{l,t} \leq f_{l,t}^y \leq \bar{F}_{l,t} \quad (4.21)$$

$$-\pi \leq \theta_{s,t}^y \leq \pi \quad (4.22)$$

- GENERATION PLANNING MODEL

Equation (4.23) records the year when a generator is installed, which triggers the investment cost in equation (4.4). Equations (4.23) and (4.24) enforce a construction delay of two years between the investment decision and the availability of a new generator.

$$Z_{s,y} = \begin{cases} \sum_{r=1}^{y-2} I_{s,r} & y \geq 3 \\ 0 & y \leq 2 \end{cases} \quad (4.23)$$

$$Z_{l,y} \geq Z_{l,y-1} \quad (4.24)$$

Because all generation investments made over time at a given node are assumed to consist of the same type of unit, they can be represented by an aggregated generator whose capacity varies over time. Equations (4.25) to (4.30) describe this aggregated generator:

$$np_{s,t}^y = \sum_{b=1}^{NB} np_{s,b,t}^y \cdot nx_{s,t}^y \quad (4.25)$$

$$np_{s,t}^y \geq \underline{p} \cdot nx_{s,t}^y \quad (4.26a)$$

$$np_{s,t}^y \geq \underline{p} \cdot Z_{s,y} - (1 - nx_{s,t}^y) \cdot M \quad (4.26b)$$

$$np_{s,b,t}^y \leq M \cdot \bar{p}_b \cdot nx_{s,t}^y \quad (4.27a)$$

$$np_{s,b,t}^y \leq \bar{p}_b \cdot Z_{s,y} \quad (4.27b)$$

$$|np_{s,t}^y - np_{s,t-1}^y| \leq \Delta \cdot Z_{s,y} \quad (4.28)$$

$$np_{s,t}^y + nrg_{s,t}^y \leq M \cdot \bar{p} \cdot nx_{s,t}^y \quad (4.29a)$$

$$np_{s,t}^y + nrg_{s,t}^y \leq \bar{p} \cdot Z_{s,y} - (1 - nx_{s,t}^y) \cdot M \quad (4.29b)$$

$$nrg_{s,t}^y \leq \Delta \cdot \delta t \cdot nx_{s,t}^y \cdot M \quad (4.30a)$$

$$nrg_{s,t}^y \leq \Delta \cdot \delta t \cdot Z_{s,y} - (1 - nx_{s,t}^y) \cdot M \quad (4.30b)$$

4.4 TEST SYSTEM

Tests were carried out on a modified version of the IEEE-RTS 24-bus system. The full system data can be downloaded from [64]. The wind power profiles used are from Pandzic et al. [71]. Only the

three wind farms located at bus 20, 21 and 23 of subsystem 1 are selected with initial capacities of 600MW, 300MW and 300MW. Wind generation accounts for 21.7% of the annual load at year 1. A line was added between buses 7 and 8 to make the system N-1 secure.

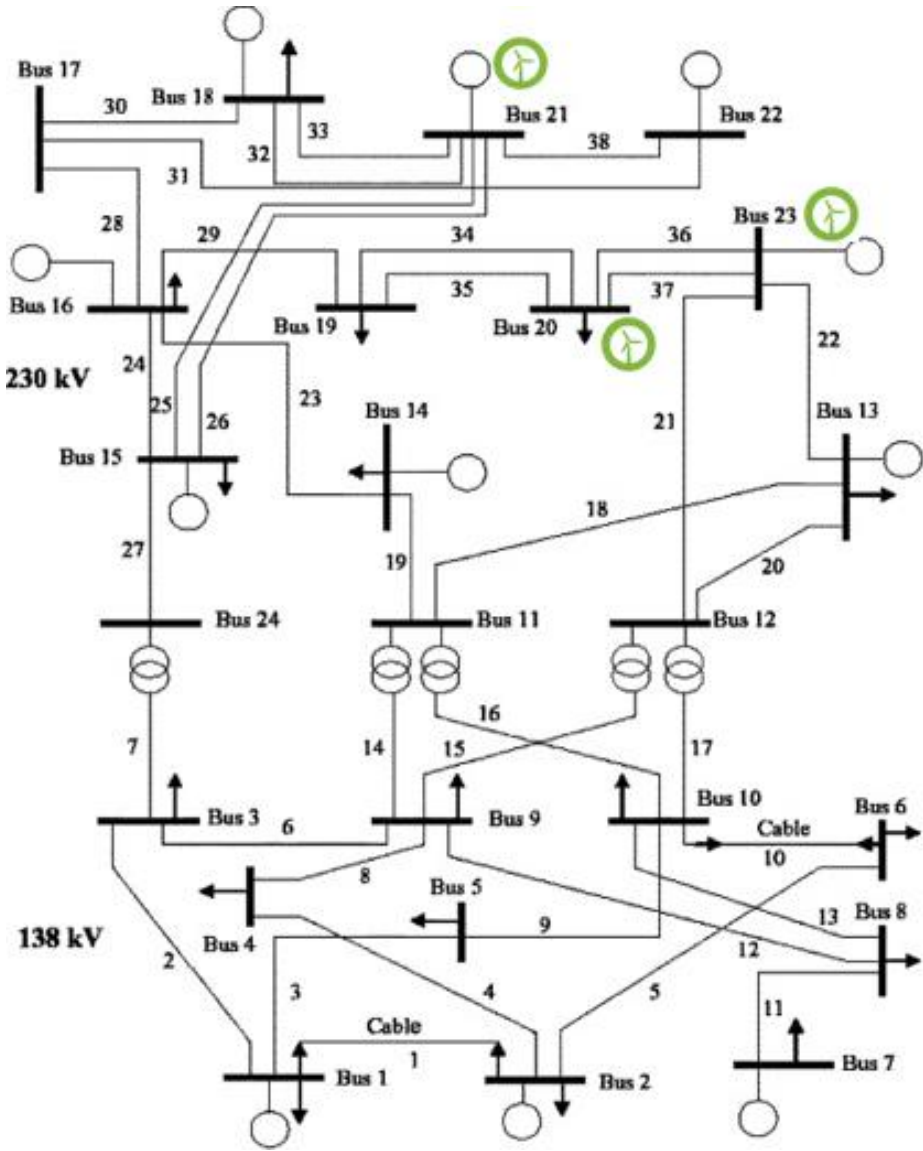


Figure 4.2. Test System Topology

Other important parameters include:

- The capacity of the transmission lines was reduced by 20%

- The cost of a BESS is assumed to be 500\$/kW plus 25\$/kWh, and its lifetime 10 years.
- The cost of a flexible generator is assumed to be 536,000 \$/MW, and its lifetime 60 years.
- The discount rate is set at 5%.
- In the base scenario, the wind generation capacity increases linearly each year by 4% of its initial capacity and the load by 3% of its initial value. By the end of the planning horizon, wind generation and load reach 196% and 172% of their initial values, respectively.
- The committed units are selected using the method as Chapter 4 showing in Table 4.2.

Table 4.2. Unit Categories

Type	No	Min-Down (hr)	Min-Up (hr)	Category
1	15-19	1	2	Fast
2	1-2, 5-6	1	2	Fast
3	24-29	1	2	Fast
4	3-4, 7-8	2	3	Fast
5	9-11	2	4	Slow
6	20-21, 30-31	16	24	Slow
7	12-14	3	4	Slow
8	32	5	8	Slow
9	22-23	24	168	Slow

All modeling was done using GAMS 23.7. The computations were carried out using the MILP solver of CPLEX 12.6 on a computer cluster with x nodes consisting of dual-core Intel Xenon 2.55 GHz processors with 32 GB RAM.

4.5 TEST RESULTS AND ANALYSIS

To analyze how the ratio of wind generation capacity to peak load and the correlation between the wind and load profiles would affect planning decisions, 9 different groups of simulations were performed. Each simulation assumes that there is only one type of representative days for a whole year. This allows us to explore how these factors affect the planning results and the interaction between the two types of resources.

- EFFECT OF WIND LEVEL AND WIND/LOAD CORRELATION

Tables 4.3 and 4.4 show the amount and timing of investments in flexible generation and in storage for 9 combinations of wind penetrations and wind/load correlations.

Table 4.3. Co-planning of Generation Capacity for 9 Combinations of Wind penetrations and Wind/load Correlations

Total Installed Gen Capacity (MW)				Investment Start Year		
	HW	AW	LW	HW	AW	LW
HC	228	0	836	17	N/A	11
AC	304	988	912	14	11	10
LC	304	1292	1368	14	9	6

Table 4.4. Co-planning of Storage for 9 Combinations of Wind Penetrations and Wind/load Correlations

Total Installed Energy Capacity (MWh)				Investment Start Year		
	HW	AW	LW	HW	AW	LW
HC	389	20	0	1	23	N/A
AC	170	440	0	1	1	N/A
LC	1611	1031	0	1	1	N/A
Total Installed Power Capacity (MW)				Investment Start Year		
	HW	AW	LW	HW	AW	LW
HC	52	8	0	1	23	N/A
AC	21	55	0	1	1	N/A
LC	256	129	0	1	1	N/A

We can draw the following conclusions from these results:

- Days with lower wind/load correlation (LC) provide more energy arbitrage opportunities for BESS. In these cases, the wind generation tends to be larger when the load is lighter, a larger BESS capacity is needed to store wind energy during valley load hours and discharge it during

peak load hours.

- This effect becomes more significant for higher wind penetrations. No BESS investment happens when the wind/load ratio (LW) is low.
- When the wind penetration is low, more conventional generation is required, and these investments occur earlier.
- For a given wind generation level, if the wind/load correlation is small, less wind power is available during peak hours and additional flexible generators are needed.
- The wind/load ratio and the correlation together determine how much flexible generation and storage are needed.
- A higher wind/load correlation (HC) means that wind power can be used to supply the load most of the time. However, a different wind/load ratio can lead to completely different planning results. As shown in Table 4.3, for a medium wind/load ratio (AC), existing resources are adequate to serve the load without the need to plan for additional generation. As the wind/load ratio increases (HW), some additional generation should be planned to deal with the high hourly wind fluctuation. As wind power generation drops, additional generations are needed to serve the increasing load.

- INVESTMENT LOCATION DISTRIBUTION

To identify the preferred locations for investments in storage and flexible generation, all buses in the system are divided into three categories depending on whether they are near a load center, along the transmission corridor, or near the wind generation. Tables 4.5, 4.6 and 4.7 show how the capacities shown in Tables 4.3 and 4.4 are geographically distributed.

Table 4.5. Total Generation Capacity (MW) with the Co-Planning Model

		HW	AW	LW
Load Center	HC	152	0	836
	AC	304	836	912
	LC	304	912	1368
Corridor	HC	76	0	0
	AC	0	152	0
	LC	0	380	0
Wind Center	HC	0	0	0
	AC	0	0	0
	LC	0	0	0

Table 4.6. Total BESS Energy Capacity (MWh) in Co-Planning Model

		HW	AW	LW
Load Center	HC	167	14	0
	AC	144	0	0
	LC	755	590	0
Corridor	HC	46	0	0
	AC	0	0	0
	LC	479	0	0
Wind Center	HC	176	6	0
	AC	26	440	0
	LC	377	442	0

Table 4.7. Total BESS Power Capacity at Each Location (MW)

		HW	AW	LW
Load Center	HC	21	5	0
	AC	18	0	0
	LC	122	74	0
Corridor	HC	9	0	0
	AC	0	0	0
	LC	81	0	0
Wind Center	HC	22	3	0
	AC	3	55	0
	LC	53	55	0

Several locational patterns are apparent from these results:

- The majority of investments in flexible generation occur near the load centers and some along transmission corridors.
- Since wind farms are often located far from load centers, more transmission capacity is required when more wind power is used in the system. Because of limitations on the available

transmission capacity, load centers tend to be a better choice for investments in flexible generation. This is particularly true under the HC and LW scenarios.

- Investments in storage capacity tend to take place near wind centers and near load centers. Unlike generators that can only produce power, the ability of a BESS to charge as well as discharge gives it more flexibility. The coordinated operation of BESS pairs located near sources and sinks of energy creates additional transmission capacity which is particularly useful during HW days. Some BESS investments happen along the transmission corridor under the LC scenario because a BESS is able to reshape the wind power output, and hence relieve the congestion on the transmission corridor.

- COMPETITION AND COMPLEMENTARITY

Flexible generation and storage provide different types of flexibility to a power system. While both are able to respond to changes in the output of renewable generation, their contributions to the system are determined not only by the amount of wind generation capacity but also by its production profile. For the LW-HC case, investments in energy storage systems are not needed because the net load is smooth enough that additional flexibility is not required. For the HW-HC case, wind power might use most of the transmission capacity, leaving little room for power from flexible generators. The energy and ramping capacity that flexible generators could provide would indeed be limited by the transmission capacity of the system.

Because of their respective advantages and limitations, in some cases these two types of resources compete, while in others they are complementary. Table 4.8 shows how much generation capacity should be built and the year when it should start being built assuming no investments in storage. Table 4.9 shows how these decisions change when generation and storage are planned

together. Table 4.10 summarizes the location of these investments.

Table 4.8. Generation Only Planning

Total Installed Gen. Capacity(MW)				Investment Start Year		
	HW	AW	LW	HW	AW	LW
HC	304	0	836	15	N/A	11
AC	304	988	912	13	11	10
LC	228	1216	1368	14	8	6

Table 4.9. Differences between Co-planning and Generation Only Planning

Total Installed Gen. Capacity(MW)				Investment Start Year		
	HW	AW	LW	HW	AW	LW
HC	-76	0	0	2	0	0
AC	0	0	0	1	0	0
LC	76	76	0	0	1	0

Table 4.10. Total Installed Capacity (MW) with Generation Only Planning

		HW	AW	LW
Load Center	HC	304	0	836
	AC	228	684	912
	LC	228	532	1368
Corridor	HC	0	0	0
	AC	76	304	0
	LC	0	532	0
Wind Center	HC	0	0	0
	AC	0	0	0
	LC	0	152	0

Competition: In general, investments in flexible generation start earlier when there is no energy storage. In a HW-HC system, the transmission network is highly stressed and constrains the response of both storage and flexible generators. Competition happens between the two resources under this scenario, especially near the load center. Co-planning results in less flexible generation investment under these scenarios.

Complementarity: Co-planning increases the amount of flexible generation capacity compared with generation-only planning. Investments in flexible generation are indeed highly dependent on the availability of transmission. The virtual transmission capacity created by storage provides more opportunities for flexible generators, especially in the HW-LC and AW-LC scenarios when large investments are made in storage.

- SIMULATIONS WITH MULTIPLE REPRESENTATIVE DAYS

The planning results discussed so far are based on a single type of representative day. In practice, a year consists of a combination of all 9 types of representative days, although one or two types might represent a majority. To explore how different combinations of representative days might affect the results, two additional tests with 9 types of representative days were carried out.

- TEST1: In this test, the HW-LC day represents 55% of the days in a year, and the other 8 types account for about 5.6% of the days each.
- TEST2: In this test, the AW-AC day represents 55% of the days in the year, and the other 8 types account for about 5.6% of the days each.

Figures 4.3 and 4.4 show how the total available BESS power and energy capacity evolves over the years with each representative day separately as well as the TEST1 and TEST2 combinations. Compared with the results from the nine simulations with a single type representative day: (1) the results from TEST1 are closest to the results from HW-LC single representative day simulation; (2) the results from TEST2 are closest to the results from AW-LC single representative day simulation. Similar conclusions can be drawn from Table 4.11, which shows the generation investments.

The following conclusion can be made looking at similarity of the results of TEST1 to HW-LC

single representative day simulation and TEST2 to AW-AC single representative day simulation:
 We can get a good enough near optimal planning results by looking only at the majority days or
 by reducing the types of minority days. This could be really practical when doing long-term
 planning for large system which has a higher requirement on computing resource and time.

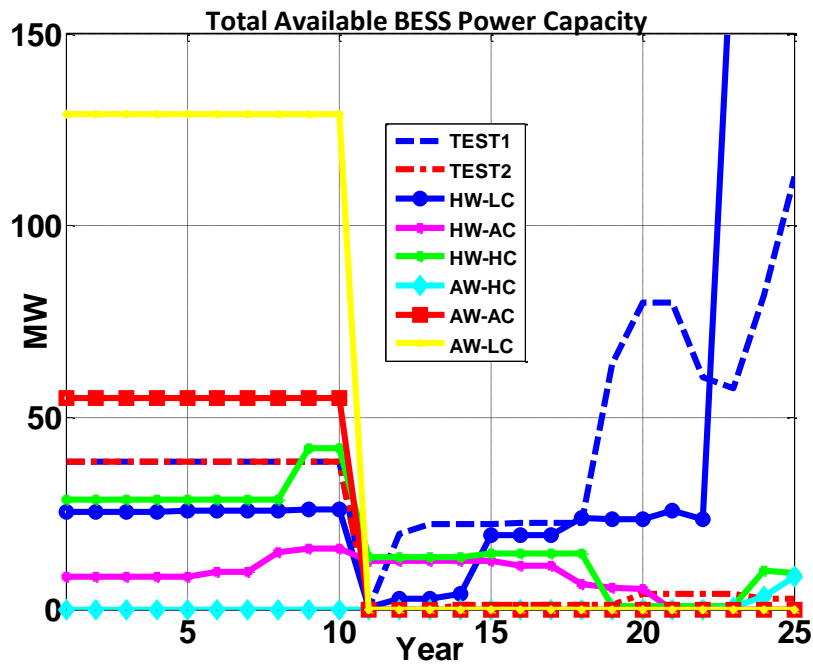


Figure 4.3. Total Available BESS Power Capacity over time

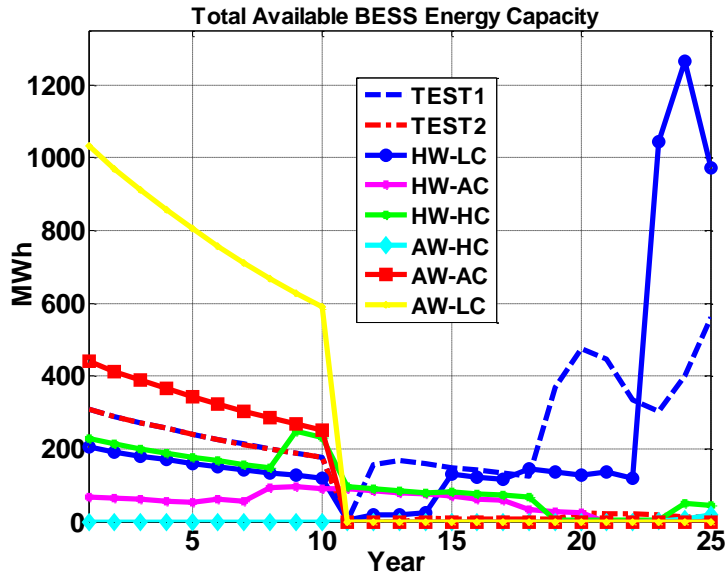


Figure 4.4. Total Available BESS Energy Capacity over time

Table 4.11. Generation Investment in TEST1 and TEST2

	Total Generation Capacity(MW)		Investment Start Year	
	TEST1	TEST2	TEST1	TEST2
Load Center	304	532	15	15
Corridor	76	76	17	18
Wind Center	76	0	20	N/A

4.6 CONCLUSIONS

In this chapter, we proposed a stochastic multi-stage method for co-planning flexible generation and BESS. Compared with the state of art, the proposed method uses more detailed and more

accurate models over a longer planning horizon. In particular, it takes into account the degradation, limited lifetime of BESS and the delay in generation installation. It also considers the reserve constraints and optimizes both the location and capacity of BESS and generators. A detailed analysis highlights the combined effects of different wind generation levels and wind/load ratio on the capacity, initiation year, preferred location of BESS and flexible generation investments.

Chapter 5. STOCHASTIC ENERGY AND ANCILLARY SERVICE CO-OPTIMIZATION WITH BESS

5.1 INTRODUCTION

Energy storage can be used in different parts of the electric grid to hedge the risk of renewable generation volatility, to provide baseload arbitrage, to increase transmission utilization, to enhance distribution system stability, to improve electric power service quality and for other purposes.

As Figure 5.1 shows, regulation service, which requires continuous and rapid control, commands the highest price compared to the price for energy and other types of reserve. As shown below, the price of regulation can be up to ten times larger than the price of spinning reserve, especially at times when the load is low, the online capacity is limited and most of the generators are running at their minimum.

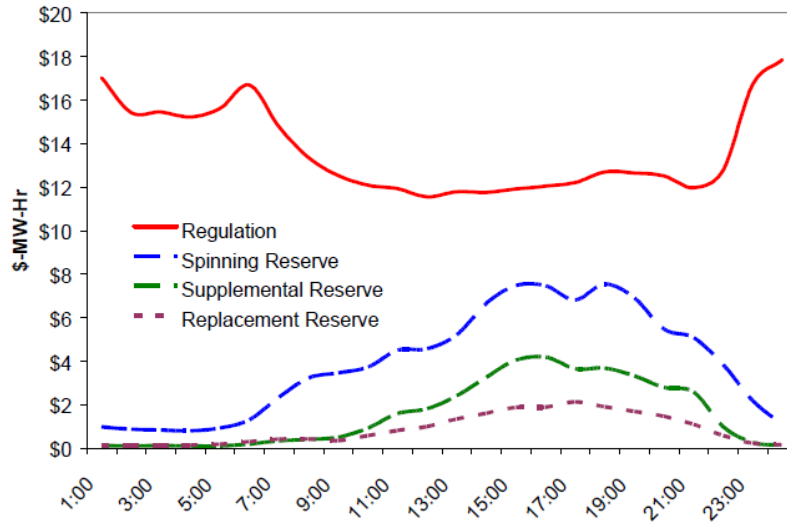


Figure 5.1. California's average hourly ancillary service prices for 2002. [109]

Based upon these prices, the faster response services are more attractive for storage. Batteries can indeed react very fast to rapid changes in wind generation to support frequency regulation. Such actions reduce the need for synchronous generators to provide inertia and primary reserve. Storage thus reduces system power imbalances and reduce the overall operation cost.

The use of energy storage for combined applications has been discussed by a number of authors. References [110] - [119] focus on applications of energy storage that increase their owner's profits or benefits. Shi et al. [110] propose a joint optimization method for commercial battery storage users to reduce their electricity bill by allowing the BESS to participate in both the energy and primary frequency regulation markets. Battery storage degradation, customer load and regulation signals uncertainties are taken into consideration in this model. Xi et al. [111] use a stochastic dynamic programming model to optimize the application of a distributed energy storage (PHEV) in different applications to achieve the maximum gain per unit of capacity. Cheng and Powell [112] propose to co-optimize the applications of BESS for energy arbitrage and frequency

regulation to achieve maximum profit. A multi-scale dynamic programming method is used to reduce the problem size. Walawalkar et al. [113] mention that greater benefit can be achieved by using electric energy storages for different purpose such as energy arbitrage, frequency regulation and voltage support. White and Zhang [114] propose a “dual-use” program to achieve the maximum profit of a PHEV by utilizing it for both peak reduction and frequency regulation simultaneously. Sarker et al. [115] propose a method for an electric vehicle aggregator to maximize its profits by participating in both the energy and the regulating reserve markets, while compensating EV owners for the degradation of their battery. Arabali et al. [116] developed a co-optimization model for grid scale energy storage to maximize its revenues in the day-ahead energy and frequency regulation markets. The uncertainty of the frequency control signal is taken into consideration in the proposed model. Byrne and Silva-Monroy [117] estimated the potential revenue of grid connected energy storage from both energy arbitrage and regulation using CAISO system operation data. Their study reveals that the revenue from frequency regulation is four times larger than that from energy arbitrage. In Donadee [118], an infinite horizon Markov decision problem (MDP) framework is used to co-optimize the application of energy storage in the energy and ancillary service markets. It is shown that the value of energy storage can be substantially increased if used for multiple purposes simultaneously. Chazarra et al. [119] proposed a mixed integer linear programming model for a pumped hydro power plant to participate in the hourly energy and secondary regulation reserve markets to maximize the income of the power plant.

References [120] and [121] take the system operator’s perspective on the optimal scheduling of energy and ancillary service to minimize the total operational cost. Lukas et al. [120] assessed the economic benefits of using energy storage for both primary reserve support and peak shaving in an islanded power system. Gobos et al. [121] proposed a robust energy and spinning reserve co-

optimization model with energy storage considering wind uncertainty. The objective function is to minimize the total energy and spinning reserve procurement cost. The energy and spinning reserve schedules for both traditional generators and storage units are optimized under both forecast and uncertain wind power generation scenarios.

Taking the system operator's perspective, we propose a comprehensive energy and reserve co-optimization model for the operation of energy storage systems. Unlike the hourly model described in [120] and [121], which only consider the energy and spinning reserve markets, we model the application of energy storage for load shaping, frequency regulation and spinning reserve support simultaneously. Combining intra-hour real-time stochastic operation with hourly day-ahead unit commitment, we demonstrate and quantify the overall benefits of deploying energy storage systems in power systems.

Compared with the state of art, our contributions can be summarized as follows:

- a. We propose a method for using BESSs for load shaping, frequency regulation, and spinning reserve service support.
- b. The regulation reserve needed is optimized through a stochastic optimization which takes into account the possible real-time net load realizations.
- c. An intra-hour real-time dispatch model is adopted to evaluate the contribution of BESS in both the regulation and spinning reserve services.
- d. The effect of BESS operation and maintenance cost on the operating results are analyzed.

The rest of this chapter is organized as follows. Section 5.2 discusses the modeling assumptions. Section 5.3 provides the detailed mathematical formulation of the co-optimization problem. Section 5.4 describes the test system. Section 5.5 presents and analyzes the results of the

optimization. Section 5.5 concludes.

5.2 MODEL ASSUMPTIONS

- REGULATION RESERVE

The amount of regulation reserve required is typically specified in most of the existing markets. With the increasing integration of renewable energy, this amount is increasing and there have been several proposals to optimize it [122-123]. Dvorkin et al. [122] proposed a non-parametric approach to allocate the required flexibility among primary, secondary and tertiary regulation intervals at a given probability level. Ding et al. [123] proposed an adjustable robust co-optimization model for the energy and ancillary services markets. The generation dispatch, AGC participation factors and spinning reserve allocations are optimized considering wind power uncertainties. In our model, the required amount of regulation is optimized based on the real-time wind power forecast. The number and type of scenarios used in this optimization can be adjusted depending on the system's accepted level for risks.

- SPINNING RESERVE

The requirements for spinning reserve has been discussed in a number of papers. To name a few, Ortega-Vazquez and Kirschen [124] propose an offline method for setting the SR requirements based on the cost of its provision and the benefit derived from its availability. In our model, we adopt the spinning reserve model mentioned in [125], i.e. the total available spinning reserve should be bigger than the capacity of the largest committed generators.

5.3 FORMULATION OF THE PROBLEM

- NOTATIONS

Sets and Indices

- t Index to the time interval, from 1 to T
- h Index to the intra-hour time interval, from 1 to H
- n Index to the wind forecast scenarios, from 1 to N

Parameters:

- C^e O&M Cost per MWh of a BESS
- P_n Probability of the n th real-time wind power scenario
- $c_i^{ru}, c_i^{rd}, c_i^{su}, c_i^{sd}$ Regulation and spinning reserve cost
- Δ_i Generator ramp rate
- δt_1 Spinning reserve ramping time
- δt_2 Regulation reserve ramping time
- $w_{w,t}^f$ Day-ahead wind power forecast
- $w_{s,t}^n$ Real-time wind power realization scenarios
- $D_{s,t}$ Load forecast

General Variables

- TC^{DA} Day-ahead total cost
- TC^{RT} Real-time total cost
- $OC_{t,i}^{DA}$ Day-ahead hourly unit operation cost

$suc_{i,t}$ Day-ahead unit startup cost

$OC_{h,i,n}^{RT}$ Intra-hour real-time unit operation cost

Variables of the day-ahead scheduling

$r_{i,t}^{ru}$ Regulation up reserve from each unit

$r_{i,t}^{rd}$ Regulation down reserve from each unit

$r_{i,t}^{su}$ Spinning up reserve from each unit

$r_{i,t}^{sd}$ Spinning down reserve from each unit

$p_{i,t}^{DA}$ Total generation of each generator

$ch_{s,t}^{DA}$ Charging power of a BESS

$p_{i,b,t}^{DA}$ Generation on each segment of the cost curve

$p_{i,t}^{DA}$ Total generation of each generator

$ch_{s,t}^{DA}$ Charging power of a BESS

$dis_{s,t}^{DA}$ Discharging power of a BESS

$SoC_{s,t}^{DA}$ State of charge of a BESS

$pf_{l,t}^{DA}$ Line flow

$\theta_{s,t}^{DA}$ Bus voltage angle

Variables for the real-time primary reserve response period

$p_{i,h,n}^1$ Total generation of each generator

$ch_{s,t,n}^1$ Charging power of a BESS

$dis_{s,t,n}^1$ Discharging power of a BESS

$SoC_{s,t,n}^1$ State of charge of a BESS

$pf_{l,t,n}^1$ Line flow

$\theta_{s,t,n}^1$ Bus voltage angle

Variables for the real-time secondary reserve response period

$p_{i,h,n}^2$ Total generation of each generator during secondary reserve response period

$ch_{s,t,n}^2$ Charging power of a BESS

$dis_{s,t,n}^2$ Discharging power of a BESS

$SoC_{s,t,n}^2$ State of charge of a BESS

$pf_{l,t,n}^2$ Line flow

$\theta_{s,t,n}^2$ Bus voltage angle

- OBJECTIVE FUNCTION

This co-optimization problem aims to minimize the sum of the day-ahead and the expected real-time correction cost:

$$\min \quad TC^{DA} + E(TC^{RT}) \quad (5.1)$$

The day-ahead cost (5.1a) includes the energy and the ancillary service costs:

$$\begin{aligned} TC^{DA} = & \sum_{i=1,t=1}^{I,T} (k_{i,b} \cdot g_{i,b,t} + suc_{i,t} + N_i) + \sum_{i=1,t=1}^{I,T} (c_i^{ru} \cdot R_{i,t}^{reg-up} + c_i^{rd} \cdot R_{i,t}^{reg-down}) \\ & + \sum_{i=1,t=1}^{I,T} (c_i^{su} \cdot R_{i,t}^{spin-up} + c_i^{sd} \cdot R_{i,t}^{spin-down}) \end{aligned} \quad (5.1a)$$

The real-time cost includes the cost of corrective actions during both the primary and secondary reserve response periods. We assume that the secondary reserve ramps through the whole intra-hour dispatch period.

$$E(TC^{RT}) = \sum_{i=1, n=1}^H P_n \cdot k_i \cdot \left(\sum_{h=1}^H (\delta t_1 \cdot p_{i,t,n}^{ru} + \delta t_2 \cdot p_{i,t,n}^{su}) \right) \quad (5.1b)$$

The startup cost and the minimum up- and down-time constraints are not listed here but can be found in [71].

- GENERATOR CONSTRAINTS

Equations (5.2) to (5.7) implement the constraints on minimum and maximum generation capacity, reserve capacity and maximum ramping:

$$P_{i,t}^{DA} = \sum_{b=1}^{NB} P_{i,b,t}^{DA} \quad (5.2)$$

$$P_{i,t}^{DA} - r_{i,t}^{rd} - r_{i,t}^{sd} \geq \underline{p}_i \cdot x_{i,t} \quad (5.3)$$

$$P_{i,b,t}^{DA} + r_{i,t}^{ru} + r_{i,t}^{su} \leq \bar{p}_{i,b} \cdot x_{i,t} \quad (5.4)$$

$$|P_{i,t}^{DA} - P_{i,t-1}^{DA}| \leq \Delta_i \quad (5.5)$$

$$r_{i,t}^{ru}, r_{i,t}^{rd} \leq \Delta_i \cdot \delta t_1 \cdot x_{i,t} \quad (5.6)$$

$$r_{i,t}^{su}, r_{i,t}^{sd} \leq \Delta_i \cdot (\delta t_1 + \delta t_2) \cdot x_{i,t} \quad (5.7)$$

- ENERGY STORAGE CONSTRAINTS

Equation (5.10) keeps track of the state of charge of each BESS while Equations (5.11) to (5.12) enforce their energy and power capacity limits. Equation (5.13) sets the final SOC of each BESS

in a way that they return to their initial SOC by the end of the scheduling horizon.

$$SoC_{s,t}^{DA} = SoC_{s,t-1}^{DA} + ch_{s,t}^{DA} - dis_{s,t}^{DA} \quad (5.10)$$

$$E_s^{\min} \leq SoC_{s,t}^{DA} \leq E_s^{\max} \quad (5.11)$$

$$ch_{s,t}^{DA}, dis_{s,t}^{DA} \leq Pe_s \quad (5.12)$$

$$SOC_{s,T}^{DA} = SOC_{s,t_0}^{DA} \quad (5.13)$$

- DAY-AHEAD SYSTEM BALANCE CONSTRAINTS

Equation (5.14) enforces the system power balance at each node. (5.15) to (5.17) set limits on the line flows.

$$\sum_{i=1}^I P_{i,t}^{DA} \cdot M_{i,s}^G - \sum_{w=1}^W wf_{w,t}^{DA} \cdot M_{w,s}^W - \sum_{l=1}^L pf_{l,t}^{DA} \cdot M_{l,s}^L = D_{s,t} + \sum_{t=1}^T \left(\frac{ch_{s,t}^{DA}}{\eta_s^{ch}} + dis_{s,t}^{DA} \cdot \eta_s^{dis} \right) \quad (5.14)$$

$$f_{l,t}^{DA} = B_{ms} \cdot (\theta_{m,t}^{DA} - \theta_{s,t}^{DA}) \quad (5.15)$$

$$-\bar{F}_{l,t} \leq f_{l,t}^{DA} \leq \bar{F}_{l,t} \quad (5.16)$$

$$-\pi \leq \theta_t^{DA} \leq \pi \quad (5.17)$$

- PRIMARY FREQUENCY RESPONSE STAGE SYSTEM CONSTRAINTS

Equation (5.18) enforces the system power balance at each node during the primary frequency response time. (5.18a) and (5.18b) set the starting point of each generator and energy storage system at the optimized value set by the day ahead problem. Equations (5.19) to (5.21) enforce the operating limits for both generators and energy storage systems.

$$\sum_{i=1}^I P_{i,h,n}^1 \cdot M_{i,s}^G - \sum_{w=1}^W wr_{w,h,n}^{RT} \cdot M_{w,s}^W - \sum_{l=1}^L pf_{l,h,n}^2 \cdot M_{l,s}^L = D_{s,h} + \sum_{t=1}^T \left(\frac{ch_{s,h,n}^1}{\eta_s^{ch}} + dis_{s,h,n}^1 \cdot \eta_s^{dis} \right) \quad (5.18)$$

$$P_{i,h,n}^1 = \begin{cases} P_{i,t}^{DA} + P_{i,t,n}^{ru} - P_{i,t,n}^{rd} & \text{if } \frac{(t-1) \cdot H}{T} + 1 \leq n \leq \frac{t \cdot H}{T} \\ P_{i,h-1,n}^1 + P_{i,t,n}^{ru} - P_{i,t,n}^{rd} & \text{else} \end{cases} \quad (5.18a)$$

$$SoC_{s,h,n}^1 = \begin{cases} SoC_{s,t}^{DA} + (ch_{s,h,n}^1 - dis_{s,h,n}^1) \cdot \delta t_1 & \text{if } \frac{(t-1) \cdot H}{T} + 1 \leq n \leq \frac{t \cdot H}{T} \\ SoC_{s,h-1,n}^{DA} + (ch_{s,h,n}^1 - dis_{s,h,n}^1) \cdot \delta t_1 & \text{else} \end{cases} \quad (5.18b)$$

$$E_s^{\min} \leq SoC_{s,h,n}^1 \leq E_s^{\max} \quad (5.19)$$

$$ch_{s,h,n}^1, dis_{s,h,n}^1 \leq Pe_s \quad (5.20)$$

$$P_{i,t,n}^{su} \leq r_{i,t}^{su} \quad P_{i,t,n}^{sd} \leq r_{i,t}^{sd} \quad (5.21)$$

- SECONDARY FREQUENCY RESPONSE STAGE SYSTEM CONSTRAINTS

Equation (5.22) enforces the system power balance at each node during the primary frequency response period. (5.22a) and (5.22b) show that the primary frequency response stage set the initial point for the secondary frequency response stage. (5.23) to (5.25) set the operating limits for both the generators and the energy storage systems.

Equation (5.26) constrains the state of charge of each energy storage to return to its day-ahead setting at the end of each hour.

$$\sum_{i=1}^I P_{i,h,n}^2 \cdot M_{i,s}^G - \sum_{w=1}^W wr_{w,h,n}^{RT} \cdot M_{w,s}^W - \sum_{l=1}^L pf_{l,h,n}^2 \cdot M_{l,s}^L = D_{s,h} + \sum_{t=1}^T \left(\frac{ch_{s,h,n}^2}{\eta_s^{ch}} + dis_{s,t,n}^2 \cdot \eta_s^{dis} \right) \quad (5.22)$$

$$P_{i,h,n}^2 = P_{i,h,n}^1 + P_{i,t,n}^{su} - P_{i,t,n}^{sd} \quad (5.22a)$$

$$SoC_{s,h,n}^2 = SoC_{s,h,n}^1 + (ch_{s,h,n}^2 - dis_{s,h,n}^2) \cdot \delta t_2 \quad (5.22b)$$

$$E_s^{\min} \leq SoC_{s,h,n}^2 \leq E_s^{\max} \quad (5.23)$$

$$ch_{s,h,n}^2, dis_{s,h,n}^2 \leq Pe_s \quad (5.24)$$

$$P_{i,t,n}^{su} \leq r_{i,t}^{su} \quad P_{i,t,n}^{sd} \leq r_{i,t}^{sd} \quad (5.25)$$

$$SOC_{s,h,n}^2 = SOC_{s,t}^{DA} \quad \text{if } h = \frac{t \cdot H}{T} \quad (5.26)$$

- ADDITIONAL SPINNING RESERVE REQUIREMENTS

The amount of regulation reserve required in the system is determined by considering the set of real-time, intra-hour wind power scenarios. Spinning reserve for unexpected large disturbance such as the lost a generator are explicitly modeled as follows. The reserve from energy storage are modeled using the same way proposed in [84].

$$\sum_{i=1}^I (r_{i,t}^{ru} + r_{i,t}^{su}) + \sum_{s=1}^S r_{s,t}^{ess} \geq P_{i,t}^{DA} \quad (5.27)$$

5.4 TEST SYSTEM

Tests were carried out on a modified version of the IEEE-RTS 24-bus system. Full system data can be downloaded from [64]. Four wind farms were added at buses 2, 18, 21, and 22, accounting for a wind penetration of up to 30% of the peak load. A line was added between buses 7 and 8 to make the system N-1 secure. The system configuration is shown in Figure 5.2. No correlation between the wind-farms was taken into account. Wind farms receive a fixed in-feed tariff of 20\$/MWh.

The day-ahead hourly forecast, the 11 real-time wind realization scenarios and the actual real-time wind power for Monte-Carlo simulation are generated using the 2004 to 2006 actual and observed wind data from NREL Eastern Wind Datasets [65]. Since only the hourly wind data is

provided, linear interpolation is used to form the 10 minute real-time wind power data.

Ten energy storage units with 25MW/50MWh configuration are distributed all over the system: near wind center (Bus19, 22, and 23), near load center (Bus 1, 2, 3, 6 and 10) and along the transmission corridor (Bus12, 14).

Other important testing parameters include:

- For real-time operation, each hour is divided into 6 intra-hour periods of 10 minutes.
- 5 minute ramping is required from the regulation reserve resources, and 10 minute ramping from the spinning reserve resource.
- The transmission capacity is reduced to 90% of its original value
- The optimization gap is set to 0.5%
- Both load curtailment and reserve insufficiency penalties are set at \$5000/MWh.
- The price for regulation reserve capacity is set to be 100% of the energy price, and the price for spinning reserve capacity at 10% of the energy price.

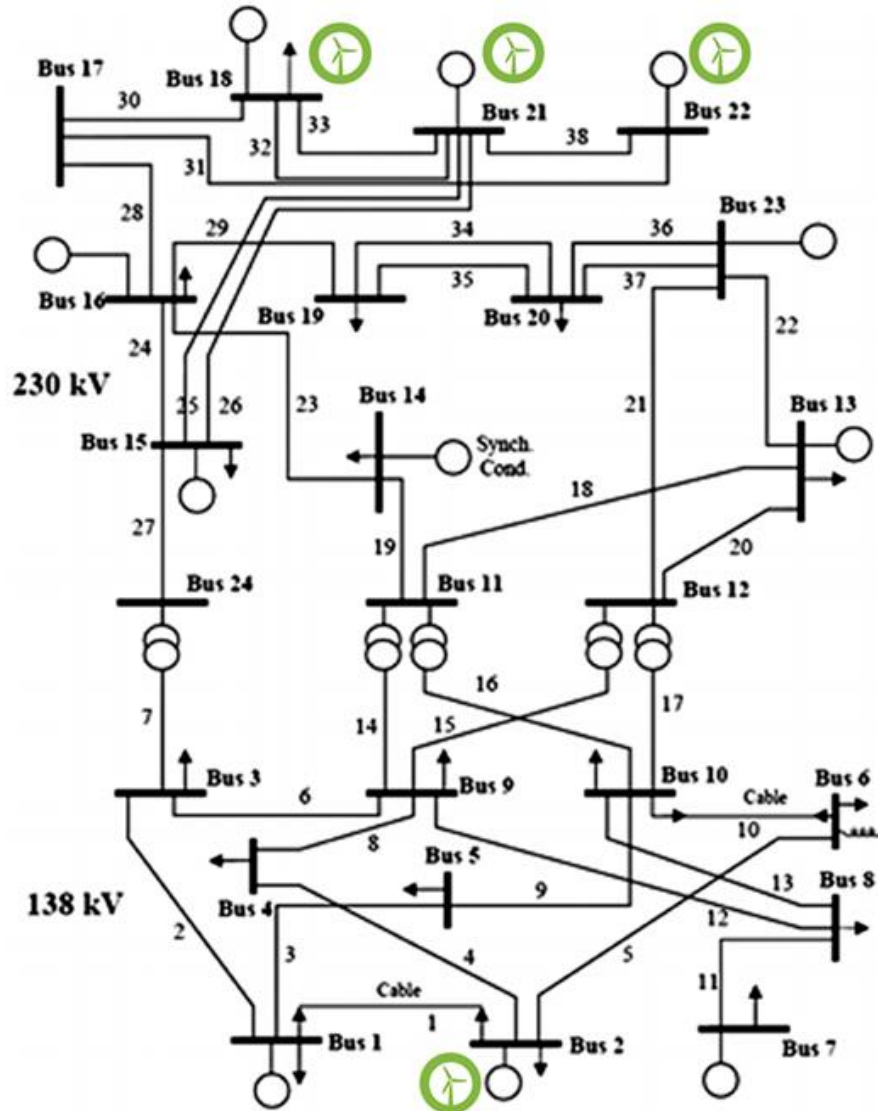


Figure 5.2. Test System Topology

Three cases are studied for analysis and comparison: Case1—Without BESS, Case2 – With BESS at no cost, Case3—With BESS operation and maintenance cost set at 2\$/MWh for each charge or discharge.

5.5 TEST RESULTS AND ANALYSIS

- SINGLE DAY OPERATION

Table 5.1 summarizes the cost savings that can be achieved with storage for a single day of operation on the test system. Since the BESS responds fast changes in the wind production and the state of the system, the savings in regulation/spinning reserve services and real-time corrective costs are significant.

Table 5.1. Comparison of Day-ahead and Expected Real-Time Costs

	NO ESS	WITH ESS	PERCENT SAVINGS
TOTAL DA	1262925	1089389	14
DA_GENERATION	1092480	1016762	7
DA_REGULATION	8792	867	90
DA_SPINNING	15641	7012	55
DA_STARTUP	55291	54903	1
EXPECTED_RT	32792	2251	93

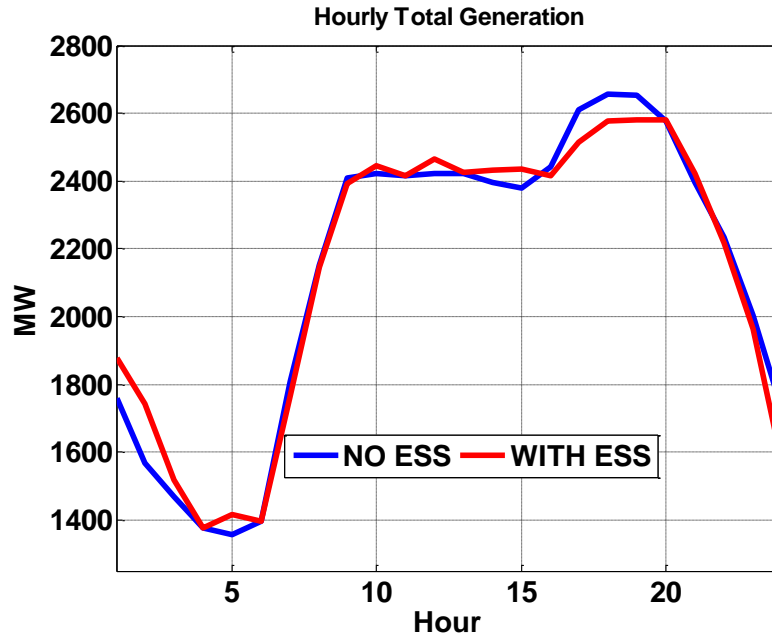


Figure 5.3. Total Hourly Generation Output

Figure 5.3 shows the effect of BESS on the load shape. BESS charge at the beginning of the day and discharge during the peak hours, which results in a smoother total generation output curve. Due to the ending hour SOC constraint, all BESS discharge its energy to back to its initial SOC state, which results in the much less total generator output for the last few hours of the scheduling period.

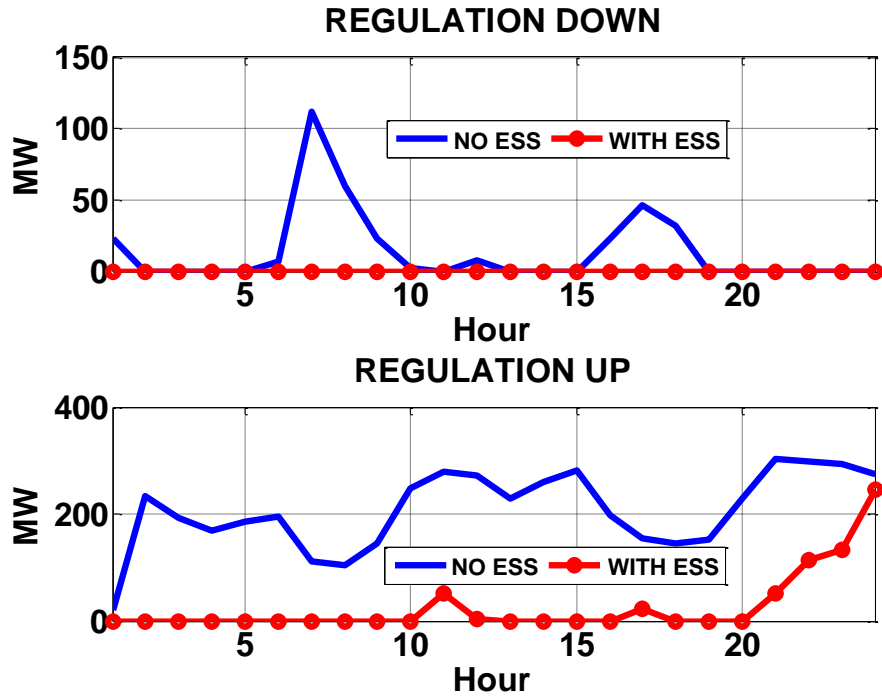


Figure 5.4. Total Hourly Regulation Reserve Provided by Generators

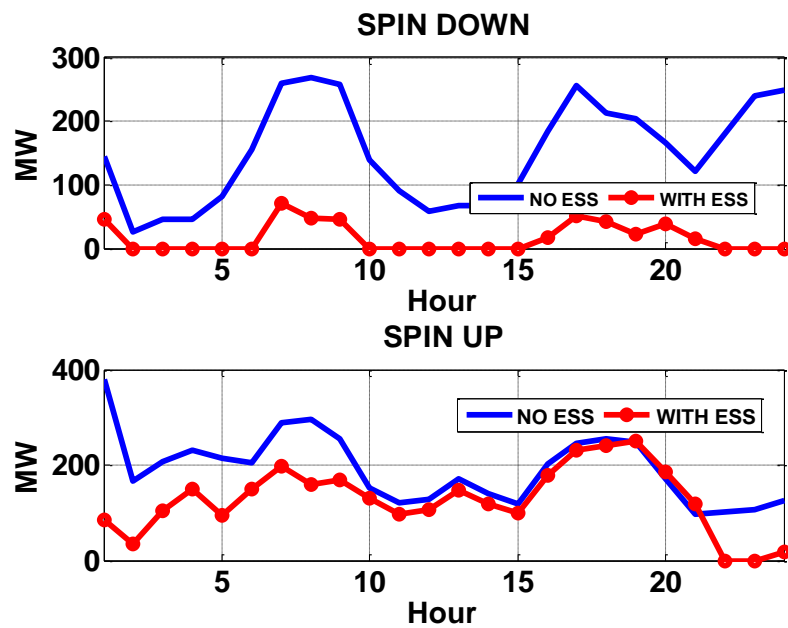


Figure 5.5. Total Hourly Spinning Reserve Provided by Generators

Figure 5.4 shows how storage provide regulation reserve and Figure 5.5 shows how it provides spinning reserve. Since storage can charge the extra energy, both the regulation down and spinning down reserve provided by generators are greatly reduced.

Storage responds fast, which make it an ideal resource for regulation. In total, 250MW/500MWh of storage capacity is installed in the system. Much less regulation up reserve is needed from generators, but some spinning up reserve is still needed due to the limited available BESS capacity as shown in Figure 5.5.

- ENERGY AND ANCILLARY SERVICE COST CHANGES

To quantify the contribution of BESS to both energy and ancillary cost savings, a simulation over a whole year was performed using the proposed method. Figure 5.6 shows the different costs incurred in different market. Figure 5.7 and Figure 5.8 show the CDF of the relative cost savings for different aspects of power system operation. The horizontal axis shows the relative number of cost savings, and the vertical axis shows the probability that $F(x > Value)$

$$\text{Relative Cost Saving} = \frac{\text{cost without BESS} - \text{cost with BESS}}{\text{cost without BESS}}$$

The following quantities are displayed on these graphs:

- DA Total (TC^{DA}) is the sum of the day-ahead generation cost, and of the procurement cost for both regulation and spinning reserve.
- DA Generation is the day-ahead generation cost, which includes the fuel costs, the no-load costs and start-up costs of all the units.
- Regulation Reserve: the cost of procuring regulation reserve in the day-ahead market.
- Spinning Reserve: the cost of procuring spinning reserve in the day-ahead market.

- RT Total (TC^{RT}) is the cost of deploying regulation and spinning reserve purchased on the real-time market

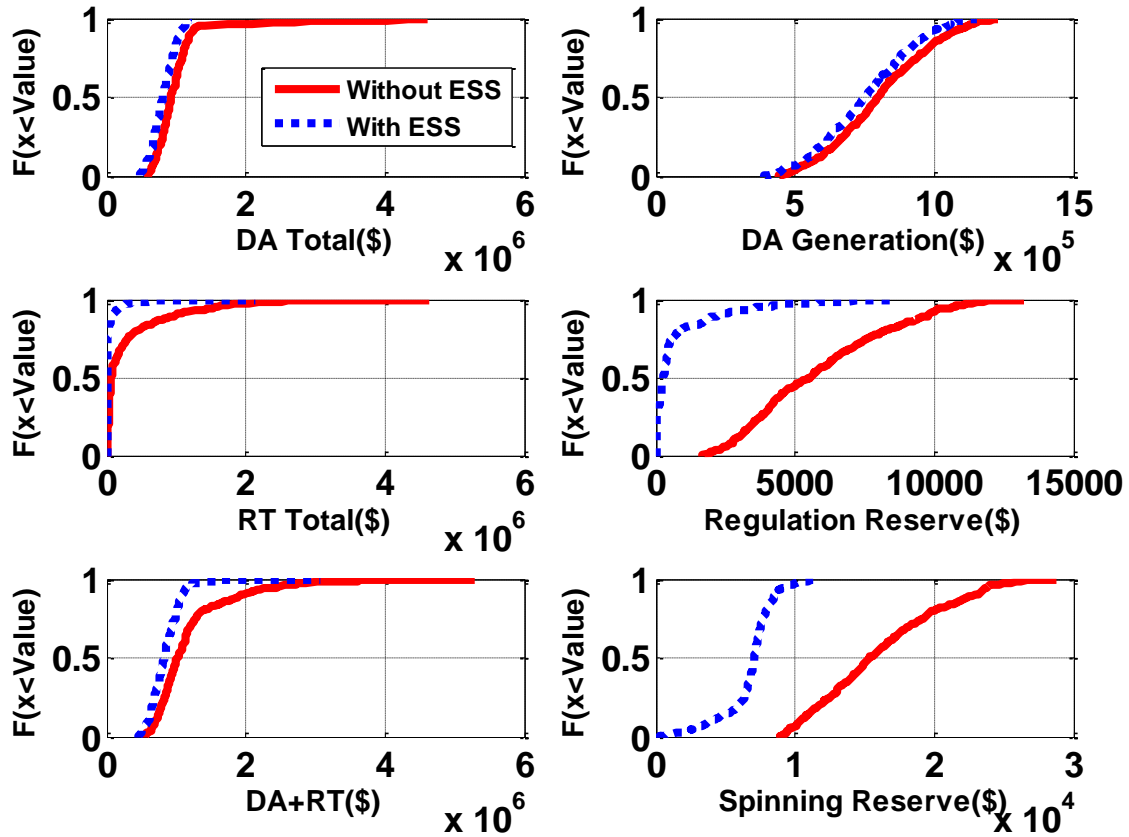


Figure 5.6. CDF of the Different Costs in Day-ahead and Real Time Market

Figure 5.6 shows that, despite the fact that they are relatively smaller, the savings brought by energy storage are more significant in the day-ahead regulation and spinning reserve procurement cost. Figures 5.7 and 5.8 illustrate the relative savings in more detail.

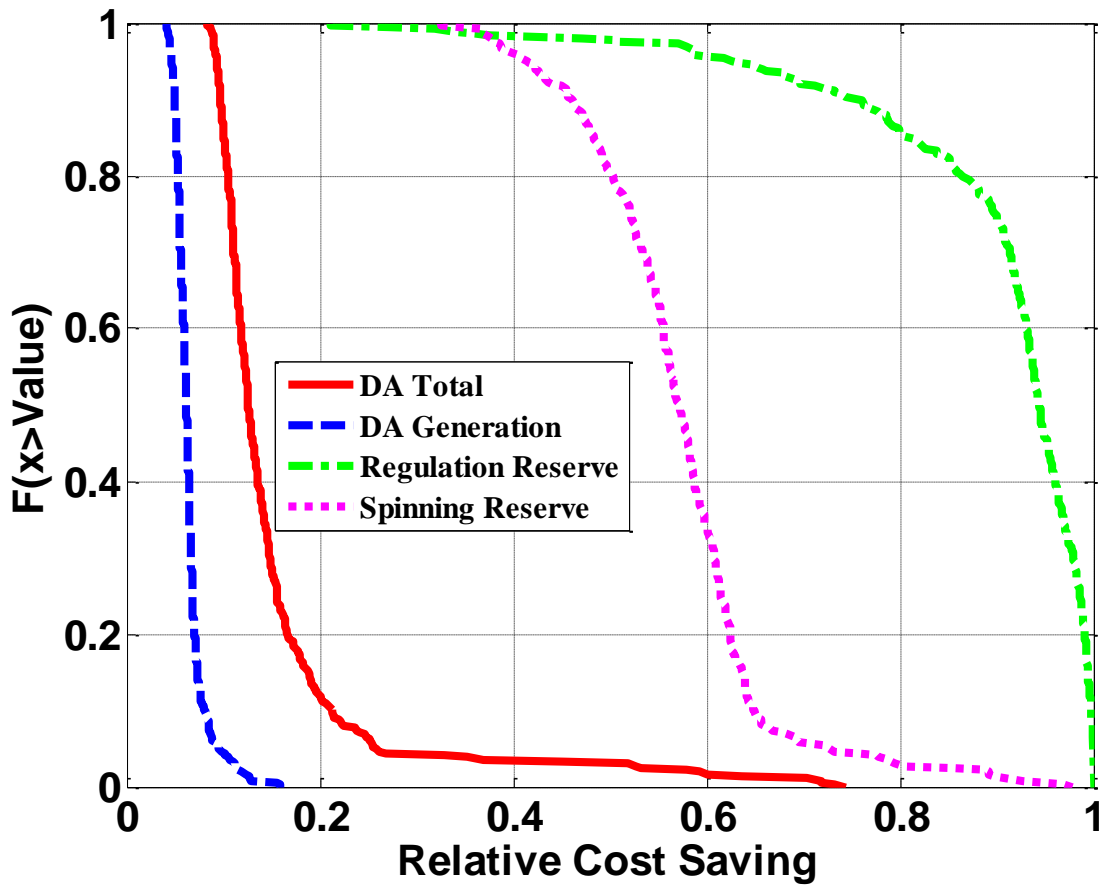


Figure 5.7. CDF of Relative Cost Savings in Day-ahead Energy and Ancillary Service Procurement Costs

- Regulation Reserve Cost: With storage, there is a 0.8 probability of achieving a 90% saving in regulation reserve procurement cost. In other words, as compared with a system without storage, in 80% of the days, the cost of procuring regulation reserve will be reduced at least 90% when storage is in operation.
- Spinning Reserve Cost: With storage, there is a 0.5 probability of achieving a 90% saving in spinning reserve procurement cost. In other words, as compared with a system without storage, in 50% of the days, the cost of procuring spinning reserve will be reduced by at least 90% when storage is in operation.

- Day-ahead generation cost: The relative savings in the day-ahead generation cost is not as large as the relative savings in ancillary services. With storage, the probability of a 10% savings in generation procurement cost is about 0.9. That is, compared with the case without storage, the cost savings is only up to 10% in 90% of the days over a whole year when storage is in operation.

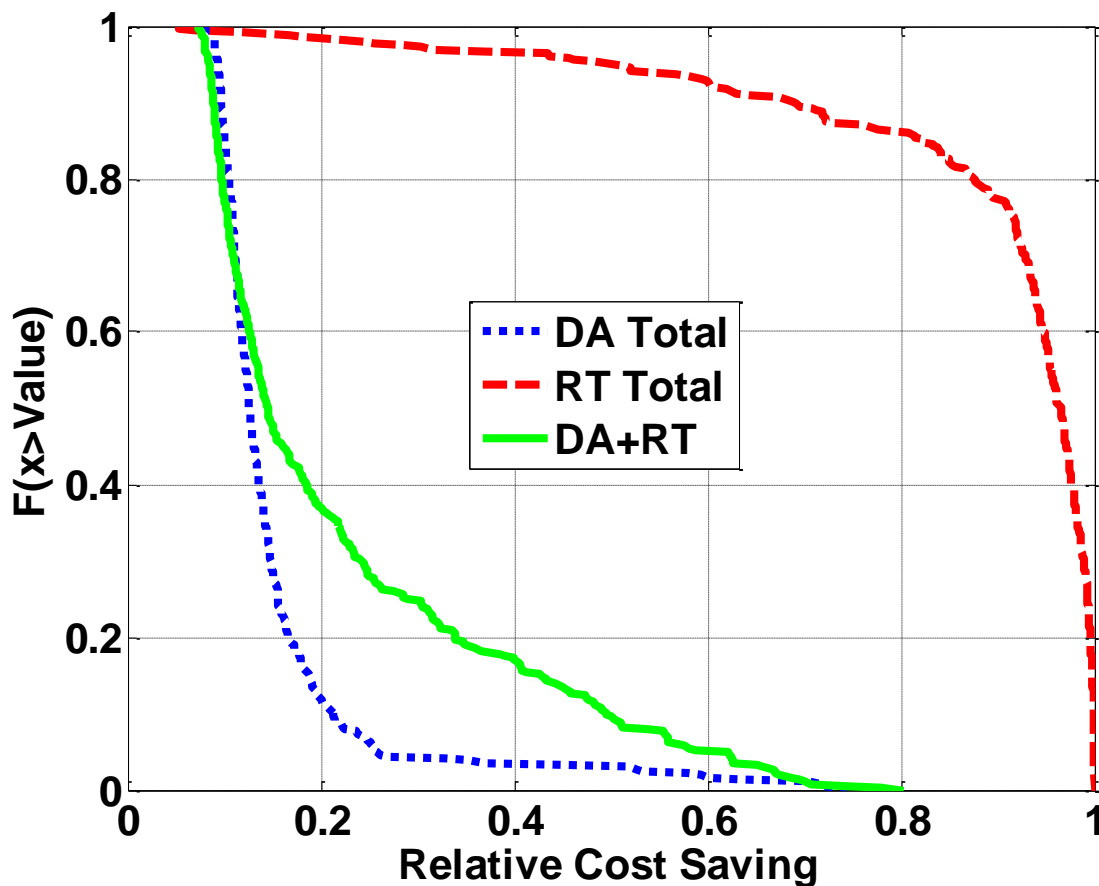


Figure 5.8. CDF of Relative Savings in Real-time, Day-ahead, and Total Cost

Figure 5.8 shows the relative savings for in real-time costs when storage is in operation. The real-time costs is defined as the cost of deploying regulation and spinning reserve. With storage, there is a probability of about 0.8 of achieving a 90% savings in the real-time cost. In other words, compared with the case without storage, the savings in the real-time cost savings is up to 90% in

80% of the days over a whole year when storage is available.

Figure 5.8 also shows the total day-ahead procurement cost (as in Figure 5.7) as well as the sum of the day-ahead and real-time costs. Since the day-ahead generation cost accounts for the majority of the total cost, the overall relative savings are dominated by the relative savings in the day-ahead generation procurement cost.

- RESERVE NEEDED

In the proposed model, the regulation reserve requirements are determined by the wind generation scenarios, while the spinning reserve should be able to deal with the loss of the largest generator committed. Figures 5.9 to 5.12 are histograms of the average hourly regulation and spinning reserve requirements for a whole year. The horizontal axis shows the average hourly reserve requirement value, and the vertical axis shows the number of days over a whole year.

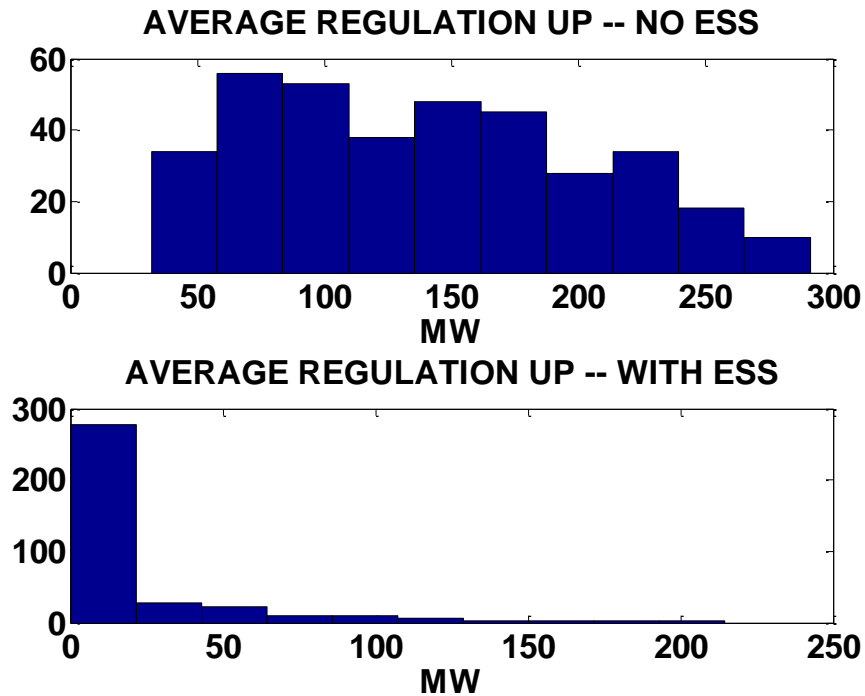


Figure 5.9. Histograms of Average Hourly Regulation Up Reserve

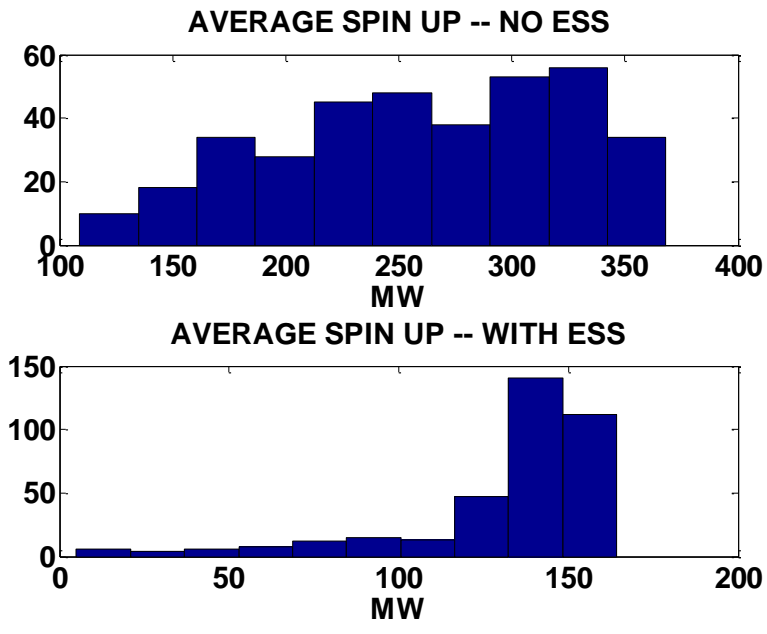


Figure 5.10. Histograms of Average Hourly Spinning Up Reserve

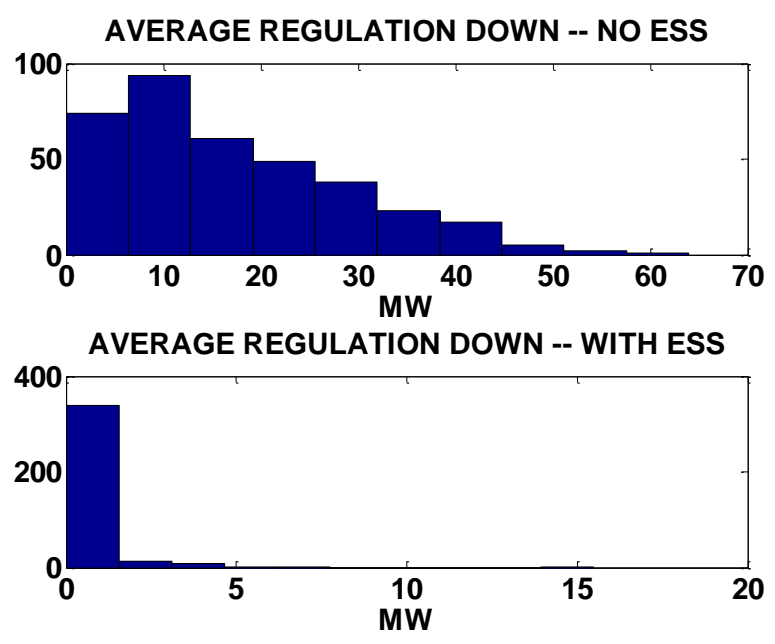


Figure 5.11. Histograms of Average Hourly Regulation Down Reserve

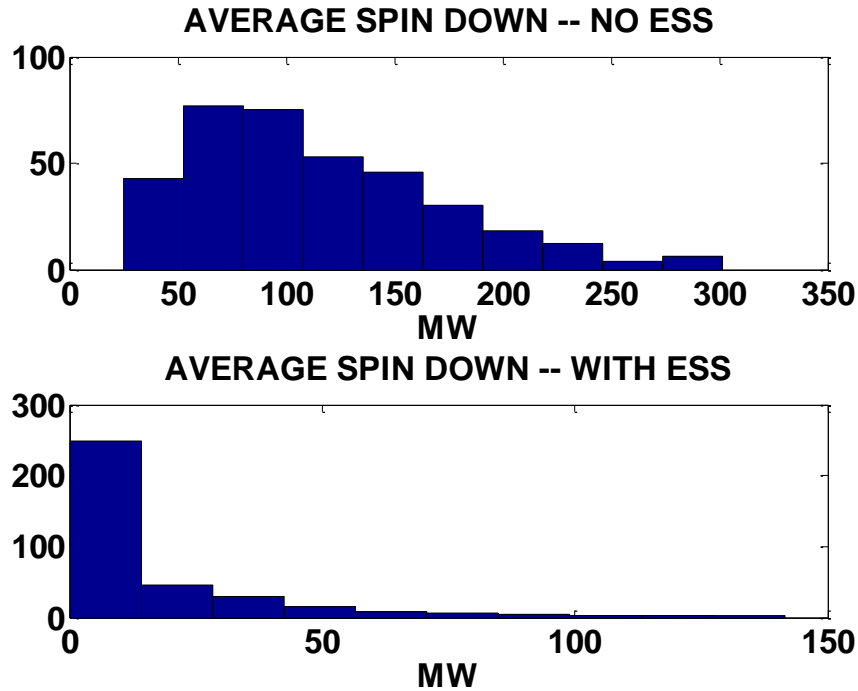


Figure 5.12. Histograms of Average Hourly Spinning Down Reserve

As shown in Figures 5.4 and 5.5 which display a single day simulation results, we observe a significant reduction in the needs for both regulation and spinning reserve from traditional generators. Figures 5.9 to 5.12 show that, when there are BESSs in the system, less ancillary services are needed most days of the year.

- EFFECT OF BESS O&M COST

To analyze the effect of the O&M cost of BESSs on their various applications, a \$2/MWh O&M cost was added to each BESS charge and discharge cycle. The effect of BESS O&M cost on the energy generation and ancillary service procurement costs, as well as on the probability of real-time load shedding and wind curtailment are illustrated in Figures 5.13 and 5.14. In these figures, the vertical axis shows the probability of $F(x < Value)$. The horizontal axis shows the relative

increase in cost between the case where a \$2/MWh O&M cost is considered and the case where it is not considered:

$$\text{Relative Cost Increase} = \frac{\text{cost considering BESS O\&M} - \text{cost not considering BESS O\&M}}{\text{cost consider BESS O\&M}}$$

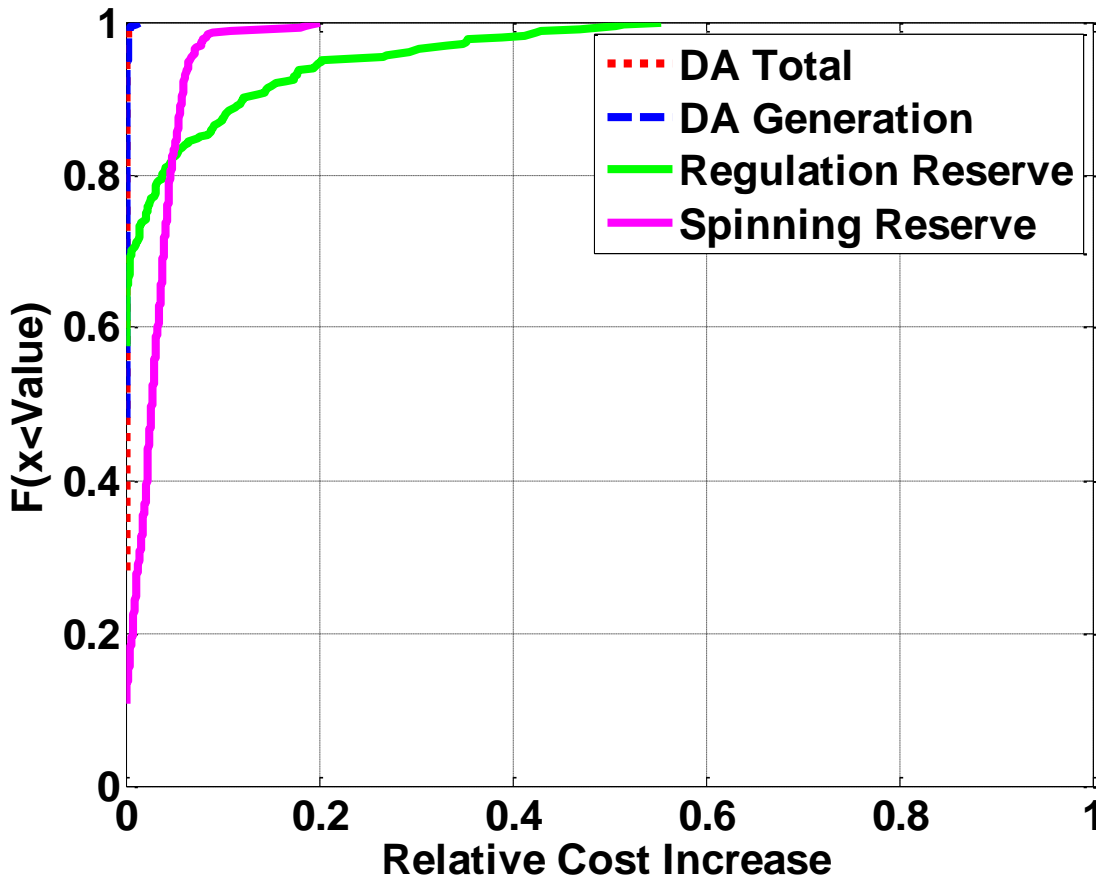


Figure 5.13. Relative increase in the day-ahead costs caused by the BESS O&M cost

Because BESSs are able to charge or discharge quickly, they reduce the need for ancillary services from generator. However, each charge or discharge incurs an O&M cost. Since these charge/discharge cycles are more frequent when they provide primary and secondary frequency response than when BESSs perform energy arbitrage, the increase in the day-ahead regulation and spinning reserve procurement costs is more significant than the increase in the cost of energy

generation as shown in Figure 5.13. However, the increased amount is not significant. With a probability of 0.9, the relative cost increase in the procurement of spinning reserve is less than 10%, and the relative cost increase in the regulation reserve procurement cost is less than 20% when a \$2/MWh BESS O&M cost is incorporated in the model. That is, when BESS O&M cost is considered, the total regulation reserve procurement cost increases by less than 20% in 90% of the days over a year, and the total spinning reserve procurement cost increase is less than 10% of the days. Over a whole year simulation, the highest relative cost increase in spinning reserve was 20% and the highest relative cost increase in regulation was about 60%.

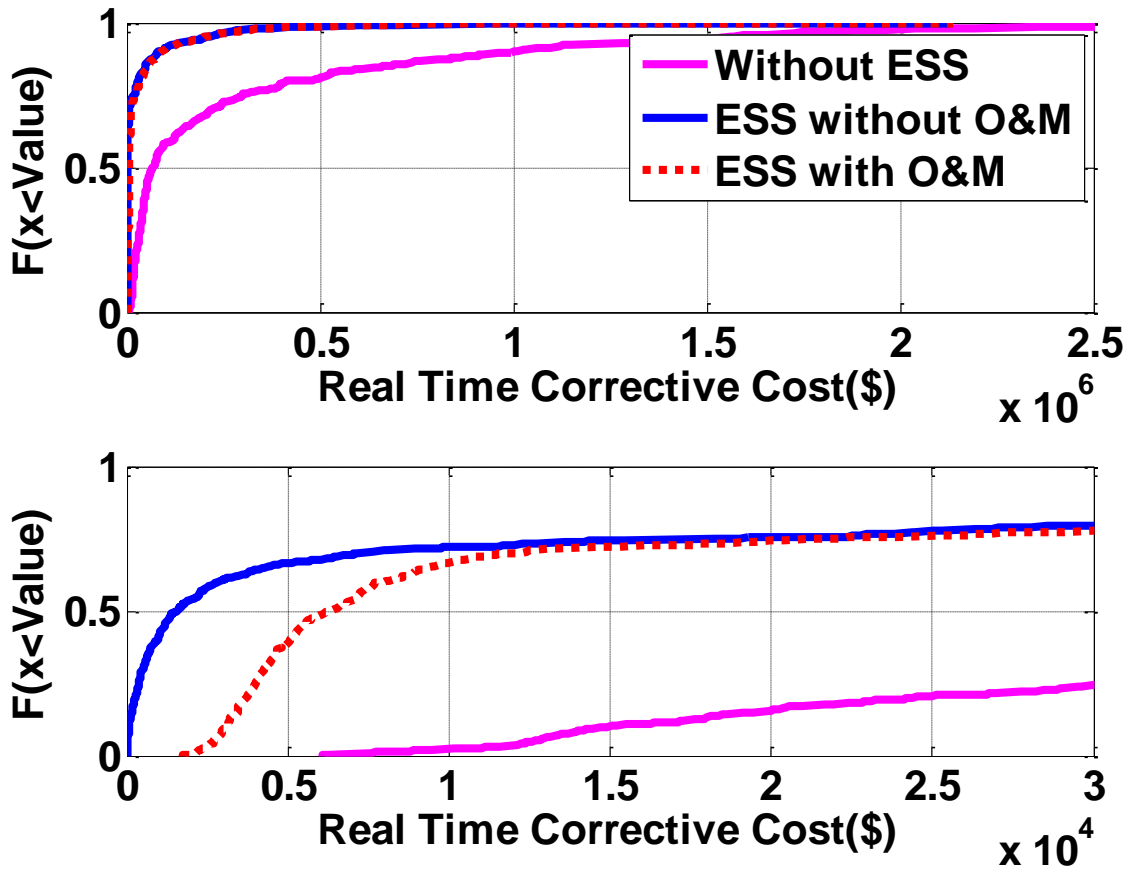


Figure 5.14. CDF of the cost of real-time corrective actions

Figure 5.14 shows the CDF of the cost of real-time corrective actions. Because the O&M cost

limits the deployment of storage BESS in the real-time market, generators are re-dispatched and wind generation is curtailed more often. This increases the cost of real-time corrective actions. However, this increase is still trivial compared with the cost when no storage is available in the system since the curve for the case when ESS has O&M cost is on top of the curve for the case when there is no O&M cost for ESS.

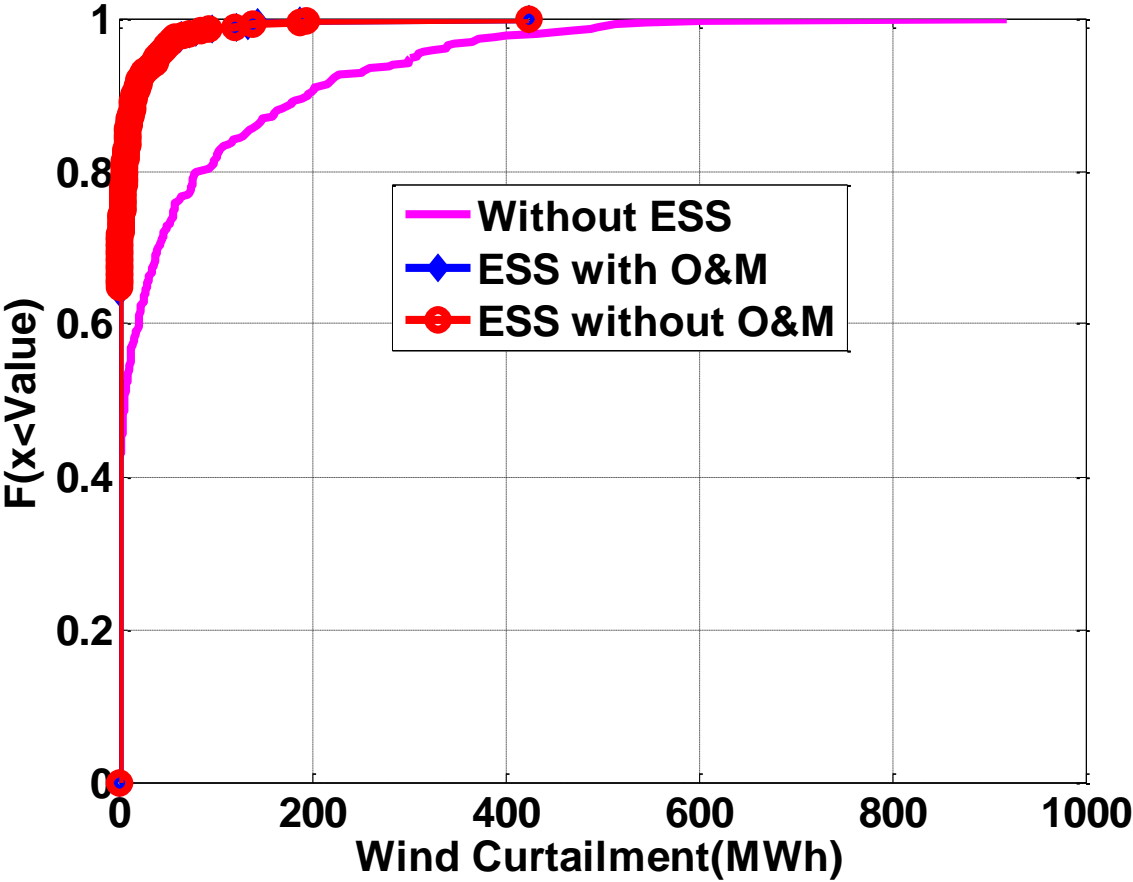


Figure 5.15. Real-time Wind Curtailment in Monte-Carlo Simulation

The proposed method optimizes the day-ahead energy production and the provision of ancillary service from both the generators and storage. The need for ancillary service is determined by the forecast real-time wind generation scenarios. Load shedding and wind curtailments are allowed

when not enough ancillary services are available, but some penalties are applied.

No load shedding was observed during the whole year simulation, and some real-time wind curtailment are seen in all three cases with storage, without storage and with storage O&M cost. Figure 5.15 shows a CDF of the amount of wind curtailment in real-time when there are insufficient ancillary services. Three conclusions can be drawn from this figure: (1) Without storage, the probability of no wind curtailment is less than 0.4, and that probability jumps to 0.65 when storage is deployed in the system; (2) Storage greatly reduces the risk of an extreme situation where a large amount of wind curtailment is needed in real-time. As shown in figure 5.15, the tail of the curve without storage is much longer than the ones with storage; (3) The effect the storage O&M on protecting the system from real-time wind curtailment is trivial because the \$2/MWh O&M cost is cheaper than the \$20 fixed in-feed tariff for wind and the cost of re-dispatching traditional generators.

5.6 CONCLUSIONS

This chapter has proposed a stochastic co-optimization method for energy and ancillary services with BESS. An hourly unit commitment model which takes into consideration the intra-hour real-time re-dispatch is adopted to quantify the contributions of storage to load shaping, regulation and spinning reserve service. A Monte-Carlo simulation spanning a whole year validates the effectiveness of the proposed method.

Chapter 6. CONCLUSIONS AND FUTURE WORK

6.1 CONCLUSIONS

The increasing need for flexibility in power systems can be solved in two ways. In the short term, advanced optimization methods could be introduced to better co-ordinate the production from renewables, traditional generations and other flexible resources. In the long-term, additional transmission assets, fast response generators and energy storage should be planned for a secure power system operation. In chapter 2 of this dissertation, several optimization methods that are widely used in day-ahead power system operation are discussed and compared in terms of modeling complexity, accuracy and computing efficiency. Chapters 3 and 4 focus on the long-term planning of flexible generation and transmission resources considering increases in wind generation capacity and load, as well as the associated uncertainties. In Chapter 3, a multi-stage co-planning model is proposed to determine the optimal size and site for battery energy storage and transmission lines. Compared with the state of art, the proposed method can handle a longer planning horizon, and consider the age and limited lifetime of BESS, as well as the time needed to build transmission. Optimal investments in storage are determined for each year at each location over the entire planning period. In Chapter 4, a multi-stage co-planning model is proposed to optimally allocate the needed battery energy storage and the flexible fast generators. The co-operation and competition relationship between storage and flexible generation is discussed in detail using nine different scenarios which represent different ratios between total wind power output and load, as well as the time correlation between wind and load changing trend coefficient. By comparing the planning results under the nine different scenarios, some common investment patterns are summarized such as the preferable locations and amounts of investments in BESS and fast generators. Chapter 5 proposed and demonstrated a stochastic model for the co-optimization

of energy and ancillary services with BESS. The benefit of allowing BESS to operate in different markets is discussed in the literature, most of the time from a BESS investor's perspective. In this chapter, we take the system operator's perspective to investigate comprehensively the contributions that a BESS can have on load shaping, as well as primary and secondary frequency support. By modeling the real-time wind/load realization scenarios in a day-ahead optimization, the r simulation.

6.2 SUGGESTED FUTURE WORK

Power system long-term planning is a hard problem due to its size and the uncertainty about the evolution of the various components of the system. Compromises between planning horizon and modeling requirements for frequency response and spinning reserve are quantified. The contributions of BESS to different aspects of power system operation are also quantified through based on a whole year accuracy are usually required. Despite the longer planning horizon and a more detailed BESS planning model, our current research is restricted to the planning BESS with transmission expansion (chapter 3) and the planning of BESS with other generation resources (chapter 4) in order to make the problem tractable. However, power systems are complex with many different elements and resources. In the future, efforts are still need in research areas which focused on a more comprehensive and tractable planning model which covering BESS, other flexible transmission and generation resources. Several simplifications may be carried out without the sacrifice of model accuracy, such as (1) reducing the number of binary decision variables by fixing the commitment status of some generators either through heuristics or looking at history commitment status; (2) reduce the number of representative days. In chapter 4, we have briefly discussed the similarity of the planning results by choosing different number of representative

days. In areas where wind and load are with sufficient temporal or geographical characteristic, the number of representative days selected could be reduced to achieve an acceptable near optimal planning solution; (3) better wind and load forecast. A better forecast could reduce the model size in two ways. First, it reduces the number of wind/load scenario considered in the model, especially under the stochastic optimization framework. Second, the consecutive years with less wind capacity /load change can be combined into an epoch, which is similar to reduce the planning horizon, and the planning problem size over several future epochs is much less than the planning problem size over each year; (4) improved optimization method. Our current model is based on stochastic optimization, and the problem size increase linearly with the number of scenarios considered. In the future, other optimization methods such as robust optimization, min-max regret optimization may be applied the planning problem.

Energy storage brings additional flexibility to power systems and reduces the need for ancillary services provided by traditional generators. However, quantifying the amounts of regulation and spinning reserve needed is not an easy task. In chapter 5 of this thesis, the regulation reserve needed is determined through stochastic optimization which looks at several real-time wind generation scenarios. In the future, other optimization methods may be considered to control the problem size in the mean while guaranteeing that sufficient regulation reserve is procured on the day-ahead.

As discussed in Chapter 1, the high investment cost of BESSs remains a major obstacle to their wider deployment in power systems. In chapter 5, a simple BESS O&M cost model is used and the effect of BESS O&M cost is discussed briefly. However, the life-cycle cost of storage depends not only on the storage cell design, battery module and the energy/power ratio, but also on parameters such as round-trip efficiency, calendar life and cycle life. All these parameters are non-linear functions of depth of discharge (DOD). In the future, a linearized storage cost model

is needed for both power system planning and operation in order to evaluate and control energy storage systems more accurately.

BIBLIOGRAPHY

- [1] M. Ortega-Vazquez and D. Kirschen, 'Estimating the Spinning Reserve Requirements in Systems With Significant Wind Power Generation Penetration', *IEEE Trans. Power Syst.*, vol. 24, no. 1, pp. 114-124, 2009.
- [2] A. Papavasiliou, S. Oren and R. O'Neill, 'Reserve Requirements for Wind Power Integration: A Scenario-Based Stochastic Programming Framework', *IEEE Trans. Power Syst.*, vol. 26, no. 4, pp. 2197-2206, 2011.
- [3] K. Bruninx, K. Van den Bergh, E. Delarue and W. D'haeseleer, 'Optimization and Allocation of Spinning Reserves in a Low-Carbon Framework', *IEEE Trans. Power Syst.*, pp. 1-11, 2015.
- [4] C. Lowery and M. O'Malley, 'Reserves in Stochastic Unit Commitment: An Irish System Case Study', *IEEE Trans. Sustain. Energy*, vol. 6, no. 3, pp. 1029-1038, 2015.
- [5] "Electricity storage: Location, location, location... and cost - Today in Energy - U.S. Energy Information Administration (EIA)", 2012. [Online]. Available: <http://www.eia.gov/todayinenergy/detail.cfm?id=6910>.
- [6] S. Ghosh and S. Kamalasan, "An Energy Function-Based Optimal Control Strategy for Output Stabilization of Integrated DFIG-Flywheel Energy Storage System", *IEEE Trans. Smart Grid*, pp. 1-10, 2016.
- [7] M. Abdullah, K. Muttaqi, D. Sutanto and A. Agalgaonkar, "An Effective Power Dispatch Control Strategy to Improve Generation Schedulability and Supply Reliability of a Wind Farm Using a Battery Energy Storage System", *IEEE Trans. Sustain. Energy*, vol. 6, no. 3, pp. 1093-1102, 2015.

- [8] F. Islam, A. Al-Durra and S. Mueeen, "Smoothing of Wind Farm Output by Prediction and Supervisory-Control-Unit-Based FESS", *IEEE Trans. Sustain. Energy*, vol. 4, no. 4, pp. 925-933, 2013.
- [9] Q. Jiang, Y. Gong and H. Wang, "A Battery Energy Storage System Dual-Layer Control Strategy for Mitigating Wind Farm Fluctuations", *IEEE Trans. Power Syst.*, vol. 28, no. 3, pp. 3263-3273, 2013.
- [10] G. Wang, M. Ciobotaru and V. Agelidis, "Power Smoothing of Large Solar PV Plant Using Hybrid Energy Storage", *IEEE Trans. Sustain. Energy*, vol. 5, no. 3, pp. 834-842, 2014.
- [11] J. Song, V. Krishnamurthy, A. Kwasinski and R. Sharma, "Development of a Markov-Chain-Based Energy Storage Model for Power Supply Availability Assessment of Photovoltaic Generation Plants", *IEEE Trans. Sustain. Energy*, vol. 4, no. 2, pp. 491-500, 2013.
- [12] N. Li, C. Uckun, E. Constantinescu, J. Birge, K. Hedman and A. Botterud, "Flexible Operation of Batteries in Power System Scheduling With Renewable Energy", *IEEE Trans. Sustain. Energy*, pp. 1-12, 2015.
- [13] P. Zou, Q. Chen, Q. Xia, G. He and C. Kang, "Evaluating the Contribution of Energy Storages to Support Large-Scale Renewable Generation in Joint Energy and Ancillary Service Markets", *IEEE Trans. Sustain. Energy*, pp. 1-11, 2015.
- [14] C. O'Dwyer and D. Flynn, "Using Energy Storage to Manage High Net Load Variability at Sub-Hourly Time-Scales", *IEEE Trans. Power Syst.*, vol. 30, no. 4, pp. 2139-2148, 2015.
- [15] R. Jabr, S. Karaki and J. Korbane, "Robust Multi-Period OPF With Storage and Renewables", *IEEE Trans. Power Syst.*, vol. 30, no. 5, pp. 2790-2799, 2015.

- [16] M. Ghofrani, A. Arabali, M. Etezadi-Amoli and M. Fadali, "Energy Storage Application for Performance Enhancement of Wind Integration", *IEEE Trans. Power Syst.*, vol. 28, no. 4, pp. 4803-4811, 2013.
- [17] L. Vargas, G. Bustos-Turu and F. Larrain, "Wind Power Curtailment and Energy Storage in Transmission Congestion Management Considering Power Plants Ramp Rates", *IEEE Trans. Power Syst.*, vol. 30, no. 5, pp. 2498-2506, 2015.
- [18] Y. Wen, C. Guo, H. Pandzic and D. Kirschen, "Enhanced Security-Constrained Unit Commitment With Emerging Utility-Scale Energy Storage", *IEEE Trans. Power Syst.*, vol. 31, no. 1, pp. 652-662, 2016.
- [19] Y. Wen, C. Guo, D. Kirschen and S. Dong, "Enhanced Security-Constrained OPF With Distributed Battery Energy Storage", *IEEE Trans. Power Syst.*, vol. 30, no. 1, pp. 98-108, 2015.
- [20] A. Del Rosso and S. Eckroad, "Energy Storage for Relief of Transmission Congestion", *IEEE Trans. Smart Grid*, vol. 5, no. 2, pp. 1138-1146, 2014.
- [21] H. Khani, M. Dadash Zadeh and A. Hajimiragha, "Transmission Congestion Relief Using Privately Owned Large-Scale Energy Storage Systems in a Competitive Electricity Market", *IEEE Trans. Power Syst.*, pp. 1-1, 2015.
- [22] Y. Wen, W. Li, G. Huang and X. Liu, "Frequency Dynamics Constrained Unit Commitment with Battery Energy Storage", *IEEE Trans. Power Syst.*, pp. 1-11, 2016.
- [23] S. Zhang, Y. Mishra and M. Shahidehpour, "Fuzzy-Logic Based Frequency Controller for Wind Farms Augmented With Energy Storage Systems", *IEEE Trans. Power Syst.*, pp. 1-9, 2015.
- [24] S. Pulendran and J. Tate, "Energy Storage System Control for Prevention of Transient Under-Frequency Load Shedding", *IEEE Trans. Smart Grid*, pp. 1-10, 2015.

- [25] M. Datta and T. Senjyu, "Fuzzy Control of Distributed PV Inverters/Energy Storage Systems/Electric Vehicles for Frequency Regulation in a Large Power System", *IEEE Trans. Smart Grid*, vol. 4, no. 1, pp. 479-488, 2013.
- [26] K. Yang and A. Walid, "Outage-Storage Tradeoff in Frequency Regulation for Smart Grid with Renewables", *IEEE Trans. Smart Grid*, vol. 4, no. 1, pp. 245-252, 2013.
- [27] D. Banham-Hall, G. Taylor, C. Smith and M. Irving, "Flow Batteries for Enhancing Wind Power Integration", *IEEE Trans. Power Syst.*, vol. 27, no. 3, pp. 1690-1697, 2012.
- [28] P. Wang, D. Liang, J. Yi, P. Lyons, P. Davison and P. Taylor, "Integrating Electrical Energy Storage Into Coordinated Voltage Control Schemes for Distribution Networks", *IEEE Trans. Smart Grid*, vol. 5, no. 2, pp. 1018-1032, 2014.
- [29] G. Mokhtari, G. Nourbakhsh and A. Ghosh, "Smart Coordination of Energy Storage Units (ESUs) for Voltage and Loading Management in Distribution Networks", *IEEE Trans. Power Syst.*, vol. 28, no. 4, pp. 4812-4820, 2013.
- [30] H. Sugihara, K. Yokoyama, O. Saeki, K. Tsuji and T. Funaki, "Economic and Efficient Voltage Management Using Customer-Owned Energy Storage Systems in a Distribution Network With High Penetration of Photovoltaic Systems", *IEEE Trans. Power Syst.*, vol. 28, no. 1, pp. 102-111, 2013.
- [31] M. Alam, K. Muttaqi and D. Sutanto, "Alleviation of Neutral-to-Ground Potential Rise Under Unbalanced Allocation of Rooftop PV Using Distributed Energy Storage", *IEEE Trans. Sustain. Energy*, vol. 6, no. 3, pp. 889-898, 2015.
- [32] S. Sun, B. Liang, M. Dong and J. Taylor, "Phase Balancing Using Energy Storage in Power Grids Under Uncertainty", *IEEE Trans. Power Syst.*, pp. 1-13, 2015.

- [33] N. Jayasekara, M. Masoum and P. Wolfs, "Optimal Operation of Distributed Energy Storage Systems to Improve Distribution Network Load and Generation Hosting Capability", *IEEE Trans. Sustain. Energy*, vol. 7, no. 1, pp. 250-261, 2016.
- [34] S. Liu, X. Wang and P. Liu, "A Stochastic Stability Enhancement Method of Grid-Connected Distributed Energy Storage Systems", *IEEE Trans. Smart Grid*, pp. 1-9, 2016.
- [35] A. Nagarajan and R. Ayyanar, "Design and Strategy for the Deployment of Energy Storage Systems in a Distribution Feeder With Penetration of Renewable Resources", *IEEE Trans. Sustain. Energy*, vol. 6, no. 3, pp. 1085-1092, 2015.
- [36] J. Tant, F. Geth, D. Six, P. Tant and J. Driesen, "Multiobjective Battery Storage to Improve PV Integration in Residential Distribution Grids", *IEEE Trans. Sustain. Energy*, vol. 4, no. 1, pp. 182-191, 2013.
- [37] D. Somayajula and M. Crow, "An Ultracapacitor Integrated Power Conditioner for Intermittency Smoothing and Improving Power Quality of Distribution Grid", *IEEE Trans. Sustain. Energy*, vol. 5, no. 4, pp. 1145-1155, 2014.
- [38] <http://energystorage.org/energy-storage/energy-storage-benefits/benefit-categories/end-user-benefits>
- [39] Y. Wang, X. Lin and M. Pedram, "A Near-Optimal Model-Based Control Algorithm for Households Equipped With Residential Photovoltaic Power Generation and Energy Storage Systems", *IEEE Trans. Sustain. Energy*, vol. 7, no. 1, pp. 77-86, 2016.
- [40] N. Paterakis, O. Erdinc, I. Pappi, A. Bakirtzis and J. Catalao, "Coordinated Operation of a Neighborhood of Smart Households Comprising Electric Vehicles, Energy Storage and Distributed Generation", *IEEE Trans. Smart Grid*, pp. 1-12, 2016.

- [41] O. Erdinc, N. Paterakis, T. Mendes, A. Bakirtzis and J. P. S. Catalao, "Smart Household Operation Considering Bi-Directional EV and ESS Utilization by Real-Time Pricing-Based DR", *IEEE Trans. Smart Grid*, vol. 6, no. 3, pp. 1281-1291, 2015.
- [42] Z. Xu, X. Guan, Q. Jia, J. Wu, D. Wang and S. Chen, "Performance Analysis and Comparison on Energy Storage Devices for Smart Building Energy Management", *IEEE Trans. Smart Grid*, vol. 3, no. 4, pp. 2136-2147, 2012.
- [43] "Lithium-ion costs to fall by up to 50% within five years | Energy Storage Update", 2016. [Online]. Available: <http://analysis.energystorageupdate.com/lithium-ion-costs-fall-50-within-five-years>.
- [44] H. Pandzic, Ting Qiu and D. Kirschen, "Comparison of state-of-the-art transmission constrained unit commitment formulations", *2013 IEEE Power & Energy Society General Meeting*, 2013.
- [45] A. Papavasiliou and S. Oren, "Multiarea Stochastic Unit Commitment for High Wind Penetration in a Transmission Constrained Network", *Operations Research*, vol. 61, no. 3, pp. 578-592, 2013.
- [46] A. Papavasiliou, S. Oren and B. Rountree, "Applying High Performance Computing to Transmission-Constrained Stochastic Unit Commitment for Renewable Energy Integration", *IEEE Trans. Power Syst.*, vol. 30, no. 3, pp. 1109-1120, 2015.
- [47] Haoyong Chen, Hao Li, Rong Ye and Bo Luo, "Robust scheduling of power system with significant wind power penetration", *2012 IEEE Power and Energy Society General Meeting*, 2012.

- [48] Jianhui Wang, M. Shahidehpour and Zuyi Li, "Security-Constrained Unit Commitment With Volatile Wind Power Generation", *IEEE Trans. Power Syst.*, vol. 23, no. 3, pp. 1319-1327, 2008.
- [49] Y. Wang, Q. Xia and C. Kang, "Unit Commitment With Volatile Node Injections by Using Interval Optimization", *IEEE Trans. Power Syst.*, vol. 26, no. 3, pp. 1705-1713, 2011.
- [50] Y. Yu, P. Luh, E. Litvinov, T. Zheng, J. Zhao and F. Zhao, "Grid Integration of Distributed Wind Generation: Hybrid Markovian and Interval Unit Commitment", *IEEE Trans. Smart Grid*, vol. 6, no. 6, pp. 3061-3072, 2015.
- [51] Long Zhao and Bo Zeng, "Robust unit commitment problem with demand response and wind energy", *2012 IEEE Power and Energy Society General Meeting*, 2012.
- [52] Peng Xiong and P. Jirutitijaroen, "An adjustable robust optimization approach for unit commitment under outage contingencies", *2012 IEEE Power and Energy Society General Meeting*, 2012.
- [53] Y. An and B. Zeng, "Exploring the Modeling Capacity of Two-Stage Robust Optimization: Variants of Robust Unit Commitment Model", *IEEE Trans. Power Syst.*, vol. 30, no. 1, pp. 109-122, 2015.
- [54] R. Jiang, J. Wang and Y. Guan, "Robust Unit Commitment With Wind Power and Pumped Storage Hydro", *IEEE Trans. Power Syst.*, vol. 27, no. 2, pp. 800-810, 2012.
- [55] D. Bertsimas, E. Litvinov, X. Sun, J. Zhao and T. Zheng, "Adaptive Robust Optimization for the Security Constrained Unit Commitment Problem", *IEEE Trans. Power Syst.*, vol. 28, no. 1, pp. 52-63, 2013.
- [56] C. Zhao and Y. Guan, "Unified Stochastic and Robust Unit Commitment", *IEEE Trans. Power Syst.*, vol. 28, no. 3, pp. 3353-3361, 2013.

- [57] A. Tuohy, E. Denny and M. O'Malley, 'Rolling Unit Commitment for Systems with Significant Installed Wind Capacity', *2007 IEEE Lausanne Power Tech*, 2007.
- [58] S. Madaeni and R. Sioshansi, "Measuring the Benefits of Delayed Price-Responsive Demand in Reducing Wind-Uncertainty Costs", *IEEE Trans. Power Syst.*, vol. 28, no. 4, pp. 4118-4126, 2013.
- [59] T. Qiu, T. Haring and D. Kirschen, 'Cost recovery in a rolling horizon unit commitment with energy storage', *2014 Power Systems Computation Conference*, 2014.
- [60] R. Jiang, J. Wang, M. Zhang and Y. Guan, "Two-Stage Minimax Regret Robust Unit Commitment", *IEEE Trans. Power Syst.*, vol. 28, no. 3, pp. 2271-2282, 2013.
- [61] Z. Wu, P. Zeng, X. Zhang and Q. Zhou, "A Solution to the Chance-Constrained Two-Stage Stochastic Program for Unit Commitment With Wind Energy Integration", *IEEE Trans. Power Syst.*, pp. 1-12, 2016.
- [62] H. Wu, M. Shahidehpour, Z. Li and W. Tian, "Chance-Constrained Day-Ahead Scheduling in Stochastic Power System Operation", *IEEE Trans. Power Syst.*, vol. 29, no. 4, pp. 1583-1591, 2014.
- [63] Y. Dvorkin, H. Pandzic, M. Ortega-Vazquez and D. Kirschen, "A Hybrid Stochastic/Interval Approach to Transmission-Constrained Unit Commitment", *IEEE Trans. Power Syst.*, vol. 30, no. 2, pp. 621-631, 2015.
- [64] http://www.ee.washington.edu/research/real/real_pe.html.
- [65] http://www.nrel.gov/electricity/transmission/eastern_wind_dataset.html
- [66] R. Hemmati, R. Hooshmand and A. Khodabakhshian, 'Comprehensive review of generation and transmission expansion planning', *IET Generation, Transmission & Distribution*, vol. 7, no. 9, pp. 955-964, 2013.

- [67] F. Munoz, B. Hobbs, J. Ho and S. Kasina, 'An Engineering-Economic Approach to Transmission Planning Under Market and Regulatory Uncertainties: WECC Case Study', *IEEE Trans. Power Syst.*, vol. 29, no. 1, pp. 307-317, 2014.
- [68] E. Martinez Cesena, T. Capuder and P. Mancarella, 'Flexible Distributed Multienergy Generation System Expansion Planning Under Uncertainty', *IEEE Trans. Smart Grid*, pp. 1-1, 2015.
- [69] K. Zach and H. Auer, 'Bulk energy storage versus transmission grid investments: Bringing flexibility into future electricity systems with high penetration of variable RES-electricity', *2012 9th International Conference on the European Energy Market*, 2012.
- [70] H. Oh, 'Optimal Planning to Include Storage Devices in Power Systems', *IEEE Trans. Power Syst.*, vol. 26, no. 3, pp. 1118-1128, 2011.
- [71] H. Pandzic, Y. Wang, T. Qiu, Y. Dvorkin and D. Kirschen, 'Near-Optimal Method for Siting and Sizing of Distributed Storage in a Transmission Network', *IEEE Trans. Power Syst.*, vol. 30, no. 5, pp. 2288-2300, 2015.
- [72] Y. Liu, W. Du, L. Xiao, H. Wang and J. Cao, 'A Method for Sizing Energy Storage System to Increase Wind Penetration as Limited by Grid Frequency Deviations', *IEEE Trans. Power Syst.*, pp. 1-9, 2015.
- [73] P. Li, R. Dargaville, F. Liu, J. Xia and Y. Song, 'Data-Based Statistical Property Analyzing and Storage Sizing for Hybrid Renewable Energy Systems', *IEEE Trans. Ind. Electron.*, vol. 62, no. 11, pp. 6996-7008, 2015.
- [74] I. Bayram, M. Abdallah, A. Tajer and K. Qaraqe, 'A Stochastic Sizing Approach for Sharing-Based Energy Storage Applications', *IEEE Trans. Smart Grid*, pp. 1-1, 2015.

- [75] Zechun Hu, Fang Zhang and Baowei Li, 'Transmission expansion planning considering the deployment of energy storage systems', *2012 IEEE Power and Energy Society General Meeting*, 2012.
- [76] F. Zhang, Y. Song and Z. Hu, 'Mixed-integer linear model for transmission expansion planning with line losses and energy storage systems', *IET Generation, Transmission & Distribution*, vol. 7, no. 8, pp. 919-928, 2013.
- [77] M. Hedayati, J. Zhang and K. Hedman, 'Joint transmission expansion planning and energy storage placement in smart grid towards efficient integration of renewable energy', *2014 IEEE PES T&D Conference and Exposition*, 2014.
- [78] I. Konstantelos and G. Strbac, 'Valuation of Flexible Transmission Investment Options Under Uncertainty', *IEEE Trans. Power Syst.*, vol. 30, no. 2, pp. 1047-1055, 2015.
- [79] S. Chen, K. Tseng and S. Choi, 'Modeling of Lithium-Ion Battery for Energy Storage System Simulation', *2009 Asia-Pacific Power and Energy Engineering Conference*, 2009.
- [80] N. Watrin, H. Ostermann, B. Blunier and A. Miraoui, 'Multiphysical Lithium-Based Battery Model for Use in State-of-Charge Determination', *IEEE Trans. Veh. Technol.*, vol. 61, no. 8, pp. 3420-3429, 2012.
- [81] P. Fortenbacher, J. Mathieu and G. Andersson, 'Modeling, identification, and optimal control of batteries for power system applications', *2014 Power Systems Computation Conference*, 2014.
- [82] *Case note World's Largest Battery Energy Storage System Fairbanks, Alaska, USA*. ABB.
- [83] *Western wind and solar integration study*. National Renewable Energy Laboratory, 2010.

- [84] Zechun Hu, Shu Zhang, Fang Zhang and Haiyan Lu, 'SCUC with battery energy storage system for peak-load shaving and reserve support', *2013 IEEE Power & Energy Society General Meeting*, 2013.
- [85] *Capital Costs for Transmission and Substations: Updated Recommendations for WECC Transmission Expansion Planning*. Western Electricity Coordinating Council, 2014.
- [86] E. Lannoye, D. Flynn and M. O'Malley, "The role of power system flexibility in generation planning," *2011 IEEE Power and Energy Society General Meeting*, San Diego, CA, 2011, pp. 1-6.
- [87] A. Shortt, J. Kiviluoma and M. O'Malley, "Accommodating Variability in Generation Planning," in *IEEE Transactions on Power Systems*, vol. 28, no. 1, pp. 158-169, Feb. 2013.
- [88] B. Hua, R. Baldick and J. Wang, "Representing Operational Flexibility in Generation Expansion Planning Through Convex Relaxation of Unit Commitment," in *IEEE Transactions on Power Systems*, vol. PP, no. 99, pp. 1-1, 2017.
- [89] V. Hinojosa and F. Gonzalez-Longatt, "Stochastic security-constrained generation expansion planning methodology based on a generalized line outage distribution factors," *2017 IEEE Manchester PowerTech*, Manchester, 2017, pp. 1-6.
- [90] D. S. Kirschen, J. Ma, V. Silva and R. Belhomme, "Optimizing the flexibility of a portfolio of generating plants to deal with wind generation," *2011 IEEE Power and Energy Society General Meeting*, San Diego, CA, 2011, pp. 1-7.
- [91] C. De Jonghe, B. F. Hobbs and R. Belmans, "Optimal Generation Mix With Short-Term Demand Response and Wind Penetration," in *IEEE Transactions on Power Systems*, vol. 27, no. 2, pp. 830-839, May 2012.

- [92] R. Hemmati, R. Hooshmand and A. Khodabakhshian, 'Comprehensive review of generation and transmission expansion planning', *IET Generation, Transmission & Distribution*, vol. 7, no. 9, pp. 955-964, 2013.
- [93] H. Saboori and R. Hemmati, "Considering Carbon Capture and Storage in Electricity Generation Expansion Planning," in *IEEE Transactions on Sustainable Energy*, vol. 7, no. 4, pp. 1371-1378, Oct. 2016.
- [94] Y. Zhan, Q. P. Zheng, J. Wang and P. Pinson, "Generation Expansion Planning With Large Amounts of Wind Power via Decision-Dependent Stochastic Programming," in *IEEE Transactions on Power Systems*, vol. 32, no. 4, pp. 3015-3026, July 2017.
- [95] R. Dominguez, A. J. Conejo and M. Carrión, "Investing in Generation Capacity: A Multi-Stage Linear-Decision-Rule Approach," in *IEEE Transactions on Power Systems*, vol. 31, no. 6, pp. 4784-4794, Nov. 2016.
- [96] H. Oh, 'Optimal Planning to Include Storage Devices in Power Systems', *IEEE Trans. Power Syst.*, vol. 26, no. 3, pp. 1118-1128, 2011.
- [97] K. Dvijotham, M. Chertkov and S. Backhaus, "Storage Sizing and Placement through Operational and Uncertainty-Aware Simulations," *2014 47th Hawaii International Conference on System Sciences*, Waikoloa, HI, 2014, pp. 2408-2416.
- [98] S. Wogrin and D. F. Gayme, "Optimizing Storage Siting, Sizing, and Technology Portfolios in Transmission-Constrained Networks," in *IEEE Transactions on Power Systems*, vol. 30, no. 6, pp. 3304-3313, Nov. 2015.
- [99] P. Xiong and C. Singh, "Optimal Planning of Storage in Power Systems Integrated With Wind Power Generation," in *IEEE Transactions on Sustainable Energy*, vol. 7, no. 1, pp. 232-240, Jan. 2016.

- [100] B. Xu *et al.*, "Scalable Planning for Energy Storage in Energy and Reserve Markets," in *IEEE Transactions on Power Systems*, early access.
- [101] K. Yasuda, K. Nishiya, J. Hasegawa and R. Yokoyama, "Optimal Generation Expansion Planning with Electric Energy Storage Systems," *Proceedings.14 Annual Conference of Industrial Electronics Society*, Singapore, 1988, pp. 550-555.
- [102] D. Pudjianto, M. Aunedi, P. Djapic and G. Strbac, "Whole-Systems Assessment of the Value of Energy Storage in Low-Carbon Electricity Systems," in *IEEE Transactions on Smart Grid*, vol. 5, no. 2, pp. 1098-1109, March 2014.
- [103] P. Yang and A. Nehorai, "Joint Optimization of Hybrid Energy Storage and Generation Capacity With Renewable Energy," in *IEEE Transactions on Smart Grid*, vol. 5, no. 4, pp. 1566-1574, July 2014.
- [104] M. Carrión, Y. Dvorkin and H. Pandžić, "Primary Frequency Response in Capacity Expansion," in *IEEE Transactions on Power Systems*, early access.
- [105] A. Kargarian, G. Hug and J. Mohammadi, "A Multi-Time Scale Co-Optimization Method for Sizing of Energy Storage and Fast-Ramping Generation," in *IEEE Transactions on Sustainable Energy*, vol. 7, no. 4, pp. 1351-1361, Oct. 2016.
- [106] Y. Liu, R. Sioshansi and A. Conejo, "Multistage Stochastic Investment Planning with Multiscale Representation of Uncertainties and Decisions," in *IEEE Transactions on Power Systems*, early access.
- [107] T. Qiu, B. Xu, Y. Wang, Y. Dvorkin and D. S. Kirschen, "Stochastic Multistage Coplanning of Transmission Expansion and Energy Storage," in *IEEE Transactions on Power Systems*, vol. 32, no. 1, pp. 643-651, Jan. 2017.

- [108] K. Poncelet, H. Höschle, E. Delarue, A. Virag and W. D'haeseleer, "Selecting Representative Days for Capturing the Implications of Integrating Intermittent Renewables in Generation Expansion Planning Problems," in *IEEE Transactions on Power Systems*, vol. 32, no. 3, pp. 1936-1948, May 2017.
- [109] B. Kirby, "Frequency Regulation Basics and Trends", *Oak Ridge National Lab*, 2004.
[Online].Available: http://www.consultkirby.com/files/TM2004-291_Frequency_Regulation_Basics_and_Trends.pdf
- [110] Y. Shi, B. Xu, D. Wang and B. Zhang, "Using Battery Storage for Peak Shaving and Frequency Regulation: Joint Optimization for Superlinear Gains," in *IEEE Transactions on Power Systems*, vol. PP, no. 99, pp. 1-1.
- [111] X. Xi, R. Sioshansi, and V. Marano, "A stochastic dynamic programming model for co-optimization of distributed energy storage," *Energy Systems*, vol. 5, no. 3, pp. 475–505, 2014.
- [112] B. Cheng and W. Powell, "Co-optimizing Battery Storage for the Frequency Regulation and Energy Arbitrage Using Multi-Scale Dynamic Programming," in *IEEE Transactions on Smart Grid*, vol. PP, no. 99, pp. 1-1.
- [113] R. Walawalkar, J. Apt, and R. Mancini, "Economics of electric energy storage for energy arbitrage and regulation in new york," *Energy Policy*, vol. 35, no. 4, pp. 2558–2568, 2007.
- [114] C. D. White and K. M. Zhang, "Using vehicle-to-grid technology for frequency regulation and peak-load reduction," *Journal of Power Sources*, vol. 196, no. 8, pp. 3972–3980, 2011.
- [115] M. R. Sarker, Y. Dvorkin and M. A. Ortega-Vazquez, "Optimal Participation of an Electric Vehicle Aggregator in Day-Ahead Energy and Reserve Markets," in *IEEE Transactions on Power Systems*, vol. 31, no. 5, pp. 3506-3515, Sept. 2016.

- [116] A. Arabali, B. Asghari and R. Sharma, "A new co-optimization model for grid scale storage units in energy and frequency regulation markets," *2016 IEEE/PES Transmission and Distribution Conference and Exposition (T&D)*, Dallas, TX, 2016, pp. 1-5.
- [117] R. H. Byrne and C. A. Silva-Monroy, "Estimating the maximum potential revenue for grid connected electricity storage: Arbitrage and the regulation market," Sandia National Laboratories, Albuquerque, NM, Tech. Rep. SAND2012-3863, December 2012.
- [118] J. Donadee, "Optimal operation of energy storage for arbitrage and ancillary service capacity: The infinite horizon approach," *2013 North American Power Symposium (NAPS)*, Manhattan, KS, 2013, pp. 1-6.
- [119] M. Chazarra, J. I. Pérez-Díaz and J. García-González, "Optimal Joint Energy and Secondary Regulation Reserve Hourly Scheduling of Variable Speed Pumped Storage Hydropower Plants," in *IEEE Transactions on Power Systems*, vol. 33, no. 1, pp. 103-115, Jan. 2018.
- [120] S. Lukas, E. Lobato, and L. Rouco, "Energy storage systems providing primary reserve and peak shaving in small isolated power systems: an economic assessment," *International Journal of Electrical Power & Energy Systems*, vol. 53, pp. 675–683, December 2013.
- [121] N. G. Cobos, J. M. Arroyo, N. Alguacil-Conde and J. Wang, "Robust Energy and Reserve Scheduling Considering Bulk Energy Storage Units and Wind Uncertainty," in *IEEE Transactions on Power Systems*, vol. PP, no. 99, pp. 1-1.
- [122] Y. Dvorkin, D. S. Kirschen and M. A. Ortega-Vazquez, "Assessing flexibility requirements in power systems," in *IET Generation, Transmission & Distribution*, vol. 8, no. 11, pp. 1820-1830, 11 2014.

- [123] T. Ding, Z. Wu, J. Lv, Z. Bie and X. Zhang, "Robust Co-Optimization to Energy and Ancillary Service Joint Dispatch Considering Wind Power Uncertainties in Real-Time Electricity Markets," in *IEEE Transactions on Sustainable Energy*, vol. 7, no. 4, pp. 1547-1557, Oct. 2016.
- [124] M. A. Ortega-Vazquez and D. S. Kirschen, "Optimizing the Spinning Reserve Requirements Using a Cost/Benefit Analysis," in *IEEE Transactions on Power Systems*, vol. 22, no. 1, pp. 24-33, Feb. 2007.
- [125] C. Liu, A. Botterud, Z. Zhou and P. Du, "Fuzzy Energy and Reserve Co-optimization With High Penetration of Renewable Energy," in *IEEE Transactions on Sustainable Energy*, vol. 8, no. 2, pp. 782-791, April 2017.

APPENDIX A

VITA